

## PC1-1-INV

### Scanning SQUID Microscopy on Chiral Superconductor Candidates $\text{Sr}_2\text{RuO}_4$ and $\text{URu}_2\text{Si}_2$

\*YUSUKE IGUCHI<sup>1</sup>

Department of Applied Physics, Stanford University<sup>1</sup>

A chiral superconductor is defined as one in which a complex superconducting gap function breaks time-reversal symmetry[1]. In this talk, I will review the superconductivity of chiral superconductor candidates  $\text{Sr}_2\text{RuO}_4$  and  $\text{URu}_2\text{Si}_2$ , and introduce our recent studies, especially of time-reversal symmetry breaking (TRS) using Scanning SQUID Microscopy (SSM). Our scanning SQUID microscope has a gradiometric SQUID layout with integrated pickup loops and field coils, enabling simultaneous measurements of the local magnetic flux and the local ac susceptibility[2].

$\text{Sr}_2\text{RuO}_4$  has been extensively studied as a possible chiral  $p$ -wave superconductor because of evidence for a nodal gap structure, spin triplet state, and TRSB[3]. However, a recent NMR Knight shift study suggested a spin singlet state in  $\text{Sr}_2\text{RuO}_4$ [4]. In addition, TRSB is still being discussed, because TRSB has been observed by  $\mu$ -SR and polar Kerr[5], but not by our SSM[6]. On the other hand, in a chiral  $p$ -wave superconductor, it is theoretically predicted that the superconducting critical temperature  $T_c$  increases linearly as the uniaxial stress increases, with a cusp at zero stress, but non-local ac susceptibility measurements and local measurements by our SSM have shown a smooth and non-linear response of  $T_c$  to uniaxial stress[7].

$\text{URu}_2\text{Si}_2$  has also been studied as a candidate for a chiral  $d$ -wave superconductor[8]. TRSB in  $\text{URu}_2\text{Si}_2$  has been reported by  $\mu$ -SR and polar Kerr[9]. We will report on our studies of TRSB in the superconducting state of  $\text{URu}_2\text{Si}_2$  using our SSM.

- [1] C. Kallin and J. Berlinsky, Rep. Prog. Phys. **79**, 054502 (2016).
- [2] J. R. Kirtley *et al.*, Rev. Sci. Instr. **87**, 093702 (2016).
- [3] A. P. Mackenzie and Y. Maeno, Rev. Mod. Phys. **75**, 657 (2003).
- [4] A. Pustogow *et al.*, arXiv:1904.00047 (2019); K. Ishida *et al.*, arXiv:1907.12236 (2019).
- [5] G. M. Luke *et al.*, Nature **394**, 558 (1998); J. Xia *et al.*, Phys. Rev. Lett. **97**, 167002 (2006).
- [6] P. G. Björnsson *et al.*, Phys. Rev. B **72**, 012504 (2005); J. R. Kirtley *et al.*, Phys. Rev. B **76**, 014526 (2007); C. W. Hicks *et al.*, Phys. Rev. B **81**, 214501 (2010).
- [7] C. W. Hicks *et al.*, Science **344**, 283 (2014); C. A. Watson *et al.*, Phys. Rev. B **98**, 09452 (2018).
- [8] T. Shibauchi *et al.*, Phil. Mag. **94**, 3747 (2014).
- [9] I. Kawasaki *et al.*, J. Phys. Soc. Jpn. **83**, 094720 (2014); E. R. Schemm *et al.*, Phys. Rev. B **91**, 140506 (2015).

Keywords: Chiral superconductor,  $\text{Sr}_2\text{RuO}_4$ ,  $\text{URu}_2\text{Si}_2$ , Scanning SQUID Microscopy

## PC1-2-INV

### Superconductivity and Electronic structure in Ca-intercalated Graphene

\*Satoru Ichinokura<sup>1</sup>

Tokyo Institute of Technology<sup>1</sup>

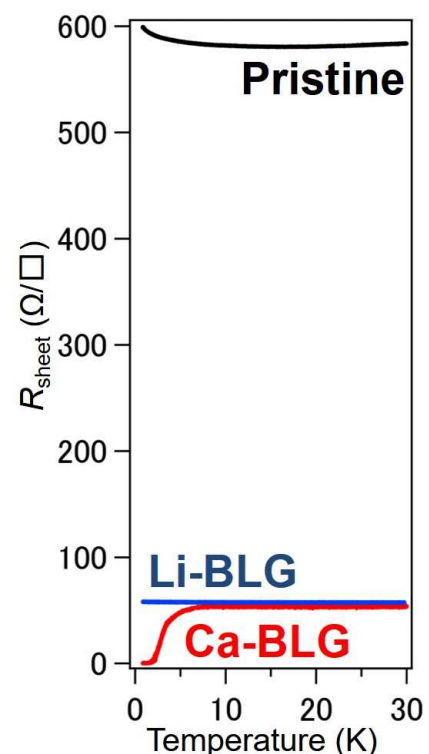
Through the enormous research focused on graphene since 2004, introducing superconductivity in graphene has grown into an attractive issue of research. To date, manipulation of stacking or intercalation of guest metal has been demonstrated to turn graphene into a superconductor by significant electronic band structures such as flat band(FB) or interlayer band(ILB). When the bilayer graphene is twisted each other by  $1.1^\circ$ , a FB is created by the band folding due to the moiré superlattice potential. Recently, it was shown that the superconductivity was driven by controlling FB at the Fermi level by field effect[1]. On the other hand, intercalation of an alkali or alkaline earth metal into graphene is believed to give ILB-driven superconductivity because they promote the occupation of the ILB, which is a criterion of the superconductivity in graphite intercalation compounds[2]. However, there was no specific evidence of superconductivity in graphene by intercalation because of difficulties in synthesizing high-quality samples and high reactivity of metal-intercalated graphene in the air.

Our group overcame these difficulties by the combination of the molecular beam epitaxy and the *in situ* 4-point-probe conductivity measurements under ultrahigh vacuum. In this paper, the author shows the electric transport properties of the Ca- and Li-intercalated bilayer-graphene on 6H-SiC(0001) substrates[3]. While the Ca-intercalated bilayer graphene exhibited the superconducting transition with  $T_c^{\text{onset}}$  of 4 K, pristine and Li-intercalated bilayer graphene did not show superconductivity down to 0.8 K, as shown in the Figure. These experimental results are explained by the occupation-criterion of ILB, as seen in their electronic structure observed by the angle-resolved photoemission spectroscopy[4] and theory[5]. The author will also report on the recent progress about Ca-intercalation into monolayer graphene.

Fig. Temperature dependence of sheet resistances  $R_{\text{sheet}}$  for pristine(black), Li-(blue) and Ca-(red)intercalated bilayer graphene under zero magnetic field.

- [1] Y. Cao, *et al.*, Nature **556**, 43 (2018).
- [2] G. Csányi, *et al.*, Nat. Phys. **1**, 42 (2005).
- [3] S. Ichinokura, *et al.*, ACS Nano **10**, 2761 (2016).
- [4] K. Kanetani, *et al.*, PNAS **109**, 19610 (2012).
- [5] E. R. Margine, *et al.*, Sci. Rep. **6** (2016).

Keywords: graphene, intercalation



## PC1-3

### Structural quantum criticality, soft phonons and strong-coupling superconductivity in $(\text{Ca}_x\text{Sr}_{1-x})_3\text{Rh}_4\text{Sn}_{13}$

Yiu Wing Cheung<sup>1</sup>, Wing Chi Yu<sup>1</sup>, Yajian Hu<sup>1</sup>, Paul J. Saines<sup>2</sup>, Malte Grosche<sup>3</sup>, Satoshi Tsutsui<sup>4</sup>, Koji Kaneko<sup>5</sup>, Kazuyoshi Yoshimura<sup>6</sup>, \*Swee K. Goh<sup>1</sup>

The Chinese University of Hong Kong, China<sup>1</sup>

University of Oxford, U. K.<sup>2</sup>

University of Cambridge, U. K.<sup>3</sup>

Japan Synchrotron Radiation Research Institute (JASRI), SPring-8, Japan<sup>4</sup>

Materials Sciences Research Center, JAEA, Japan<sup>5</sup>

Kyoto University, Japan<sup>6</sup>

Approaching a quantum critical point (QCP) has been an effective route to stabilize superconductivity. While the role of magnetic QCPs has been extensively discussed, similar exploration of a structural QCP is scarce due to the lack of suitable systems with a continuous structural transition that can be conveniently tuned to 0 K. In this presentation, I will demonstrate the existence of a structural QCP in  $(\text{Ca}_x\text{Sr}_{1-x})_3\text{Rh}_4\text{Sn}_{13}$  (Figure 1 and Ref. [1]), examine the evolution of the phonon spectrum as a function of the calcium content from inelastic x-ray scattering (Figure 2 and Ref. [2]) and heat capacity data [3]. Specifically, the inelastic x-ray scattering data unambiguously point to the softening of phonon modes around the **M** point of the Brillouin zone on cooling towards the structural transition. At  $x = 0.85$ , the soft mode energy squared at the **M** point extrapolates to zero at  $(-5.7 \pm 7.7)$  K (Figure 2(h)), providing the first compelling microscopic evidence of a structural QCP in  $(\text{Ca}_x\text{Sr}_{1-x})_3\text{Rh}_4\text{Sn}_{13}$ . Our spectroscopic, thermodynamic and transport data show that the tuning of the phonon spectra in  $(\text{Ca}_x\text{Sr}_{1-x})_3\text{Rh}_4\text{Sn}_{13}$  offers a systematic route to realize strong-coupling superconductivity.

We thank T. Matsumoto, M. Imai, Y. Tanioku, H. Kanagawa, J. Murakawa, K. Moriyama, W. Zhang, K. T. Lai, C. Michioka, H. C. Chang and D. A. Tompsett for collaboration.

- [1] Goh *et al.*,  
Phys. Rev. Lett.  
**114**, 097002 (2015)  
[2] Cheung *et al.*,  
Phys. Rev. B (R)  
**98**, 161103 (2018)  
[3] Yu *et al.*, Phys.  
Rev. Lett. **115**,  
207003 (2015)

Keywords:  
structural  
quantum critical  
point, soft  
phonons, strong-  
coupling  
superconductivity

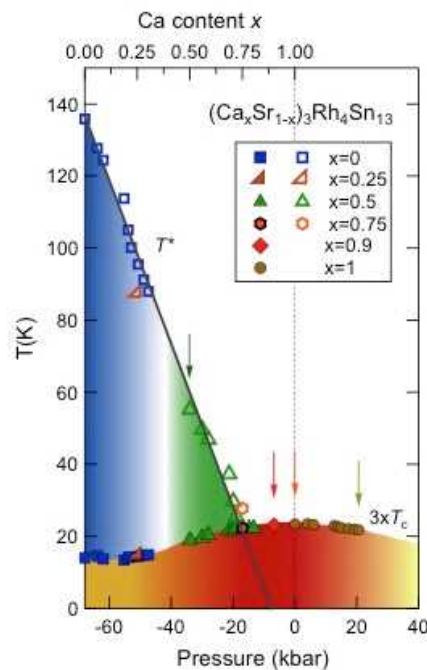


Figure 1

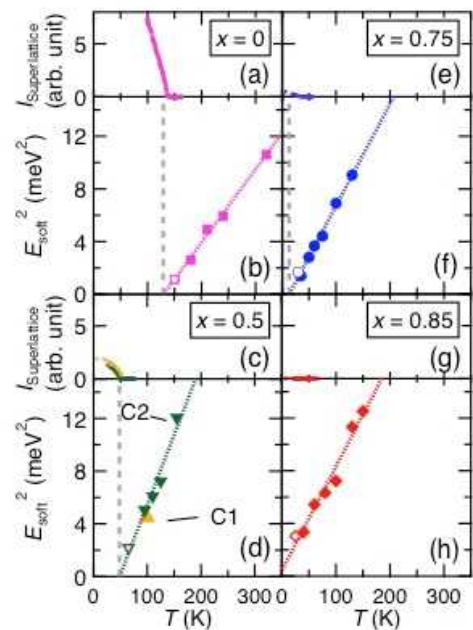


Figure 2

## PC2-1-INV

### Superconductivity in layered tin pnictides with a van der Waals-type structure

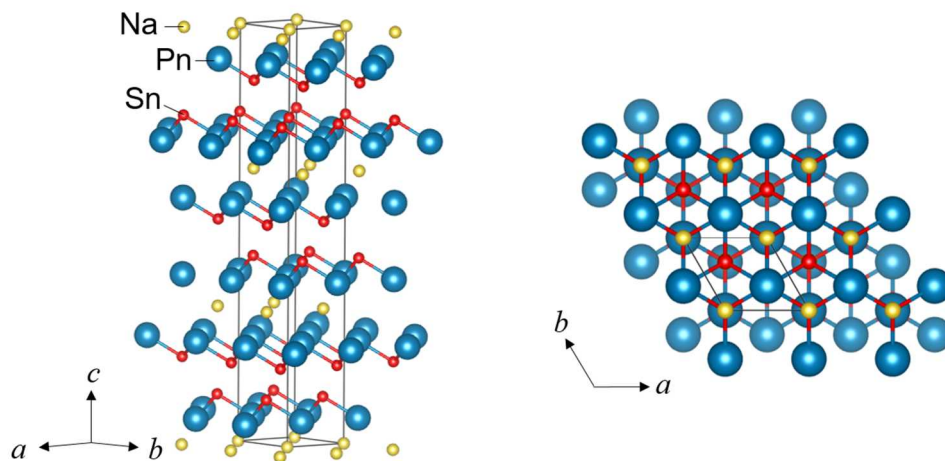
\*Yosuke Goto<sup>1</sup>, Yoshikazu Mizuguchi<sup>1</sup>

Tokyo Metropolitan University<sup>1</sup>

A layered crystal structure is an attractive stage to explore superconductors with a high transition temperature ( $T_c$ ) and to discuss the mechanisms of unconventional superconductivity, as exemplified by the cuprates and the Fe-based superconductors. The discovery of a basic structure, which works as a superconducting layer, such as the  $\text{CuO}_2$  plane and the  $\text{Fe}_2\text{An}_2$  ( $\text{An} = \text{P, As, S, Se, Te}$ ) layer, have opened new physics and chemistry fields on low-dimensional superconductors because many structural analogues could be designed by changing the structure or the alignment of the spacer layers as well as superconducting layers.

Recently, we reported SnPn-based (Pn: pnictogen) layered compounds  $\text{NaSn}_2\text{As}_2$  and  $\text{Na}_{1-x}\text{Sn}_2\text{P}_2$  [1,2] as a new class of van der Waals (vdW)-type superconductors. The crystal structure of these compounds is characterized by two layers of a buckled honeycomb network of SnPn, bound by the vdW forces and separated by Na ions, as shown in Figure 1. Measurements of electrical resistivity and specific heat indicate the bulk nature of superconductivity with transition temperature ( $T_c$ ) of 1.3 K for  $\text{NaSn}_2\text{As}_2$  and 2.0 K for  $\text{Na}_{1-x}\text{Sn}_2\text{P}_2$ . Temperature-dependent magnetic penetration depth [3] and thermal conductivity [4] of  $\text{NaSn}_2\text{As}_2$  indicate that the superconducting state can be classified into a fully gapped  $s$ -wave state with atomic-scale disorder.

In 2018, Cheng et al. reported the  $T_c$  of  $\text{NaSn}_2\text{As}_2$  as 1.6 K [4], which is slightly higher than that reported in our previous work. Furthermore, they observed charge-density-wave-like anomaly in resistivity and specific heat at around 190 K. We found that off-stoichiometry in this compound, namely, Na doping on the Sn sites ( $\text{Na}_{1+x}\text{Sn}_{2-x}\text{As}_2$ ) increases  $T_c$  to around 2.1 K [5]. Local structure analysis using extended X-ray absorption fine structure also detected the anomaly at around 190 K [6]. In the conference, we discuss detailed electronic structure of SnPn-based layered materials, as well as the synthesis of novel compounds.



#### Reference

- [1] Y. Goto et al. *J. Phys. Soc. Jpn.* **86**, 123701 (2017).
- [2] Y. Goto et al. *Sci. Rep.* **8**, 12852 (2018).
- [3] K. Ishihara et al. *Phys. Rev. B* **98**, 20503 (2018).
- [4] E. J. Cheng et al. *EPL* **123**, 47004 (2018).
- [5] H. Yuwen et al. *Jpn. J. Appl. Phys.* **58**, 083001 (2019).
- [6] G. Pugliese et al. *J. Phys.: Cond. Mater.* DOI: 10.1088/1361-648X/ab2bd4.

Keywords: pnictide, layered structure

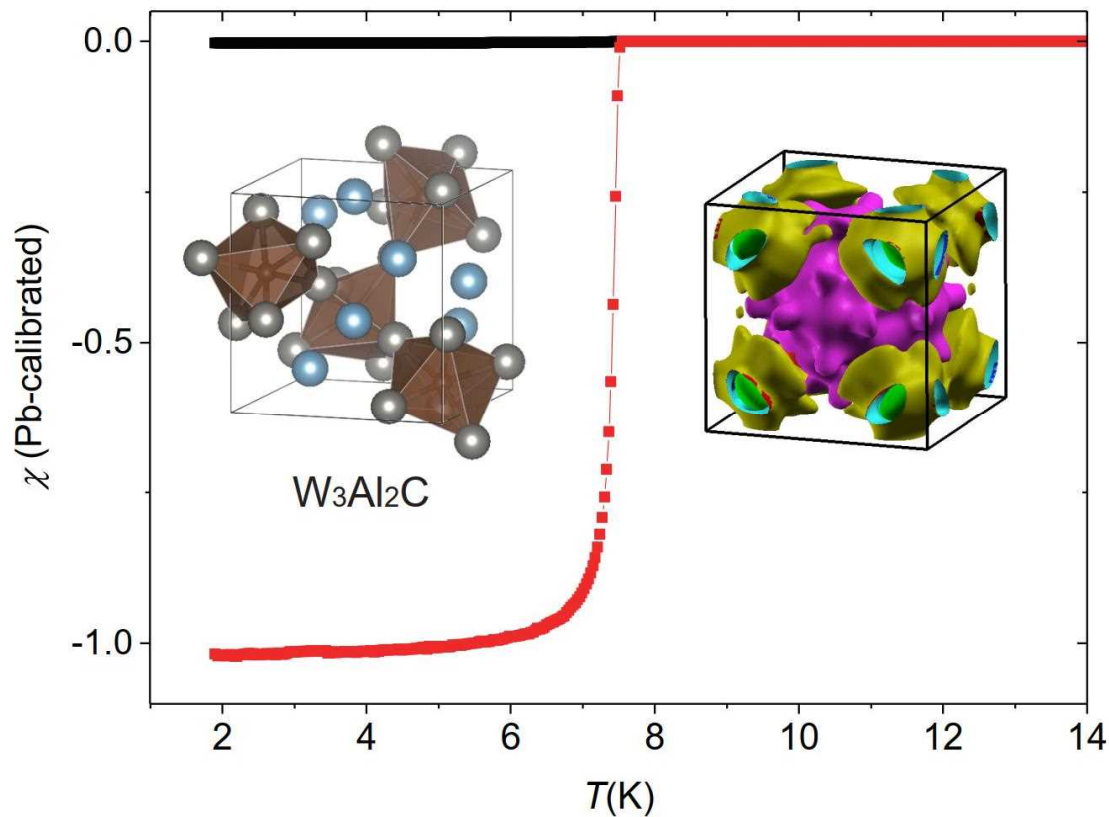
## PC2-2

### Superconductivity with strong electron-phonon coupling in noncentrosymmetric $W_3Al_2C$

\*Tianping Ying<sup>1</sup>, Yanpeng Qi<sup>2</sup>, Hideo Hosono<sup>1</sup>

Tokyo Institute of Technology, Japan<sup>1</sup>  
ShanghaiTech University, China<sup>2</sup>

We report the discovery of superconductivity in  $W_3Al_2C$  ( $T_c = 7.6$  K) synthesized by high-pressure method.  $W_3Al_2C$  is isostructural to  $Mo_3Al_2C$  (space group  $P4_132$ ) but with stronger spin-orbit coupling (SOC). Different from the  $Mo_3Al_2C$  with metallic nature, the resistivity of the normal state of  $W_3Al_2C$  shows a non-metallic behavior. A specific heat jump of  $\Delta C_{es}/\gamma T_c = 2.7$  and gap energy of  $2\Delta(0)/\gamma T_c = 5.43$  are observed, which are much larger than that of  $Mo_3Al_2C$  (2.1 and 4.03) and the expectation of the Bardeen-Cooper-Schrieffer (BCS) theory (1.43 and 3.52). However, the Sommerfeld coefficient of  $W_3Al_2C$  is less than half of that of its Mo counterpart and the specific heat below  $T_c$  shows a power-law divergence following  $C_{es}/\gamma T_c \sim (T/T_c)^{3.3}$  rather than an exponential relation. Theoretical calculations show that the Fermi surface of  $W_3Al_2C$  is dominated by  $W$ - $5d$  electrons and the inclusion of SOC significantly changes its band structure, density of states (DOS) and Fermi surface topology. The realization of superconductivity by replacing  $4d$  Mo towards  $5d$  W provides a candidate for the search of potential triplet superconductors with enhanced SOC.



Keywords: superconductivity, noncentrosymmetric, spin-orbit coupling

## PC2-3

### Pressure-induced superconductivity and topological quantum phase transitions in topological materials

\*Yanpeng Qi<sup>1</sup>

School of Physical Science and Technology, ShanghaiTech University<sup>1</sup>

Superconductivity and topological quantum states are two frontier fields of research in modern condensed matter physics. The realization of superconductivity in topological materials is highly desired; however, superconductivity in such materials is far from being thoroughly investigated. In this talk, we will discuss the electronic properties of some topological materials by applying high pressure. Pressure-induced topological quantum phase transitions and superconductivity is observed in some topological materials. The superconducting transition temperature  $T_c$  increases with applied pressure and a dome like phase diagrams were observed, which provides insights into the interplay between superconductivity and topological physics. Our theoretical calculations suggest the presence of pressure-induced topological quantum phase transitions as well as a structural–electronic instability.

Keywords: Superconductivity, High pressure, Topological materials

## PC2-4

### Effective model construction of $\text{LaNiO}_2$ ; a possible nickelate analogue of the cuprate superconductors

\*Hirofumi Sakakibara<sup>1</sup>, Hidetomo Usui<sup>2</sup>, Katsuhiko Suzuki<sup>3</sup>, Takao Kotani<sup>1</sup>, Hideo Aoki<sup>4,5</sup>, Kazuhiko Kuroki<sup>6</sup>

Dept. of Applied Math. and Phys., Tottori Univ., Japan<sup>1</sup>

Dept. of Phys. and Mat. Sci., Shimane Univ., Japan<sup>2</sup>

Research Organization of Sci. and Tech., Ritsumeikan Univ., Japan<sup>3</sup>

AIST, Japan<sup>4</sup>

Dept. of Phys., The Univ. of Tokyo, Japan<sup>5</sup>

Dept. of Phys., Osaka Univ., Japan<sup>6</sup>

Searching for analogues of cuprates has been considered as a possible path toward discovery of new high- $T_c$  superconductors. An infinite layered nickelate  $\text{LaNiO}_2$  has been considered as a possible candidate for such an analogue of cuprates because of its  $d^9$  electron configuration [1,2]. First principles calculations have shown that the  $d_{x^2-y^2}$  bandwidth is narrower than that of the cuprates, and in addition, two electron pockets originating from La 5d orbitals are present. In the present study, in order to study the possibility of superconductivity in  $\text{LaNiO}_2$ , we construct an effective two-orbital model for  $\text{LaNiO}_2$  that takes into account the Ni  $d_{x^2-y^2}$  and  $d_{3z^2-r^2}$  orbitals. Such a model has been constructed for the cuprates by some of the present authors, which lead to a successful reproduction of the experimentally observed trend of  $T_c$  [3]. The on-site interactions are estimated within the random phase approximation [4,5]. The estimation of the interaction parameters for the nickelate shows that the on-site interaction within the  $d_{3z^2-r^2}$  orbital is relatively small due to its hybridization with the La orbitals. The fluctuation exchange study for the two-orbital model of  $\text{LaNiO}_2$  results in d-wave superconductivity similarly to the cuprates, with a somewhat reduced  $T_c$  due to the narrower bandwidth.

[1] V. I. Anisimov, D. Bukhvalov, and T. M. Rice, Phys. Rev. B **59**, 7901 (1999)

[2] K.-W. Lee and W. E. Pickett, Phys. Rev. B **70**, 165109 (2004).

[3] H. Sakakibara *et al.*, Phys. Rev. Lett. **105**, 057003 (2010).

[4] H. Sakakibara *et al.*, J. Phys. Soc. Jpn. **86**, 044714 (2017); H. Sakakibara and T. Kotani, Phys. Rev. B **99**, 195141 (2019).

[5] F. Aryasetiawan *et al.*, Phys. Rev. B **70**, 195104 (2004); S.W. Jang *et al.*, Sci. Rep. **6**, 33397 (2016).

Keywords: Superconductivity, Cuprates, First-principle calculation, Hubbard model

## PC3-1-INV

### Strong pinning theory: a review

\*Roland Willa<sup>1</sup>

Karlsruhe Institute of Technology<sup>1</sup>

For more than two decades the description of vortex pinning was dominated by the qualitative theory of weak collective pinning, where the cumulative (statistical) action of many weak defects prevent vortex motion. Proposed already in the late sixties, the theory of strong vortex pinning [1,2] takes the opposite approach: few strong defects plastically deform the flux-lines and individually pin the vortex lattice. A complete framework has been developed over the last years to quantitatively predict macroscopic observables within the strong pinning regime, among which the critical current [3], the excess-current characteristic at zero temperature [4], the Campbell response to ac perturbations [5], and vortex creep [6]. I will revisit these analytic developments, explore with the help of analytic and numerical tools the regimes of higher defect densities [7], and bring the results in contact with recent experiments.

#### References

- [1] R. Labusch, *Cryst. Lattice Defects* **1**, 1 (1969).
- [2] A.I. Larkin and Y.N. Ovchinnikov, *J. Low Temp. Phys.* **34**, 409 (1979).
- [3] G. Blatter, V.B. Geshkenbein, and J.A.G. Koopmann, *Phys. Rev. Lett.* **92**, 067009 (2004).
- [4] A.U. Thomann, V.B. Geshkenbein, and G. Blatter, *Phys. Rev. Lett.* **108**, 217001 (2012) and *Phys. Rev. B* **96**, 144516 (2017).
- [5] R. Willa, V.B. Geshkenbein, R. Prozorov, and G. Blatter, *Phys. Rev. Lett.* **115**, 207001 (2015), R. Willa, V.B. Geshkenbein, and G. Blatter, *Phys. Rev. B* **92**, 134501 (2015), and *Phys. Rev. B* **93**, 064515 (2016).
- [6] M. Buchacek, R. Willa, V.B. Geshkenbein, and G. Blatter, *Phys. Rev. B* **98**, 094510 (2018) and *Phys. Rev. B* **100**, 014501 (2019).
- [7] R. Willa, A.E. Koshelev, I.A. Sadovskyy, and A. Glatz, *Supercond. Sci. Technol.* **31**, 014001 (2018) and *Phys. Rev. B* **98**, 054517 (2018).

Keywords: strong pinning, theory, vortex matter



## PC3-2-INV

### Fulde-Ferrell-Larkin-Ovchinnikov Phases in Layered Organic Superconductors

\*S. Uji<sup>1</sup>, S. Sugiura<sup>1</sup>, T. Isono<sup>1</sup>, N. Kikugawa<sup>1</sup>, T. Terashima<sup>1</sup>, H. Akutsu<sup>2</sup>, Y. Nakazawa<sup>2</sup>, D. Graf<sup>3</sup>, P. Day<sup>4</sup>

National Institute for Materials Science, Tsukuba 305-0003, Japan<sup>1</sup>

Osaka University, Toyonaka, Osaka 560-0043, Japan<sup>2</sup>

National High Magnetic Field Laboratory, Tallahassee, Florida 32310, USA<sup>3</sup>

University College London, London, United Kingdom<sup>4</sup>

In conventional superconductors, the superconducting order parameter is spatially homogeneous. However, when the superconductivity is in the clean limit and the orbital effect is strongly quenched, so-called Fulde and Ferrell, and Larkin and Ovchinnikov (FFLO) phase with an inhomogeneous order parameter can be stabilized in fields above the Pauli limit  $H_{\text{Pauli}}$ . Highly two-dimensional layered organic superconductors are best candidates for the FFLO phase studies. In the FFLO phase, the order parameter is given by  $\Delta(\mathbf{r}) = \Delta_0 \cos(\mathbf{q}\mathbf{r})$ , where  $\mathbf{q}$  is the center-of-mass momentum of the Cooper pairs. When a magnetic field is applied parallel to the layers, flux lines penetrate the insulating layers, forming Josephson vortices (JVs). The JVs are easily driven by a perpendicular current, leading to nonzero interlayer resistance in the SC phase.

When the wavelength of the FFLO order parameter oscillation  $\lambda_{\text{FFLO}} = 2\pi/q$  becomes commensurate with the JV lattice constant  $l$ , the JVs are collectively pinned and dips periodically appear in the field dependence of the interlayer resistance. This commensurability (CM) effect is a powerful tool to estimate the order parameter oscillation in the FFLO phase. So far, we have found the CM effects in the FFLO phases for three different layered organic superconductors [Fig. 1] [1,2]. For these superconductors, the FFLO phases appear above  $\sim H_{\text{Pauli}}$  at low temperatures. On reasonable assumptions, we can estimate  $\lambda_{\text{FFLO}}$ , which decreases as the field approaches  $H_{c2}$ .

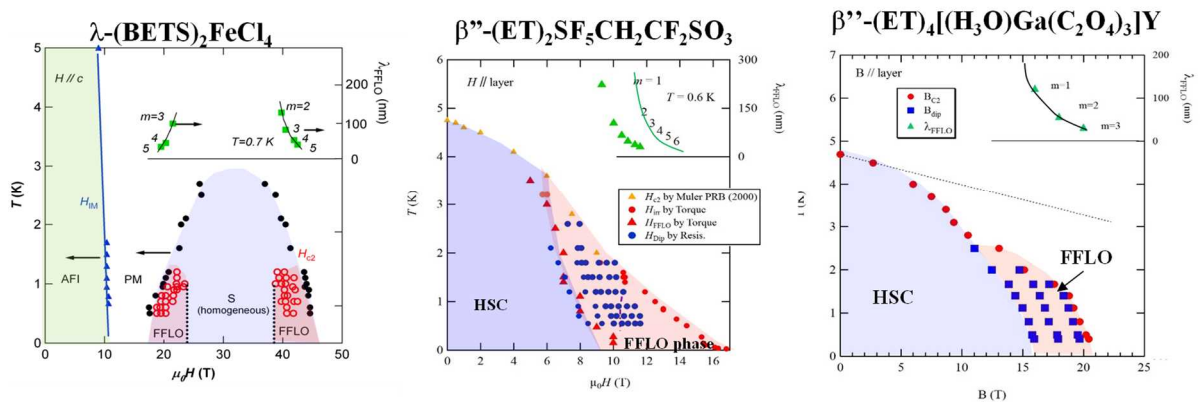


Figure 1: Superconducting phase diagrams for three different organic layered superconductors. Red regions show FFLO phases.

[1] Uji et al., Phys. Rev. Lett. 97, 157001 (2006), Phys. Rev. B 85, 174530 (2012), J. Phys. Soc. Jpn. 82, 034715 (2013), J. Phys. Soc. Jpn. 84, 104709 (2015), Phys. Rev. B 95, 165133 (2017), Phys. Rev. B 97, 144505 (2018).

[2] S. Sugiura et al., npj Quantum Matter 4, 7, 1 (2019).

Keywords: Organic superconductor, FFLO, high magnetic field

## PC3-3-INV

### Observation of vortices driven by dc current using scanning tunneling spectroscopy

\*Shin-ichi Kaneko<sup>1</sup>, Takashi Ogawa<sup>1</sup>, Kazuki Tsuchiya<sup>1</sup>, Koshiro Kato<sup>1</sup>, Koichiro Ienaga<sup>1</sup>, Hideaki Sakata<sup>2</sup>, Satoshi Okuma<sup>1</sup>

Department of Physics, Tokyo Institute of Technology<sup>1</sup>

Department of Physics, Tokyo University of Science<sup>2</sup>

We have constructed a scanning-tunneling-microscopy/spectroscopy (STM/S) system which allows us to conduct transport and STM measurements at low temperatures and high fields for the same sample. We study configurations of vortices in weak pinning amorphous  $\text{Mo}_x\text{Ge}_{1-x}$  films under dc currents  $I$  both in plastic-flow and flux-flow regimes. The applied field is well below the peak-effect field. First, we drive the vortices by  $I$  for a long time until the steady state is reached. After freezing the vortex configuration by switching off  $I$ , we perform STS measurements. We observe a triangular vortex lattice within a scanning area of  $240 \times 240 \text{ nm}^2$  for all  $I$  studied, not only in the flux-flow region at high  $I$  where the vortex configuration is considered to be an ordered lattice, but also in the plastic-flow region at low  $I$  where the configuration is expected to be disordered [1]. We find, however, that at low  $I$ , the orientation of the lattice with respect to the flow direction differs when we change the scanning area. Furthermore, real-time measurements of the tunneling spectrum at a fixed tip position show an intermittent vortex motion. These results indicate that the vortex flow at low  $I$  corresponds to that of vortex polycrystals with domain sizes larger than  $240 \times 240 \text{ nm}^2$ . This is different from simulations predicting the formation of flow channels at the domain boundaries. At high  $I$ , on the other hand, we obtain images of a vortex lattice with the same orientation over a wide area, consistent with the results of a mode-locking resonance [2]. We will also show the significance of the present STS system for the study of nonequilibrium phenomena in the vortex system [3,4].

[1] C. J. Olson, C. Reichhardt, and F. Nori, Phys. Rev. Lett. **81**, 3757 (1998).

[2] S. Okuma, D. Shimamoto, and N. Kokubo, Phys. Rev. B **85**, 064508 (2012).

[3] S. Okuma, Y. Tsugawa, and A. Motohashi, Phys. Rev. B **83**, 012503 (2011).

[4] M. Dobroka *et al.*, New J. Phys. **90**, 053023 (2017); **21**, 043007 (2019).

Keywords: vortex dynamics, plastic flow, scanning tunneling spectroscopy

## PC3-4

### Thermoelectric study of the anomalous metallic state in amorphous superconducting thin films

\*Koichiro Ienaga<sup>1</sup>, Taiko Hayashi<sup>1</sup>, Yutaka Tamoto<sup>1</sup>, Shin-ichi Kaneko<sup>1</sup>, Satoshi Okuma<sup>1</sup>

Department of Physics, Tokyo Institute of Technology<sup>1</sup>

The superconductor-insulator transition in a two-dimensional electron system is known as a quantum phase transition [1]. This transition is driven by magnetic field or disorder and has been studied in disordered superconducting thin films [2]. On the other hand, an unusual metallic phase intervening between the superconducting phase and the insulating phase has been reported in various thin-film systems including amorphous, granular, and highly crystalline films [3]. This state is called an anomalous metal and shows characteristic features reminiscent of superconductivity, e.g., residual resistivity much smaller than the normal resistivity just above the transition temperature, and giant positive magnetoresistance. Many theoretical models for the metallic state have been constructed assuming the existence of Cooper pairs and superconducting vortices [3]. However, whether the vortices are really present in the metallic phase has not been completely verified from resistivity measurements.

In this study, we performed a Nernst measurement using a dilution refrigerator. We studied an amorphous  $\text{Mo}_x\text{Ge}_{1-x}$  thin film with a thickness of 12 nm prepared by rf sputtering. The field-induced superconductor-metal-insulator transition was observed in the zero-temperature limit from the magnetoresistance measurement. We measured Nernst signals by sweeping the field at high temperatures just below the transition temperature, and found vortex Nernst signals in wide field ranges corresponding to the thermal vortex liquid phase [4]. With decreasing temperature, the field range where the vortex signals are observable decreases but remains finite toward zero temperature, indicating the existence of a quantum vortex liquid state. Moreover, the observed quantum vortex liquid state is located within the anomalous metallic phase defined by the magnetoresistance. These results strongly suggest that the metallic ground state is induced by mobile vortices due to quantum fluctuations.

[1] M. P. A. Fisher, G. Grinstein, and S. M. Girvin, *Phys. Rev. Lett.* **64**, 587 (1990); M. P. A. Fisher, *Phys. Rev. Lett.* **65**, 923 (1990).

[2] A. M. Goldman and N. Marcović, *Physics Today* **51**, 39 (1998).

[3] A. Kapitulnik, S. A. Kivelson, and B. Spivak, *Rev. Mod. Phys.* **91**, 011002 (2019).

[4] K. Behnia and H. Aubin, *Rep. Prog. Phys.* **79**, 046502 (2016).

Keywords: Nernst effect, two-dimensional superconductor, anomalous metal, quantum vortex liquid

## PC3-5

# Local Density of States of Quasi-particles around a Vortex Core in a Square Superconducting Plate under Random Impurity Potentials

\*Takayuki Tamai<sup>1</sup>, Masaru Kato<sup>1</sup>

Department of Physics and Electronics, Osaka Prefecture University, Japan<sup>1</sup>

For applications of superconductors, pinning of vortices is important. There are several kinds of pinning sites. A nanorod is one of examples of these pinning sites. On the other hand, there are superconductors such as amorphous superconductors where impurities uniformly distribute. In order to investigate behaviors of vortices in these superconductors into, we include the random impurity potential to the Bogoliubov-de Gennes (BdG) equation. We self-consistently solve this BdG equation for a square superconducting plate, using the Finite Element Method and obtain the order parameter  $\Delta(\mathbf{r})$  and local density of states (LDOS) of quasi-particles. Examples of  $\Delta(\mathbf{r})$  and LDOS are shown in Figs. 1 and 2. We find the deformation of a vortex and spatial variation of the LDOS from these figures.

In order to explain these results of the effect of impurity potential on the vortex core, we consider two simple impurity potentials, a Gaussian potential and a sinusoidal potential.

We solve the BdG equation with these two impurity potentials.

In this presentation, we will show  $\Delta(\mathbf{r})$  and LDOS and *core radius of the vortex* under these impurity potentials.

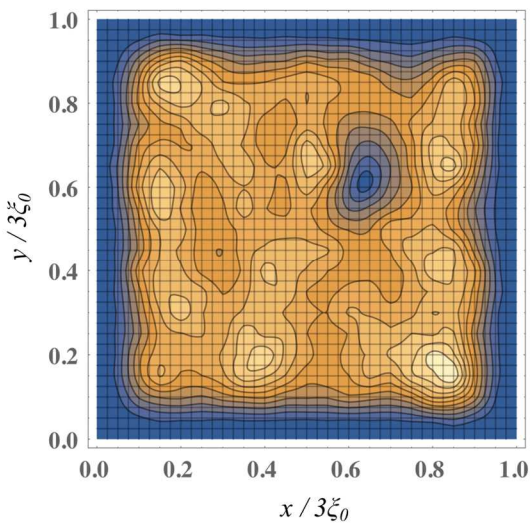


Fig. 1.  $\Delta(\mathbf{r})$  in the case of  $V_{impmax}/E_c = 0.5$

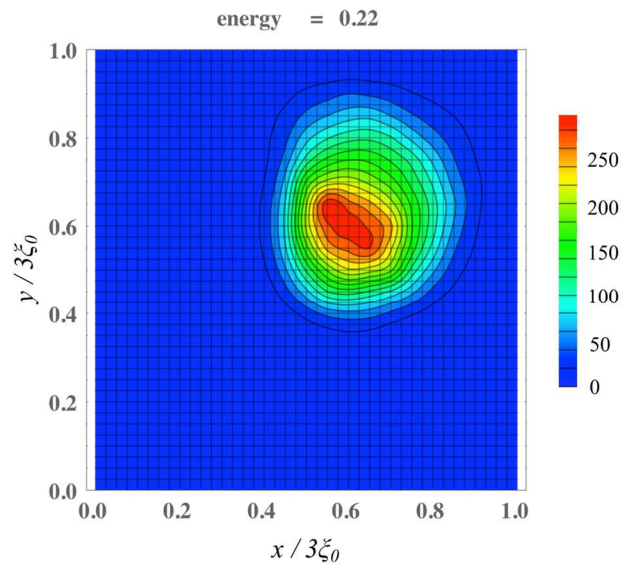


Fig. 2. LDOS in the case of  $V_{impmax}/E_c = 0.5$

Keywords: Vortex, Bogoliubov-de Gennes equation, Local density of states, Finite element method

## PC4-1-INV

### Non-magnetic Pair-breaking Scattering in Iron-based Superconductors

\*Ruslan Prozorov<sup>1</sup>, Makariy A. Tanatar<sup>1</sup>, Kyuil Cho<sup>1</sup>, Marcin Kończykowski<sup>2</sup>

Ames Laboratory and Department of Physics & Astronomy, Iowa State University, Ames, Iowa 50011, USA<sup>1</sup>

Laboratoire des Solides Irradiés, École Polytechnique, Institut Polytechnique de Paris, F-91128 Palaiseau, France<sup>2</sup>

After more than ten years of intense research, it is commonly accepted that iron-based superconductors have sign-changing order parameter that is usually nodeless but can also be nodal [1-3]. Details of the superconducting gap structure and relative strengths of inter-band and intra-band potentials of the pairing matrix can be probed experimentally by studying the response to controlled non-magnetic disorder [1,3-5]. Point-like scattering is induced by MeV electron irradiation at 22 K to avoid fast recombination. Measurements of the superconducting transition,  $T_c$ , alone are insufficient and other quantities are needed to arrive to the objective conclusions. We use anisotropic resistivity to examine nematic response as well as Matthiessen's rule in the normal state [4,5] and precision measurements of London penetration depth in the superconducting state [1-3,6]. Knowing the response to a controlled disorder, we can also analyze other properties in materials where natural "as-grown" disorder often determines the thermodynamic behavior and explains the large differences between clean (and nodal) stoichiometric compounds, such as AsP122 [2] and charge-doped (and nodeless) BaCo122 and BaK122 [3-6]. Finally, it is important to understand the role of scattering in the behavior of quantum phase transitions beneath the dome of superconductivity. The quantum critical point is found near optimal doping in AsP122 [2] and, surprisingly, in BaCo122 [6] where quantum phase transition not only exists but seems to be protected from scattering by the superconducting state revealing a novel aspect of the interplay of superconductivity and magnetism [6].

[1] R. Prozorov and V. G. G. Kogan, Rep. Prog. Phys. **74**, 124505 (2011).

[2] K. Hashimoto *et al.*, Science **336**, 1554 (2012).

[3] K. Cho *et al.*, Sci. Adv. **2**, 1600807 (2016).

[4] R. Prozorov *et al.*, Phys. Rev. X **4**, 41032 (2014).

[5] R. Prozorov *et al.*, npj Quan. Mater. **4**, 34 (2019).

[6] K. R. Joshi *et al.*, arXiv:1903.00053 (2019).

Keywords: iron-based superconductor, pair-breaking scattering, quantum phase transition, electron irradiation

## PC4-2-INV

### Zero-Energy Vortex Bound State in the Topological Superconductor Fe(Se,Te)

\*Tadashi Machida<sup>1</sup>, Yue Sun<sup>2</sup>, Sungseong Pyon<sup>3</sup>, Shyun Takeda<sup>4</sup>, Ching-Kai Chiu<sup>5</sup>, Yuhki Kohsaka<sup>1</sup>, Tetsuo Hanaguri<sup>1</sup>, Takao Sasagawa<sup>4</sup>, Tsuyoshi Tamegai<sup>3</sup>

RIKEN Center for Emergent Matter Science, Japan<sup>1</sup>

Department of Physics and Mathematics, Aoyama Gakuin University, Japan<sup>2</sup>

Department of Applied Physics, The University of Tokyo, Japan<sup>3</sup>

Laboratory for Materials and Science, Tokyo Institute of Technology, Japan<sup>4</sup>

Kavli Institute for Theoretical Sciences, University of Chinese Academy of Sciences, China<sup>5</sup>

A vortex core of a topological superconductor is an ideal platform of Majorana fermions. Although several experimental efforts have been made to detect Majorana fermions in the vortex cores as a zero-energy vortex bound state (ZVBS) [1,2], existence of the Majorana fermions is still controversial. Using a dilution-refrigerator scanning tunneling microscope [3], we have systematically examined a large number of vortices in the superconducting topological surface state of FeTe<sub>0.6</sub>Se<sub>0.4</sub>. We found that a certain number of vortices possess the ZVBS below 20  $\mu\text{eV}$  suggesting its Majorana bound-state origin, but others do not. Interestingly, emergence of the ZVBS is not related to the preexisting quenched disorders, and the fraction of vortices with the ZVBS decreases with increasing magnetic field [4]. Moreover, our time dependent measurements of tunneling spectra on a creeping vortex indicate that the ZVBS disappears after the creep (Fig. 1). These findings suggest that inter-vortex interaction plays an important role in the ZVBS formation [5].

[1] D. Wang *et al.*, *Science* **362**, 333 (2018)

[2] M. Chen *et al.*, *Nat. Commun.* **9**, 970 (2018)

[3] T. Machida *et al.*, *Rev. Sci. Instrum.* **89**, 093707 (2018)

[4] T. Machida *et al.*, *Nat. Mater.* **18**, 811 (2019)

[5] C.-K. Chiu *et al.*, arXiv:1904.13374 (2019)

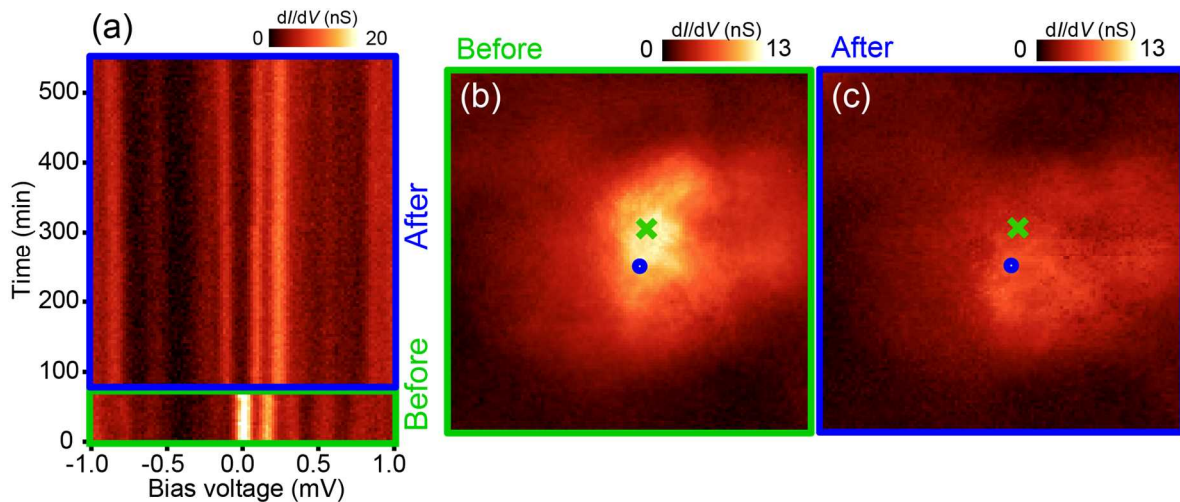


**Fig. 1:** (a) Time dependence of the tunneling spectra taken at a vortex core. (b) and (c) The zero bias conductance maps on 16 nm x 16 nm FOV before (b) and after (c) the vortex jump. Green cross and blue circle indicate the highest intensity points before and after the jump, respectively.

Keywords: Topological superconductor, Majorana fermion, Scanning tunneling microscope, Vortex

## PC4-3-INV

### Quantum critical transport phenomena in the nematic $\text{FeSe}_{1-x}\text{S}_x$

\*Matija Čulo<sup>1</sup>, S. Licciardello<sup>1</sup>, J. Ayres<sup>1</sup>, M. Berben<sup>1</sup>, Y.-T. Hsu<sup>1</sup>, S. Kasahara<sup>2</sup>, Y. Matsuda<sup>2</sup>, T. Shibauchi<sup>3</sup>, N. Maksimovic<sup>4</sup>, J. G. Analytis<sup>4</sup>, N. E. Hussey<sup>1</sup>

High Field Magnet Laboratory (HFML-EMFL) and Institute for Molecules and Materials, Radboud University, Toernooiveld 7, 6525 ED, Nijmegen, Netherlands<sup>1</sup>

Department of Physics, Kyoto University, Sakyo-ku, Kyoto 606-8502, Japan<sup>2</sup>

Department of Advanced Materials Science, University of Tokyo, Kashiwa, Chiba 277-8561, Japan<sup>3</sup>

Department of Physics, University of California and Materials Science Division, Lawrence Berkeley National Laboratory, Berkeley, California 94720, USA<sup>4</sup>

Many high-temperature superconductors in their normal state show marked deviations from Fermi liquid (FL) theory, the standard model of metals. The most prominent is the linear temperature dependence of resistivity believed to be related to the maximum (Planckian) dissipation allowed by quantum mechanics. Such behavior is often ascribed to the existence of a quantum critical point (QCP) located inside the superconducting dome in vicinity of which a coupling between critical fluctuations of an order parameter and low-energy quasi-particle excitations gives rise to novel non-FL physics. In a host of metallic systems that exhibit this so-called quantum critical behavior, evidence for electronic nematicity, a correlated electronic state with broken rotational symmetry, has been reported. In all cases, however, the nematicity is found to be intertwined with other forms of order, such as antiferromagnetism or charge density wave, that might themselves be responsible for the existence of the QCP. The iron-chalcogenide family  $\text{FeSe}_{1-x}\text{S}_x$  is unique in this respect since the superconductivity emerges from an electronic nematic state which exists in isolation and therefore provides a unique opportunity to study the influence of nematic fluctuations on high-temperature superconductivity. Substitution of Se with S effectively suppresses the nematic transition which is believed to terminate inside the superconducting dome at the QCP  $x = 0.16$ . In this talk, we report the results of our dc transport experiments – at both ambient and applied pressures – in magnetic field strengths strong enough to suppress the superconductivity and access the field-induced normal state and reveal classic signatures of quantum criticality: an enhancement in the coefficient of the  $T^2$  resistivity on approaching the QCP and, at the QCP itself, a strictly  $T$ -linear resistivity that extends over a decade in temperature. We also report a detailed study of the normal state transverse magnetoresistance in  $\text{FeSe}_{1-x}\text{S}_x$  across the nematic QCP that reveals unambiguously and for the first time, the coexistence of two charge sectors in a quantum critical system: one associated with the fermionic quasiparticles and possibly associated with the quantum critical excitations. Finally, we present our most recent Hall effect measurements performed on the same series of single-crystalline  $\text{FeSe}_{1-x}\text{S}_x$  samples which indicate that a conventional, multi-band model fails to capture the longitudinal and Hall resistivities self-consistently, suggesting that there exists a component in the Hall resistivity associated with the quantum critical sector.

Keywords: High temperature superconductivity, Quantum criticality, Electronic nematicity, Electrical transport

## PC4-4-INV

### Spin-orbit coupling and its influence on superconductivity in iron-based superconductors

Jianqing Guo<sup>1</sup>, Li Yue<sup>1</sup>, Kazuki Iida<sup>2</sup>, Kazuya Kamazawa<sup>2</sup>, Lei Chen<sup>1</sup>, Tingting Han<sup>1</sup>, Yan Zhang<sup>1</sup>, \*Yuan Li<sup>1</sup>

International Center for Quantum Materials, School of Physics, Peking University, Beijing 100871, China<sup>1</sup>

Neutron Science and Technology Center, Comprehensive Research Organization for Science and Society (CROSS), Tokai, Ibaraki 319-1106, Japan<sup>2</sup>

In this talk, I will present our inelastic neutron scattering efforts to determine low-energy spin excitations in a variety of iron-based superconductors, in which spin-orbit coupling leads to anisotropic response in spin space. To prepare the scientific context I will first introduce our earlier works on BaFe<sub>2</sub>As<sub>2</sub> and FeSe<sub>1-x</sub>S<sub>x</sub>, where regardless of whether long-range magnetic order is present, we show that the magnetic excitations at low temperatures are preferentially polarized along the *c*-axis [1,2]. In our most recent work on the tetragonal and *c*-axis oriented magnetic phase of Sr<sub>1-x</sub>Na<sub>x</sub>Fe<sub>2</sub>As<sub>2</sub>, we find the first spectroscopic evidence that the itinerant charge carriers actually "prefer" to be assisted by *c*-axis polarized magnetic excitations in their formation of superconducting Cooper pairs [3], namely, only the weak *c*-axis response exhibits a spin resonant mode in the superconducting state. Our results naturally explains why the superconductivity competes strongly with the tetragonal magnetic phase in Sr<sub>1-x</sub>Na<sub>x</sub>Fe<sub>2</sub>As<sub>2</sub>, and provide a fresh view on how to make a good superconductor out of a magnetic "Hund's metal".

#### References

- [1] C. Wang *et al.*, *Phys. Rev. X* **3**, 041036 (2013).
- [2] M. Ma *et al.*, *Phys. Rev. X* **7**, 021025 (2017).
- [3] J. Guo *et al.*, *Phys. Rev. Lett.* **122**, 017001 (2019).

Keywords: iron-based superconductors, neutron scattering, spin anisotropy, strongly correlated electron systems



## PC4-5

### Infrared Spectroscopic Studies of the Phonon Dynamics in Iron-based Superconductors

\*Xianggang Qiu<sup>1</sup>, Run Yang<sup>1</sup>, Bing Xu<sup>1</sup>

Institute of Physics, Chinese Academy of Sciences<sup>1</sup>

The temperature dependence optical reflectivity has been measurement on iron-based superconductors of different families. The optical conductivity has been obtained by using the two-Drude component model. It has been found that the phonons show red- or blue-shift in different samples. Interestingly, the phonon conductivity exhibits a Fano lineshape, suggesting possible coupling between phonon and electrons or spin. Based on the temperature evolution of the lineshape and peak shift, we discuss the possible role played by electron-phonon and spin fluctuation in the occurrence of superconductivity in iron-based superconductors.

Keywords: Infrared spectroscopy, iron-based superconductor, electron-phonon coupling

## **PC5-1-INV**

### **Orbitals and Nematicity in La-1111 Single Crystals**

\*Bernd Büchner<sup>1</sup>

IFW Dresden and University Dresden, Germany<sup>1</sup>

While there is broad consensus that superconductivity in Fe based superconductors is due to an unconventional, most likely electronic pairing, many important aspects of the normal and superconducting state are still unexplored. In particular, the role of orbital degrees of freedom for the normal state electronic properties, nematicity, and pairing is discussed very controversial. In my talk I will present results on a series of large La-1111 single crystals which have been grown for the first time using a method based on anomalous solid state reaction. We have reexamined the phase diagram and studied magnetism and nematic order by means of NMR and strain dependent transport measurements. The possible formation of polaron-like structures will be discussed and evidence for an unusual state with suppressed long range order and soft nematic fluctuations will be presented.

## PC5-2-INV

### Composition - Temperature Phase Diagram of Iron-Based Superconductors Tuned by Disorder

Marcin Konczykowski<sup>1</sup>, Takasada Shibauchi<sup>2</sup>, Yuta Mizukami<sup>2</sup>, Shigeru Kasahara<sup>3</sup>, Yuji Matsuda<sup>3</sup>

Laboratoire des Solides Irradiés, CNRS, Ecole Polytechnique, 91128 Palaiseau, France<sup>1</sup>

Department of Advanced Materials Science, University of Tokyo, Japan<sup>2</sup>

Department of Physics, Kyoto University, Kyoto, Japan<sup>3</sup>

Two phase transition lines forming composition – temperature phase diagram of iron-based superconductors (IBS): antiferromagnetic Spin Density Wave (SDW) and superconducting (SC) can be tuned in large extent by controlled disorder. I will present measurements of magnetization and electronic transport of  $\text{Ba}(\text{FeAs}_{1-x}\text{Px})_2$  crystals, modified by point disorder induced by low temperature electron irradiation or by correlated disorder produced by swift heavy ions. Strong depression of SDW transition by both types of disorders is consistent with itinerant magnetism of IBS. SDW transition of Lifshitz type preserves its character even in strongly disordered material. Depression of superconducting transition temperature  $T_c$  by point disorder is proportional to the dose and reaches values below 1/3 of initial  $T_c$  without saturation. In contrast, increase of normal state resistivity induced by columnar defects has almost no effect on  $T_c$ . It is consistent with absence of pair-braking effect of intraband scattering channel prevailing for this type of disorder. The region of particular interest is that of slightly underdoped materials where magnetic and superconducting orders co-exist. The sequence of transitions (in the function of temperature on cooling) from normal, paramagnetic to antiferromagnetic and finally to superconducting state can be modified by disorder to direct transition from paramagnetic metal to superconductor. Extension of the SDW transition line can be traced inside of the superconducting dome by abrupt change of the critical current. This transition line follows the evolution with irradiation dose of SDW phase of the ground state and disappears at sufficiently high disorder. This confirms disorder induced downward shift in composition of putative Quantum Critical Point [1].

[1] Yuta Mizukami, *et al.* Journal of the Physical Society of Japan, 86, 083706 (2017)

Keywords: phase diagram, disorder

## PC5-3-INV

### Probing the superconducting gap structure of iron-based superconductors by angle-resolved specific heat measurements

\*Yue Sun<sup>1</sup>, Shunichiro Kittaka<sup>2</sup>, Toshiro Sakakibara<sup>2</sup>, Kazushige Machida<sup>3</sup>, Tsuyoshi Tamegai<sup>4</sup>

Department of Physics and Mathematics, Aoyama Gakuin University, Japan<sup>1</sup>

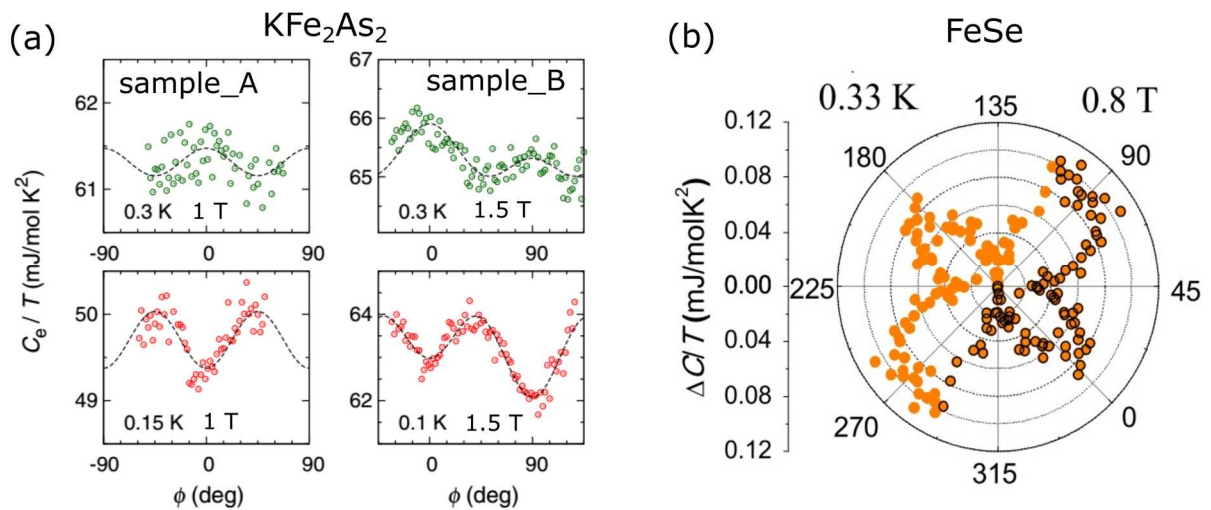
Institute for Solid State Physics (ISSP), The University of Tokyo, Japan<sup>2</sup>

Department of Physics, Ritsumeikan University, Japan<sup>3</sup>

Department of Applied Physics, The University of Tokyo, Japan<sup>4</sup>

Superconducting (SC) gap structures are intimately related to the pairing mechanism, which is pivotal for high temperature superconductors. This issue is also crucial for the iron-based superconductors (IBSs). SC gap structure of IBSs has already been confirmed not to be a conventional *s*-wave, but some of them may have large anisotropy or nodes. On the other hand, the 3D nature of the band structure of IBSs, with strong warping along the  $k_z$ -direction, suggests that a 3D space-resolved technique is required. The field angle-resolved specific heat (ARSH) measurement not only has the space-resolution, but also probes the quasi-particles in bulk, which is ideal for studying the SC gap structure of IBSs.

In this report, we will first introduce the principle and experimental details of the ARSH measurement system. Then, we will use two IBSs ( $\text{KFe}_2\text{As}_2$  and  $\text{FeSe}$ ) as examples to discuss the SC gap structure probed by ARSH measurements. For  $\text{KFe}_2\text{As}_2$ , a fourfold oscillation with minima in  $H \parallel [100]$  direction is observed in the electronic specific heat  $C_e$  as shown in Fig. (a), which indicates the presence of line nodes on the Fermi surface where the Fermi velocity is parallel to the  $[100]$  direction. In  $\text{FeSe}$ , ARSH measurements show a clear fourfold symmetric oscillation with sign change when the field rotates in the  $ab$ -plane (Fig. (b)), which indicates the existence of node or gap minimum. Such a symmetric oscillation is only observed under small fields and temperatures lower than 2 K, which suggests that it comes from the small gap. When the field is rotated out of the  $ab$ -plane, the oscillation symmetry gradually changes with increasing field, which confirms the node or minimum in the gap are in vertical line shape along the  $k_z$  direction.



## PC5-4-INV

### Unique defect structure and advantageous vortex pinning properties in $\text{CaKFe}_4\text{As}_4$

\*Shigeyuki Ishida<sup>1</sup>, Akira Iyo<sup>1</sup>, Hiraku Ogino<sup>1</sup>, Hiroshi Eisaki<sup>1</sup>, Nao Takeshita<sup>1</sup>, Kenji Kawashima<sup>1,2</sup>, Keiichi Yanagisawa<sup>3</sup>, Yuuga Kobayashi<sup>3</sup>, Koji Kimoto<sup>3</sup>, Hideki Abe<sup>3</sup>, Motoharu Imai<sup>3</sup>, Jun-ichi Shimoyama<sup>4</sup>, Michael Eisterer<sup>5</sup>

National Institute of Advanced Industrial Science and Technology<sup>1</sup>

IMRA Materials R&D Co., Ltd.<sup>2</sup>

National Institute for Materials Science<sup>3</sup>

Aoyama Gakuin University<sup>4</sup>

TU Wien<sup>5</sup>

The enhancement of critical current density ( $J_c$ ) is one of the key issues towards superconductivity applications. After the discovery of iron-based superconductors (IBSs), which are considered as candidate materials for high-field applications, high  $J_c$  values have been achieved by various techniques to introduce artificial pinning centers, while a further improvement of  $J_c$  is desired. Among various IBSs, 122 materials such as  $\text{Ba}_{1-x}\text{K}_x\text{Fe}_2\text{As}_2$  have been intensively studied owing to their small anisotropy. Meanwhile, recent studies demonstrated the high application potentiality of  $\text{CaKFe}_4\text{As}_4$  (CaK1144) [1-3]. Here, we report unprecedented vortex pinning properties in the CaK1144 system arising from the inherent defect structure. Scanning transmission electron microscopy (STEM) revealed the existence of nanoscale intergrowths of the  $\text{CaFe}_2\text{As}_2$  phase, which is unique to CaK1144 formed as a line compound. The  $J_c$  properties in CaK1144 are found to be distinct from other IBSs characterized by a significant anisotropy with respect to the magnetic field orientation as well as a novel pinning mechanism significantly enhanced with increasing temperature. We propose a comprehensive explanation of the  $J_c$  properties based on the unique intergrowths acting as pinning centers.

[1] S. J. Singh, *et al.* Phys. Rev. Mater. 2, 074802 (2018).

[2] S. Pyon, *et al.* Phys. Rev. B 99, 104506 (2019).

[3] S. Ishida, *et al.* npj Quantum Materials, 4, 27 (2019).

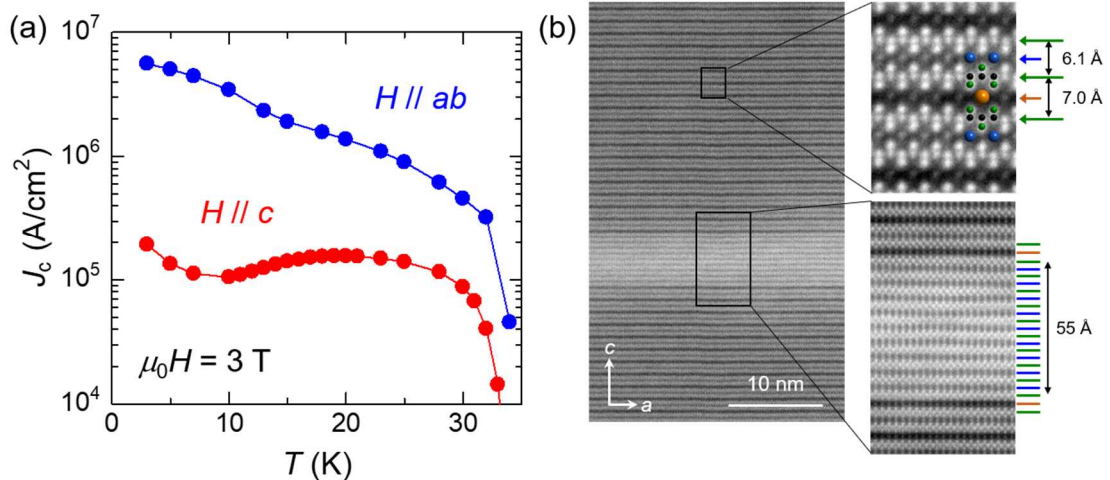


Fig. (a) Temperature dependence of  $J_c$  of CaK1144 single crystal under 3 T for  $H // c$  (red) and  $ab$  (blue), (b) STEM images around CaK1144 matrix and Ca122 intergrowth.

Keywords: Iron-based superconductors,  $\text{CaKFe}_4\text{As}_4$ , Critical current density, Defect structure

## PC5-5

### Critical Current Density and Its Enhancement by Particle Irradiation in $\text{KCa}_2\text{Fe}_4\text{As}_4\text{F}_2$

\*Tsuyoshi Tamegai<sup>1</sup>, Sunseng Pyon<sup>1</sup>, Yuto Kobayashi<sup>1</sup>, Teng Wang<sup>2</sup>, Gang Mu<sup>2</sup>, Satoru Okayasu<sup>3</sup>, Ataru Ichinose<sup>4</sup>

Department of Applied Physics, The University of Tokyo<sup>1</sup>

Shanghai Institute of Microsystem and Information Technology, Chinese Academy of Sciences<sup>2</sup>

Japan Atomic Energy Agency, Advanced Science Research Center<sup>3</sup>

Central Research Institute of Electric Power Industry, Electric Power Engineering Research Laboratory<sup>4</sup>

$\text{KCa}_2\text{Fe}_4\text{As}_4\text{F}_2$  is a new iron-based superconductor (IBS) with  $T_c \sim 33$  K having a layered structure, where  $\text{Fe}_2\text{As}_2$  double layer in  $\text{KFe}_2\text{As}_2$  is sandwiched by  $\text{Ca}_2\text{F}_2$  layers. This is another stoichiometric IBS similar to  $\text{CaKFe}_4\text{As}_4$ , where we have reported a very large critical current density ( $J_c$ ) due to the presence of novel layered defects parallel to the  $ab$ -plane [1]. In the present study, we have grown high-quality single crystals of  $\text{KCa}_2\text{Fe}_4\text{As}_4\text{F}_2$  and characterized  $J_c$  properties including its anisotropy and homogeneity.

Single crystals of  $\text{KCa}_2\text{Fe}_4\text{As}_4\text{F}_2$  are grown by the flux method.  $J_c$  as functions of magnetic field ( $H//c$ -axis) at temperatures between 2 K and 30 K are shown in Fig. 1. The self-field  $J_c$  at 2 K reaches  $\sim 8$  MA/cm<sup>2</sup>, which is larger than any other IBSs. However, unlike the case of  $\text{CaKFe}_4\text{As}_4$ , no defect structures are found by TEM observations. Magneto-optical imaging shows that shielding currents flow rather homogeneously throughout the crystal. For  $H//ab$ , the average  $J_c$  is much smaller than that for  $H//c$ -axis, probably due to the large anisotropy of this material. Effects of particle irradiation on the enhancement of  $J_c$  will also be reported.

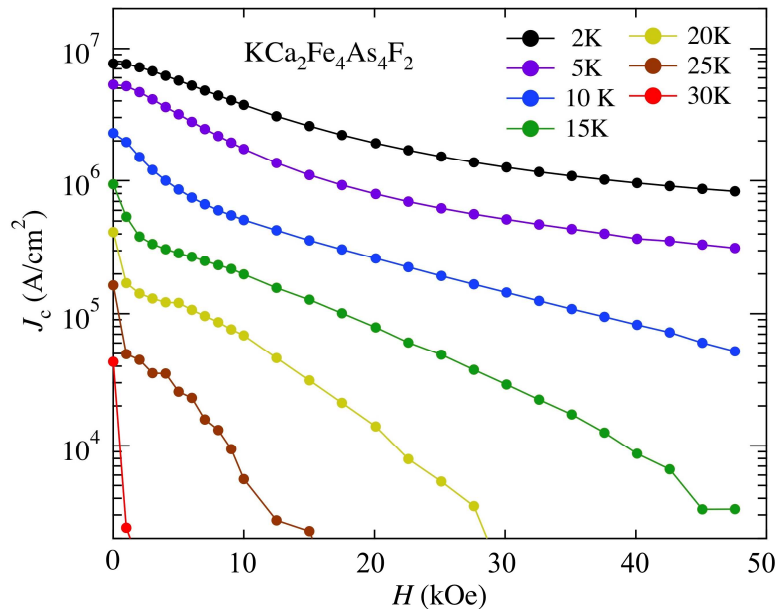


Fig. 1 Magnetic field ( $H//c$ ) dependence of  $J_c$  in  $\text{KCa}_2\text{Fe}_4\text{As}_4\text{F}_2$  at various temperatures.

[1] S. Pyon *et al.*, Phys. Rev. B **99**, 104506 (2019).

Keywords:  $\text{KCa}_2\text{Fe}_4\text{As}_4\text{F}_2$ , critical current density, irradiation effect, anisotropy

## PC6-1-INV

### Pseudogap and Superconductivity in Cuprate Superconductors Solved by *Ab initio* and Machine Learning Studies

\*Masatoshi Imada<sup>1,2</sup>

Toyota Physical and Chemical Research Institute<sup>1</sup>

Waseda Research Institute for Science and Engineering, Waseda University<sup>2</sup>

We first summarize how the *d*-wave superconducting and stripe states are severely competing in the simple Hubbard models, which is elucidated by using combined variational Monte Carlo, tensor network and Lanczos methods [1,2]. The result is not consistent with the experimental indications. On the other hand, *ab initio* Hamiltonian of carrier doped cuprates recently derived without any adjustable parameters [3,4] well reproduces the experimental phase diagram.

We next discuss renewed understanding of the superconducting mechanism. An experimental long-standing puzzle was the featureless structure in the spectral function indicated by the angle resolved photoemission spectroscopy (ARPES) spectra, in contrast to the case of conventional strong-coupling BCS superconductors in the history. We discuss how the puzzle has been solved with the help of quantum-cluster dynamical mean-field studies of the Hubbard model [5,6] and a completely independent machine learning studies purely based on the ARPES data [7]. An emergent dark fermion theory is discussed in detail [8].

This series of work has been done in collaboration with S. Sakai, M. Civelli, K. Ido, T. Ohgoe, A.S. Darmawan, Y. Nomura, Y. Yamaji, M. Hirayama, T. Misawa, and T. J. Suzuki.

- [1] Kota Ido, Takahiro Ohgoe, and Masatoshi Imada, *Phys. Rev. B* **97** 045138 (2018).
- [2] Andrew S. Darmawan, Yusuke Nomura, Youhei Yamaji, and Masatoshi Imada, *Phys. Rev. B* **98**, 205132 (2018).
- [3] Motoaki Hirayama, Youhei Yamaji, Takahiro Misawa, and Masatoshi Imada, *Phys. Rev. B* **98** 134501 (2018).
- [4] Motoaki Hirayama, Takahiro Misawa, Takahiro Ohgoe, Youhei Yamaji, and Masatoshi Imada, *Phys. Rev. B* **99**, 245155 (2019).
- [5] Takahiro Ohgoe, Motoaki Hirayama, Takahiro Misawa, Kota Ido, Youhei Yamaji, Masatoshi Imada, arXiv:1902.00122
- [6] Shiro Sakai, Marcello Civelli, Masatoshi Imada, *Phys. Rev. Lett.* **116**, 057003 (2016).
- [7] Shiro Sakai, Marcello Civelli, and Masatoshi Imada, *Phys. Rev. B* **94**, 115130 (2016).
- [8] Youhei Yamaji, Teppei Yoshida, Atsushi Fujimori, Masatoshi Imada, arXiv: 1903.08060.
- [9] Masatoshi Imada and Takafumi J. Suzuki, *J. Phys. Soc. Jpn.* **88**, 024701 (2019).

Keywords: Cuprate superconductors, Pseudogap, First principles calculation, Superconducting mechanism

## PC6-2-INV

### Exotic electronic properties revealed in a clean CuO<sub>2</sub> sheet of multilayered high-*T<sub>c</sub>* superconductor

\*Takeshi Kondo<sup>1</sup>

Institute for Solid State Physics, The University of Tokyo, Japan<sup>1</sup>

The  $T_c$  value in cuprates is sensitive to the number of CuO<sub>2</sub> layers per unit cell, and it is maximized in triple-layer systems. Significantly, the cuprates are categorized into two kinds according to the chemical situation of CuO<sub>2</sub> layers in crystal. One is single- and double-layer systems, where the CuO<sub>2</sub> plane is adjacent to the dopant layer, which possesses random atomic vacancies, thus generally causes spatially inhomogeneous state in the underlying conduction sheet. The situation is changed in the triple and more layered systems (the second category), where inner CuO<sub>2</sub> planes are sandwiched by outer CuO<sub>2</sub> planes, thus protected from the outermost dopant layers. The cleanness in CuO<sub>2</sub> plane seems to get improved with increasing the number of CuO<sub>2</sub> plane per unit cell. In this study, we have particularly selected a five-layered system with lightly doped inner CuO<sub>2</sub> planes, which are ideally flat and homogeneously hole-doped, thus provide an excellent platform to unveil inhere properties of the lightly doped electronic state in cuprates. The investigation of this compound is especially significant since the electronic properties would share those of triple-layer systems, which commonly have the highest  $T_c$  in homologous series of cuprate families. I will present recent results of multilayered cuprates investigated by laser-based angle-resolved photoemission spectroscopy (laser-ARPES) with high energy and momentum resolutions.



## PC6-3-INV

### Visualizing the Cuprate Pair Density Wave State

\*Kazuhiro Fujita<sup>1</sup>, Zengyi Du<sup>1</sup>, Hui Li<sup>1,2</sup>, Sanghyun Joo<sup>1,3,4</sup>, Elizabeth P. Donoway<sup>1</sup>, Jinho Lee<sup>3,4</sup>, J. C. Davis<sup>5,6</sup>, Ganda D. Gu<sup>1</sup>, Peter D. Johnson<sup>1</sup>

Brookhaven National Laboratory<sup>1</sup>  
Stony Brook University<sup>2</sup>  
Seoul National University<sup>3</sup>  
Institute for Basic Science<sup>4</sup>  
University College Cork<sup>5</sup>  
University of Oxford<sup>6</sup>

When Cooper pairs are formed with finite center-of-mass momentum, the defining characteristic [1,2] is a spatially modulating superconducting energy gap  $D(\mathbf{r})$ . Recently, this concept has been generalized to the pair density wave (PDW) state predicted to exist in a variety of strongly correlated electronic materials such as the cuprates [3,4]. It is also the fact that a possible presence of a cuprate PDW state emerges from recent experimental studies. An example of the observed signature is a spatial modulation of the Josephson current detected in Cooper-pair tunneling that is established by Scanned Josephson Tunneling Microscopy [5]. Another indication is obtained by a simultaneous imaging of the local-density-of-states  $N(\mathbf{r}, E)$  that reveals electronic modulations with wavevectors  $\mathbf{Q}=(1/8,0);(0,1/8)$  and  $2\mathbf{Q}=(1/4,0);(0,1/4)$  inside a vortex core when a high magnetic field is applied [6]. These signatures are indeed anticipated when the PDW coexists with homogeneous superconductivity. In this talk, I will present the recent development of the cuprate PDW studies as stated above and discuss a possible role of the PDW in the cuprate.

- [1], P. Flude, and R. A. Ferrel, *Phys. Rev.***135**, A550 (1965).
- [2], A. I. Larkin, and Yu. N. Ovchinnikov, *Sov. Phys. JETP***20**, 762 (1965).
- [3], E. Fradkin, S. A. Kivelson, J. M. Tranquada, *Rev. Mod. Phys.* **87**, 457 (2015).
- [4], D. F. Agterberg, *et al.*, Preprint at <https://arxiv.org/abs/1904.09687> (2019).
- [5], M. H. Hamidian, *et al.*, *Nature* **532**, 343-347 (2016).
- [6], S. D. Edkins, *et al.*, *Science* **364**, 976-980 (2019).

Keywords: Cuprates, Pair Density Wave

## PC7-1-INV

### ARPES study of high-temperature cuprate superconductor Bi2212 across critical dopings

\*Makoto Hashimoto<sup>1</sup>

SLAC National Accelerator Laboratory<sup>1</sup>

In the hole-doped cuprate high-temperature superconductors, the special doping  $p = 0.19$  with various anomalies has attracted considerable research interest, with close connection to the pseudogap and strange metal [1]. In this talk, we present systematic angle-resolved photoemission (ARPES) studies across  $p = 0.19$  in Bi2212. The results provide important insights into the nature of this special doping and the phenomenology of the cuprates [2, 3]. Further, we plan to discuss significant superconducting fluctuations on a single coherent, hole-like Fermi surface in heavily overdoped regime [4].

- [1] M. Hashimoto, *et al.*, Nature Phys. **10**, 483–495 (2014).
- [2] Y. He\*, M. Hashimoto\*, *et al.*, Science **362**, 62 (2018).
- [3] S. Chen\*, M. Hashimoto\*, *et al.*, submitted.
- [4] Y. He\*, *et al.*, in preparation.

Keywords: cuprate, ARPES, pseudogap, strange metal

## PC7-2-INV

### Superconductivity in a unique type of copper oxides

\*C. Q. Jin<sup>1</sup>

Institute of Physics, Chinese Academy of Sciences<sup>1</sup>

The mechanism of superconductivity of cuprates remains one of the biggest challenges in condensed matter physics. High-T<sub>c</sub> cuprates crystallize into layered perovskite structure featured with copper-oxygen octahedral coordination. Due to the strong Jahn Teller effect plus Coulomb interactions the octahedron in high T<sub>c</sub> cuprates is elongated, placing the 3d<sub>x<sup>2</sup>-y<sup>2</sup></sub> orbital level at top, almost degenerate with the O2p orbital, wherein the doped holes reside. This situation is considered to be unique of the cuprates that sustains d-wave pairing symmetry and high T<sub>c</sub>.

Here we present the high pressure synthesis of Ba<sub>2</sub>CuO<sub>4-y</sub> superconductor. Interestingly the cuprate possesses extraordinarily compressed octahedron along the *c*-axis direction. In the compressed octahedron the 3d<sub>z<sup>2</sup></sub> orbital level would be lifted above 3d<sub>x<sup>2</sup>-y<sup>2</sup></sub> orbital level. The compound shows bulk superconductivity with critical temperature (T<sub>c</sub>) above 70 K confirmed by Meissner effect,  $\mu$ SR measurements. The T<sub>c</sub> is more than 30 K higher than that for the isostructural hole doped La<sub>2</sub>CuO<sub>4</sub>. The present work sheds renewed light on comprehensive understanding of the pairing and T<sub>c</sub> determining mechanism of cuprate superconductors.

Acknowledgments: We thank all collaborators who contributed to the work.

[1] W. M. Li *et al.*, PNAS **116**, 12156(2019)

Keywords: Copper Oxide Superconductor, Compressed Local Coordination, Orbital Order

## PC7-3

### Electron-doping Effect and the Electronic State in the Undoped (Ce-free) Superconductor $T'-La_{1.8}Eu_{0.2}CuO_{4-\delta}$

\*Toshiki Sunohara<sup>1</sup>, Takayuki Kawamata<sup>1</sup>, Kota Shiosaka<sup>1</sup>, Tomohisa Takamatsu<sup>1</sup>, Takashi Noji<sup>1</sup>, Masatsune Kato<sup>1</sup>, Yoji Koike<sup>1</sup>

Department of Applied Physics, Graduate School of Engineering, Tohoku University, Japan<sup>1</sup>

In undoped (Ce-free)  $RE_2CuO_4$  ( $RE =$  rare earth) with the  $Nd_2CuO_4$ -type ( $T'$ -type) structure, the superconductivity has been observed without carrier doping by removing excess oxygen [1]. To clarify the electronic states of the undoped superconductor, it is necessary to investigate the doped carrier-concentration dependence of  $T_c$  in  $RE_2CuO_4$  with a single kind of blocking layer. It has been reported so far that  $T_c$  decreases through the hole doping in Sr- and Ca-substituted  $T'-La_{1.8}Eu_{0.2}CuO_{4-\delta}$  ( $T'$ -LECO) [2, 3]. Accordingly, we have synthesized samples of  $T'-La_{1.8}Eu_{0.2}CuO_{4-y}F_y$  ( $T'$ -LECOF) and investigated the electron-doping effect on  $T_c$ .

$T'$ -LECOF samples were obtained by the fluorination of  $T'$ -LECO samples prepared by the low-temperature synthesis method [4] using  $NH_4F$ . Superconducting samples of  $T'$ -LECOF were obtained by the reduction annealing in vacuum. From the powder X-ray diffraction and EPMA measurements, it has been found that the obtained samples are confirmed to be of the single phase and that the content of F is confirmed to be almost the same as the nominal one. The magnetic susceptibility measurements have revealed that  $T_c$  increases with increasing  $y$ , exhibits the maximum value of  $\sim 23K$  at  $y = 0.025$  and decreases. The dome-like dependence of  $T_c$  on the doped carrier concentration shown in the figure is explained in terms of the pairing mediated by spin fluctuations based on the  $d-p$  model calculation [5].

[1] O. Matsumoto *et al.*, Phys. Rev. B **79**, 100508(R) (2009).

[2] T. Takamatsu *et al.*, Appl. Phys. Express **5**, 073101 (2012).

[3] T. Takamatsu *et al.*, Phys. Procedia **58**, 46 (2014).

[4] T. Takamatsu *et al.*, Physica C **471**, 679 (2011).

[5] K. Yamazaki *et al.*, J. Phys: Conf. Ser. **871**, 012009 (2017).

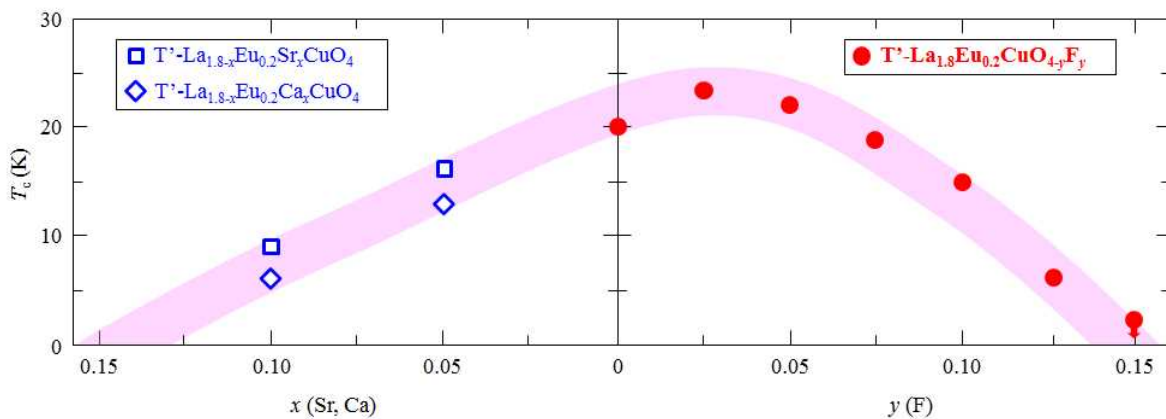


Fig. Dependence of  $T_c$  on the doped carrier concentration for  $T'-La_{1.8-x}Eu_{0.2}M_xCuO_{4-y}F_y$  ( $-M = Sr, Ca$ ).

Keywords: Undoped superconductor, Cuprate, Low-temperature synthesis, Strongly correlated electron system

## PC7-4

### Rectification by Superconducting Diodes Made of REBCO Films

\*Yuji Tsuchiya<sup>1</sup>, Keisuke Suzuki<sup>1</sup>, Tomohide Hori<sup>1</sup>, Yusuke Ichino<sup>1</sup>, Yutaka Yoshida<sup>1</sup>

Nagoya University<sup>1</sup>

A superconducting diode with an asymmetric  $I_c$  has been proposed as a novel rectifying element operating at cryogenic conditions [1]. It has an opposite current-voltage properties compared with the semiconductor diode. In the cryogenic applications, the superconducting diode has a potential to be used as an efficient rectifiers or current limiters. In our previous study, we fabricated the tailored REBCO films to achieve a large rectification rate and developed an prototype element made of the REBCO film [2]. In this study, the rectification properties of the superconducting diodes were investigated at various magnetic fields and temperatures in order to optimize the operating conditions.

BaHfO<sub>3</sub>-doped SmBa<sub>2</sub>Cu<sub>3</sub>O<sub>y</sub> films were fabricated on LaAlO<sub>3</sub> substrates with a thicknesses of 1000 nm using a pulsed laser deposition method. The films were processed into micro bridges with a width of 100  $\mu$ m. Current-voltage characteristics including the reverse current were measured at 0-9 T and 40-90 K by the four-probe method. An asymmetry  $Asym.$  was defined as a ratio between a differential and an average amplitude of  $I_c$  for the different current direction.

Figure 1(a) shows  $I$ - $V$  characteristics in the REBCO film at 65 K and 0.3 T along the in-plane direction. It is apparent that the  $I_c$  is about twice as different depending on the current direction.  $Asym.$  was plotted for the temperature and the magnetic field as shown in Fig. 1(b). The optimal temperature for the  $Asym.$  was about 65 K which corresponds to the temperature of the sub-cooled liquid nitrogen. Therefore, we conclude that the superconducting diode made of the REBCO film is expected to be used in the liquid nitrogen. On site, we will discuss an origin of the asymmetric  $I_c$  to optimize the diode with the larger rectification rate.

This research was partly supported by JST-ALCA, JST-A-STEP, KAKENHI (19K22154), REFEC, and NU-AIST alliance project.

[1] X. Jiang et al., Phys. Rev. B 49, 9244 (1994).

[2] Y. Tsuchiya *et al.*: Abstracts of ISS conference (2018).

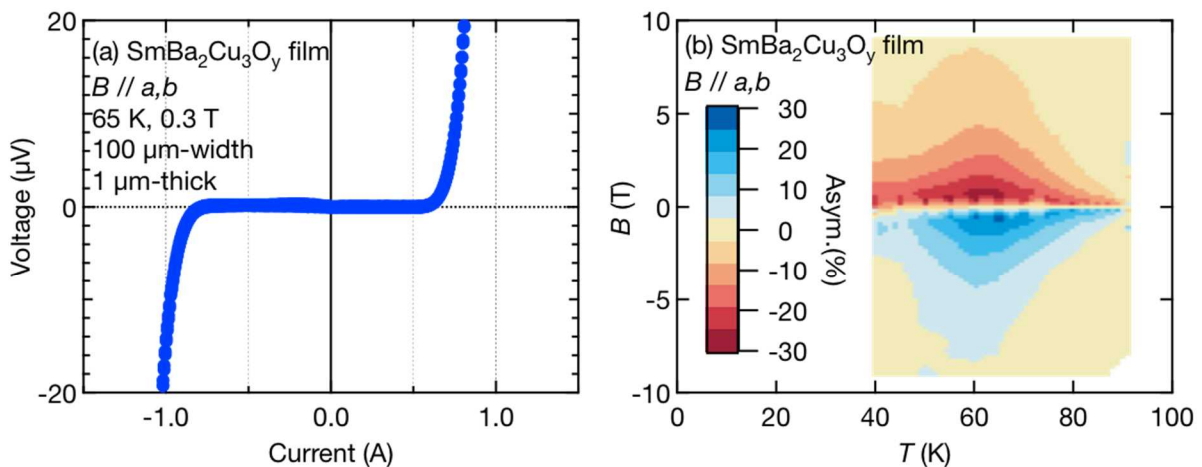


Fig. 1 (a) Asymmetric current-voltage characteristics in SmBa<sub>2</sub>Cu<sub>3</sub>O<sub>y</sub> films at 65 K and 0.3 T. (b) Temperature and field mapping of the asymmetry of the critical current.

Keywords: REBCO film, Superconducting diode, Critical current

## PCP1-1

### Spatiotemporal Dynamics of Driven Josephson Junction Networks

\*Takaaki Kawaguchi<sup>1</sup>

Department of Physics, Toho University, Japan<sup>1</sup>

Spatiotemporal dynamics of phases in Josephson junction networks (JJNs) is studied using a computer simulation based on a phase model which is related to the resistively shunted junction model. We consider JJNs which consist of a two-dimensional array of superconducting grains where each pair of the nearest-neighbor sites is connected by a Josephson junction. The JJNs are driven by external currents with spatiotemporal modulation. We investigate the current-voltage characteristics of the driven JJNs for some types of the spatiotemporal modulation of external currents. The dynamics of JJNs shows complicated behaviors in the current-voltage characteristics. There exist a sort of collective phenomena in the dynamics of JJNs under certain conditions on some controllable parameters of the present system. The collective dynamics is affected significantly by the spatiotemporal modulation of external currents. We clarify the novel collective effects on the dynamics of JJNs.

Keywords: Josephson Junction Network

## PCP1-2

### Vortex lattice melting transition : Effects of artificial nanorods

\*Takashi Kusafuka<sup>1</sup>, Masaru Kato<sup>1</sup>, Osamu Sato<sup>1,2</sup>

Osaka Pref. Univ.<sup>1</sup>

Osaka Pref. Univ. Col. Tech.<sup>2</sup>

It is known that vortices in a mesoscopic superconductor show peculiar structures, which depend on the shape of the superconductor. Ooi et al [1] found that melting transition temperatures of vortex lattices in a square superconducting plate become maximum when the vortex number is a square number. Then using the molecular dynamics method (MD), Kato and Kitago [2] investigated the vortex lattice melting transition in a pure superconductor. They showed standard deviation of vortex position increases rapidly with increasing temperature.

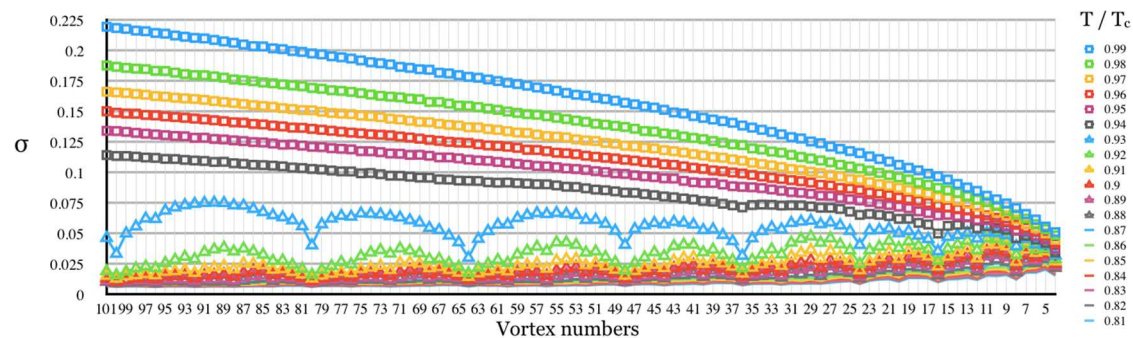
We investigated this melting of vortex lattice in a dirty square mesoscopic superconductor, using MD. We found when the vortex number is a multiple of 4, the vortex lattice becomes rather stable. [Fig.1: The standard deviations of 4 to 101 vortices in the square superconducting plate including 100 impurities as a function of the number of vortices.] So we consider other shape superconductors because of stable vortex state in the superconducting plate.

It is known that the superconducting properties are improved by adding nanorods to superconductor [3]. We investigate the melting transition of the vortex lattice in a square superconductor with nanorods, or nanorods array.

[1] S. Ooi, T. Mochiku, M. Tachiki, and K. Hirata PRL 114, 097001 (2015)

[2] M. Kato, H. Kitago, J. Phys. Conf. Ser. 871, 012028 (2017)

[3] J. L. MacManus-Driscoll et al., Nat. Mater. 3, 439 (2004)



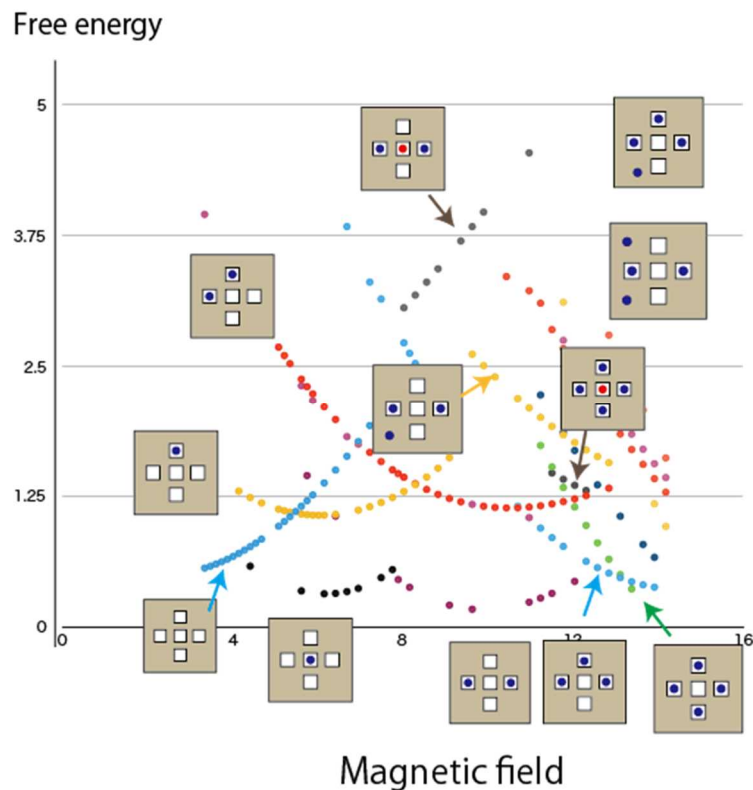
## PCP1-3

### Peculiar vortex states in mesoscopic superconductors with antidots

\*Osamu Sato<sup>1</sup>, Masaru Kato<sup>2</sup>

Osaka Prefecture University College of Technology<sup>1</sup>  
Osaka Prefecture University<sup>2</sup>

The vortex configurations in a mesoscopic superconducting square plate with antidots under uniform magnetic fields are obtained by solving the Ginzburg-Landau (GL) equation using the finite element method (FEM). In this study, dimensions of the samples are  $30\xi_0 \times 30\xi_0$ , where  $\xi_0$  is the coherence length at zero temperature, and the Ginzburg-Landau parameter and temperature set to  $\kappa=10$  and  $T=0.8T_c$  where  $T_c$  is the superconducting transition temperature. The sample has 5 antidots, one is located at the center of the sample, and the other four antidots are located away from the center point in the directions parallel to the four sides of the square sample. Generally, the GL equation has not only the most stable state solution but also metastable state solutions. In the most stable states in each magnetic field, the number of vortices that pass through the sample  $n$  increases monotonically as increasing the field  $H$ . The most stable states where  $n=3$  is realized in very narrow field region, this is because the sample has four-fold rotational symmetry. It is predicted theoretically anti-vortex can appear in the most stable state near below transition temperature from the discussion of the symmetry. We found metastable states where anti-vortex appears in a certain magnetic field region even in rather low temperature condition.



Keywords: Ginzburg-Landau equation, mesoscopic superconductor, antidot, anti-vortex



## PCP1-4

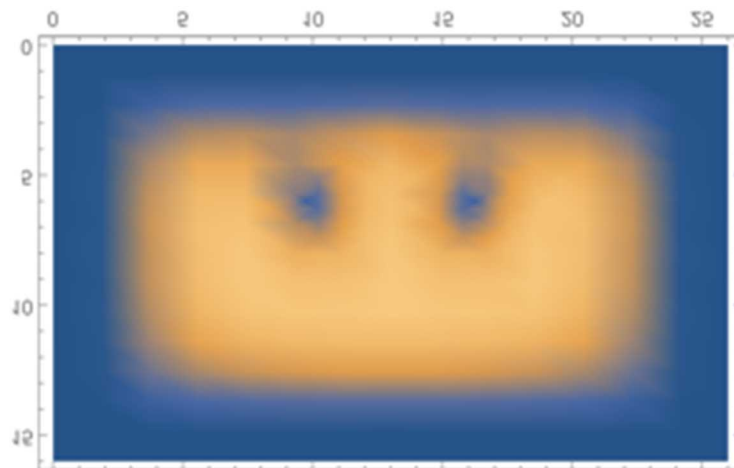
### Structures of vortices in a superconductor under spatially varying fields

\*Hayato Yokoji<sup>1</sup>, Masaru Kato<sup>1</sup>

Department of Physics and Electronics, Osaka Prefecture University, Japan<sup>1</sup>

We study behavior of vortices in a type II superconductor under spatially varying fields. Because in application of superconductors, such as an electromagnet, spatially varying fields appear. In previous study, we found directions of vortices are not parallel to the field in a chiral helimagnet /superconductor bilayer structure [1,2]. The origin of this behavior may come from interaction between vortices or screening current at edges of the superconductor.

In this study, we investigate structures of vortices in a superconductor under spatially varying fields by solving the Ginzburg-Landau equation, in order to clarify the origin of previous results. First, we obtain structures of vortices under a constant field tilted  $\pi/4$  from z-axis to investigate influences of edge currents [Fig.1]. In this case, vortices are parallel to the field, therefore, edges of the superconductor do not affect the vortex structures. We conclude previous results may come from interaction between two vortices that are not parallel. We will show structures of vortices under various fields.



[1] S.Fukui, M. Kato, Y. Togawa, *Supercond. Sci. Technol.*, **29**, 125008 (2016).

[2] S.Fukui, M. Kato, Y. Togawa, O. Sato, *J.Phys. Soc. Jpn.*, **87**, 084701 (2018).

Keywords: Vortex, Ginzburg-Landau Equation, Vortex-vortex interaction, Finite Element Method

## PCP1-5

### Transition temperature in a dirty mesoscopic superconductor: Transition from localized superconductivity to extended superconductivity

\*Masaru Kato<sup>1</sup>, Takayuki Tamai<sup>1</sup>

Department of Physics and Electronics, Osaka Prefecture University<sup>1</sup>

Transition temperature ( $T_c$ ) of a mesoscopic superconductor is enhanced [1]. This is because superconducting electrons are confined in a small space, an effective density of states is enhanced. This phenomenon is clearly appeared as gigantic enhancement of  $T_c$  in a dirty nano-size superconductor. (Fig.1) In this case, superconducting electrons are localized in a small region, and effective density of states is enhanced [2]. (Fig.2)

However, just below this transition temperature, superconductivity remains localized. If we defined true  $T_c$  as the temperature when zero resistivity occurs, true  $T_c$  is lower than the enhanced  $T_c$ . In order to find this true  $T_c$ , we must solve the full Bogoliubov-de Gennes (BdG) equations, instead of the linearized BdG equations [2].

In this study, we investigate how localized superconductivity in a dirty mesoscopic superconductor extend to whole superconductor, with decreasing the temperature. Also, we investigate how  $T_c$  depends on the size and structure of the superconductor.

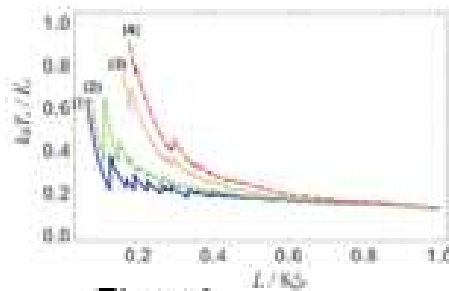


Figure 1

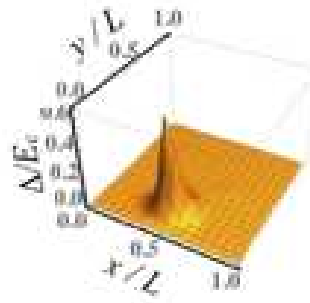


Figure 2

[1] M. Umeda and M. Kato, Physica C, 560 (2019) 45.

[2] M. Umeda and M. Kato, J. Appl. Phys., to be appeared.

Keywords: Transition temperature, Dirty mesoscopic superconductor, Bogoliubov-de Gennes equations, Localization

## PCP1-6

### **Magneto-optical imaging of field profile on niobium surface with microstructures of niobium hydrides and a single grain boundary**

\*Shuuichi Ooi<sup>1</sup>, Minoru Tachiki<sup>1</sup>, Akihiro Kikuchi<sup>1</sup>, Shunichi Arisawa<sup>1</sup>, Taro Konomi<sup>2</sup>, Eiji Kako<sup>2</sup>, Hiroshi Sakai<sup>2</sup>, Kensei Umemori<sup>2</sup>

National Institute for Materials Science<sup>1</sup>  
High Energy Accelerator Research Organization<sup>2</sup>

Improvement of the quality factor (Q-factor) of superconducting radio-frequency (SRF) cavities, usually made from Nb, for the acceleration of charged particles is desired practically, because the energy consumption by the dissipation in SRF cavities leads to the increase of the cooling cost. Since the dissipation by a motion of vortex (quantized magnetic flux) cause a residual surface resistance even at very low temperatures ( $\sim 2$  K), removal of vortices from a SRF cavity may make Q-factor better. However, there remain small amount of vortices even in the cooling with a magnetic shield, because the expulsion of vortices from superconducting Nb is not perfect due to unintended pinning. Therefore, exploration of the origins of the pinning is important. To study what kind of defects or microstructures influence on the pinning of vortices, we have observed magnetic-field profiles by a magneto-optical imaging technique on a Nb surface with microstructures, formed by the precipitation of niobium hydrides during a cooling into cryogenic temperatures, and with a single grain boundary. In the presentation, experimental results indicating that the grain boundary works as a guide for the vortex motion in some conditions and the surface microstructures trap vortices considerably.

Keywords: vortex, Niobium, Grain boundary, Magneto-optical imaging

## PCP1-7

### Reversible-Irreversible Transition Induced by Increased Shear Amplitude and Vortex Density

\*Shun Maegochi<sup>1</sup>, Koichiro Ienaga<sup>1</sup>, Kiyoshi Miyagawa<sup>1</sup>, Shin-ichi Kaneko<sup>1</sup>, Satoshi Okuma<sup>1</sup>

Tokyo Institute of Technology Japan<sup>1</sup>

When a periodic ac shear is applied to many-particle assemblies with disordered configuration, the particles gradually self-organize to avoid future collisions and transform into an organized configuration. For a small shear amplitude  $d$ , the particles finally settle into a reversible state where all the particles return to their initial position after each shear cycle, while they reach an irreversible state for  $d$  larger than a threshold amplitude  $d_c$  [1]. Using periodically sheared vortices in amorphous  $\text{Mo}_x\text{Ge}_{1-x}$  films with random pinning, we have studied the critical behavior of the reversible-to-irreversible transition (RIT). From the time-dependent voltage generated by vortex motion, we have observed organization of vortex configuration called random organization [2,3]. The relaxation time for the system to reach the steady state, plotted against  $d$ , shows a power-law divergence at the threshold amplitude  $d_c$ , indicative of a nonequilibrium RIT. The critical exponent is in agreement with the value expected for an absorbing phase transition in the two-dimensional directed-percolation universality class [4,5]. In our previous experiments, RIT was induced by increasing  $d$  at a fixed vortex density  $n$ , that is, at a fixed magnetic field  $B$ . This situation is qualitatively equivalent or similar to the one where  $n$  (i.e.,  $B$ ) is increased at fixed  $d$ . However, it is not evident whether the same critical behavior of RIT is observed irrespective of the parameters ( $d$  or  $n$  [6]) used in the experiment. This is an important issue in examining the universality of RIT. We will present the data in favor of the notion.

[1] L. Corté *et al.*, Nat. Phys. **4**, 420 (2008); N. Mangan *et al.*, Phys. Rev. Lett. **100**, 187002 (2008).

[2] S. Okuma, Y. Tsugawa, and A. Motohashi, Phys. Rev. B **83**, 012503 (2011).

[3] M. Dobroka *et al.*, New J. Phys. **19**, 053023 (2017).

[4] S. Maegochi, K. Ienaga, S. Kaneko, and S. Okuma, preprint.

[5] H. Hinrichsen, Adv. Phys. **49**, 815 (2000).

[6] E. Tjhung and L. Berthier, Phys. Rev. Lett. **114**, 148301 (2015).

Keywords: Vortex, Nonequilibrium phenomenon

## **PCP1-9**

### **Observation of Flux States and Vortex Penetration in Perforated Square Loops of Superconducting Amorphous MoGe Films**

\*Nobuhito Kokubo<sup>1</sup>, Satoru Okayasu<sup>2</sup>, Tsutomu Nojima<sup>3</sup>

Department of Engineering Science, University of Electro-Communications, Chofu, Tokyo, 182-8585, Japan<sup>1</sup>

Advanced Science Research Center, Japan Atomic Energy Agency, Tokai, Ibaraki 319-1195, Japan<sup>2</sup>

Institute for Materials Research, Tohoku University, Sendai 980-8577, Japan<sup>3</sup>

We report the magnetic visualizations of flux states in perforated square loops of superconducting amorphous MoGe films cooled in magnetic fields. Scanning superconducting quantum interference device microscopy measurements clearly revealed how the magnetic field is distributed in the loops at different magnetic fields. We found various flux states with different configurations, including vortices trapped in between holes and/or sample edges. Counting the number of trapped vortices for each image, we found that the vortices are completely excluded from the loop when the applied field is below a threshold field. We also found that the threshold field depends not only on the sample size, but also the arrangements of holes. These findings are useful for trapping or eliminating vortices in square loops, which can be crucial elements for designing various devices for quantum information processing, memory, and metrology.

Keywords: Mesoscopic superconductors, Flux States, Scanning SQUID microscope

## PCP1-10

### Vortex penetration and expulsion in NbSe<sub>2</sub> mesoscopic superconductors detected by small tunnel junction method

\*Hikari Tomori<sup>1</sup>, Naoki Hoshi<sup>1</sup>, Dai Inoue<sup>1</sup>, Akinobu Kanda<sup>1</sup>

University of Tsukuba<sup>1</sup>

By using the mechanical exfoliation method developed in the graphene research, one can obtain exfoliated films with atomically flat and defect-free surfaces. Such high uniformity is advantageous for researches of physical phenomena that are easily hindered by defects or surface roughness. Here, we use exfoliated films of a layered superconductor to investigate vortices in mesoscopic superconductors.

To electrically detect vortex penetration, expulsion, and positional change in a mesoscopic superconductor, we attached a superconductor/insulator/normal metal (SIN) junction to the superconductor (small tunnel junction method). In this structure, the junction voltage under a small current is sensitive to the supercurrent underneath the junction, which is changed by the behavior of vortices. In this study, NbSe<sub>2</sub> is used as the layered superconductor, a cleaved film of MoS<sub>2</sub> is used as the tunnel barrier, and Cr/Au electrodes are used as the normal metal. In the sample fabrication, we first formed a stacked structure NbSe<sub>2</sub>/MoS<sub>2</sub>, and then a Cr/Au electrode was connected to the stacked structure to form a tunnel junction with area of about 1 mm<sup>2</sup>, and a current lead was directly connected to the NbSe<sub>2</sub> flake. Finally, the sample was etched into a rectangular shape with size of ~ 4 mm<sup>2</sup> by reactive ion etching.

In the magnetic field dependence of the voltage of the SIN junction under a constant small biasing current, for small and increasing magnetic fields, almost periodic voltage jumps were observed, corresponding to one-by-one single vortex penetration. On the other hand, highly irregular voltage jumps were observed in other magnetic field regions. In the presentation, we will discuss these experimental results and their interpretation in detail.

Keywords: Vortex, NbSe<sub>2</sub>

## PCP2-1

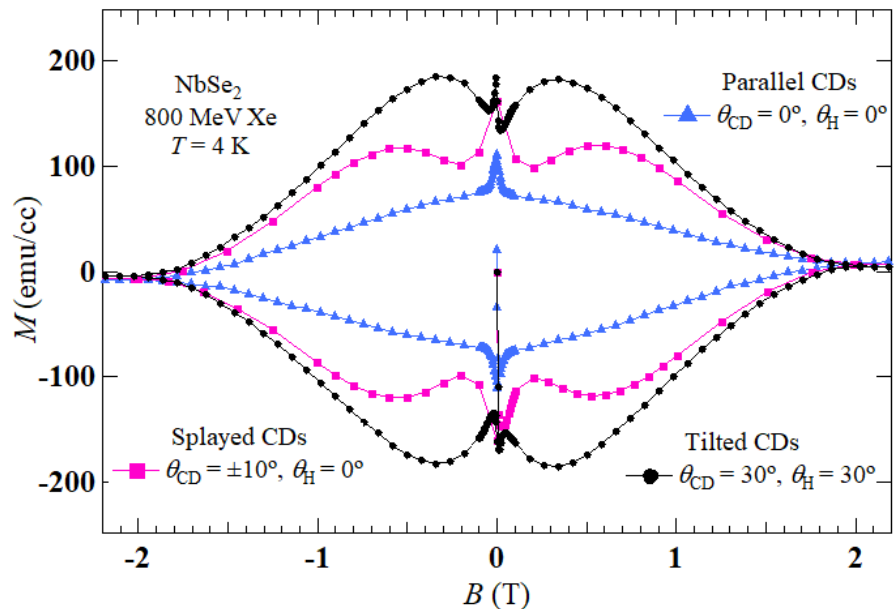
### Effects of 800 MeV Xe Irradiation on 2H-NbSe<sub>2</sub> Single Crystals

\*WENJIE LI<sup>1</sup>, Tsuyoshi Tamegai<sup>1</sup>, Sunseng Pyon<sup>1</sup>, Ayumu Takahashi<sup>1</sup>, Daisuke Miyawaki<sup>1</sup>, Yuto Kobayashi<sup>1</sup>, Ataru Ichinose<sup>2</sup>

Department of Applied Physics, The University of Tokyo, Bunkyo-ku, Tokyo 113-8656, Japan<sup>1</sup>  
Central Research Institute of Electric Power Industry, 2-6-1 Nagasaka, Yokosuka-shi, Kanagawa 240-0196, Japan<sup>2</sup>

Introduction of columnar defects in a clean single crystal of superconductor strongly enhances the critical current density ( $J_c$ ). This has been confirmed by many experiments [1,2] and explained by theoretical analyses. Several conditions of heavy-ion irradiation, such as the energy, density, and the incident direction of heavy ions strongly affect the structure of columnar defects and enhancement of  $J_c$ . An anomalous peak effect has been observed in iron-based superconductors at  $\sim 1/3$  of the dose equivalent matching field,  $B\Phi$ , when the columnar defects are introduced from two symmetric directions with respect to the  $c$ -axis at angles of  $\sim \pm 20^\circ$  [3]. Actually, a similar peak effect has been observed in YBa<sub>2</sub>Cu<sub>3</sub>O<sub>7</sub> with tilted columnar defects but with natural splay [1]. Despite these extensive research on iron-based superconductors and cuprate superconductors, there have been few studies on the effect of columnar defects in conventional superconductors. Recently, a peak effect has been observed in NbSe<sub>2</sub>, which is a canonical conventional layered superconductor, with tilted columnar defects [4]. To understand how the configuration of columnar defects affects the  $J_c$  in NbSe<sub>2</sub>, effects of 800 MeV Xe irradiation on NbSe<sub>2</sub> single crystals have been investigated. We introduced three kinds of columnar defects (parallel, tilted, and splayed columnar defects with respect to the  $c$ -axis) in NbSe<sub>2</sub> single crystals. Pronounced peak effects in M-H

loops have been observed in the case of samples introduced tilted or splayed columnar defects when the field is applied to the average direction of columnar defects (Fig. 1). It should be noticed that with a large matching field of  $B\Phi = 8$  T, the superconducting transition temperature hardly changes. We will discuss the origin of the anomalous peak effect in NbSe<sub>2</sub> with tilted or splayed columnar defects.



- [1] L. Civale et al., Phys. Rev. Lett. 67, 648 (1991).
- [2] T. Tamegai et al., Supercond. Sci. Technol. 25, 084008 (2012).
- [3] A. Park et al., Phys. Rev. B 97, 064516 (2018).
- [4] S. Eley et al., Sci. Rep. 8, 13162 (2018).

Keywords: NbSe<sub>2</sub>, columnar defects, peak effect

## PCP2-2

### Spectroscopy of exfoliated NbSe<sub>2</sub> thin films using NbSe<sub>2</sub>/MoS<sub>2</sub> superconductor-semiconductor heterostructures

Hikari Tomori<sup>1</sup>, \*Akinobu Kanda<sup>1</sup>

Department of Physics, University of Tsukuba, Japan<sup>1</sup>

Owing to the rapidly developing technology of mechanical exfoliation of layered materials and transfer/stacking of atomic layers, first developed in the graphene research, atomically thin superconducting transition metal dichalcogenide NbSe<sub>2</sub> has attracted much attention. Peculiar features such as superconductivity in high-quality monolayer with suppressed superconducting energy gap and two-band superconductivity have been reported.[1,2] In such measurements, so-called van der Waals tunnel junctions (stacked superconductor-semiconductor heterostructures) were used. However, it is known that reproducing the above results is quite difficult. Thus, here we focus on the transport property of such van der Waals superconductor-semiconductor heterostructures.

In our experiment, van der Waals NbSe<sub>2</sub>/MoS<sub>2</sub> heterojunctions were made in a glove box, and Ti/Au electrodes are connected to them to perform tunnel spectroscopy of NbSe<sub>2</sub>. We find that the superconducting energy gap of NbSe<sub>2</sub> derived from the tunnel conductance is generally smaller than the value expected from the BCS theory, and it strongly depends on the thickness of MoS<sub>2</sub> layers, indicating that the tunnel conductance does not correspond to the density of states of NbSe<sub>2</sub>. Origin of the disagreement will be discussed in the presentation.



## PCP2-3

### Intercalation of alkaline earth metals and rare-earth ions into 2H-NbSe<sub>2</sub>

\*Yukinori Yamaguchi<sup>1</sup>, T. Nishio<sup>1</sup>

Department of Physics, Tokyo University of Science, Japan<sup>1</sup>

The intercalation of alkali and alkaline earth metals with liquid ammonia or organic solvents into the FeSe superconductor results in a significant increase in the superconducting transition temperature ( $T_c$ ). [1,2] Although the mechanism of the increase of  $T_c$  has not been known, this study indicates that intercalation with liquid ammonia or organic solvents is a technique effective for increasing  $T_c$ . Meanwhile, transition metal dichalcogenide compounds (TMDC) are known to have the layered structure which resembles that of FeSe. In particular, 2H-NbSe<sub>2</sub>, one of TMDC, exhibits superconductivity below 7 K [3] and can be a material suitable for the intercalation. In this study, we report on the synthesis of  $(\text{NH}_3)_y\text{A}_x\text{NbSe}_2$ , where A is an alkaline earth metal element or Yb ( $x$  is a nominal value), by intercalating alkaline earth metals into NbSe<sub>2</sub> with liquid ammonia as a solvent. We also present the synthesis of  $(\text{C}_2\text{H}_8\text{N}_2)_y\text{A}_x\text{NbSe}_2$  by the ethylenediamine ( $\text{C}_2\text{H}_8\text{N}_2$ ) solvent. Physical properties of intercalated samples were measured. Magnetization of the samples indicates that all the samples exhibit superconductivity and different  $T_c$  values. Powder x-ray diffraction patterns (Fig. 1) show changes in the  $c$ -axis associated with intercalation for the samples. We discuss a relation between  $T_c$  and the  $c$ -axis length. Its implication in charge-density-wave is also discussed. The details will be explained in the presentation.

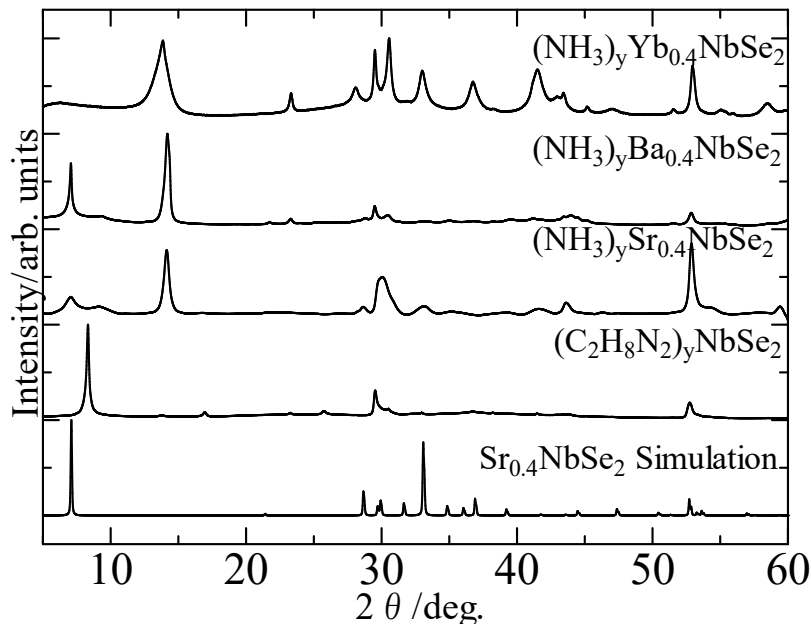


Fig. 1 Patterns of powder x-ray diffraction for samples

- [1] T.P.Ying et al., Sci. Rep. 2 (2012) 426.
- [2] T. Hatakeda et al., J. Phys. Soc. Jpn. 82, 123705 (2013)
- [3] E. Morosan et al., Nature Phys. 2, 544 (2006).

## PCP2-4

### Observation of surface structure in Hf doped ZrTe<sub>3</sub> by STM

\*Sora Kobayashi<sup>1</sup>, Shun Ohta<sup>1</sup>, Satoshi Demura<sup>2</sup>, Atsushi Nomura<sup>1</sup>, Hideaki Sakata<sup>1</sup>

Department of Physics, Tokyo University of Science, Japan<sup>1</sup>  
College of Science and Technology, Nihon University, Japan<sup>2</sup>

In transition metal trichalcogenide ZrTe<sub>3</sub>, one dimensional charge density wave (CDW), which have the wave vector  $q_{CDW} \cong (0.07, 0, 0.333)$  appears along the a-axis at about 63K, and filamentary superconductivity appears at 2K [1]. STM measurements at 4.2K in ZrTe<sub>3</sub> have revealed not only the CDW but also black streaks extending along the a-axis. The number of the streaks was found to increase when ZrTe<sub>3</sub> was grown at high temperature [2]. Since changes in physical properties due to crystal growth temperature has been reported in ZrTe<sub>3</sub>[3], the streaks seems to greatly affect the physical properties in this material.

Transition metal trichalcogenide HfTe<sub>3</sub> also exhibits quasi-one-dimensional properties. In HfTe<sub>3</sub>, it has been reported that a one-dimensional CDW along the a-axis at about 82K and superconductivity appears at about 1.4K [4,5]. However, in HfTe<sub>3</sub>, the details of the CDW or existence of the streaks observed in ZrTe<sub>3</sub> have not been reported. This seems to be due to the fact that HfTe<sub>3</sub> is unstable against humidity in atmosphere unlike ZrTe<sub>3</sub>.

In this study, the sample Hf<sub>x</sub>Zr<sub>1-x</sub>Te<sub>3</sub>, in which the Zr site of ZrTe<sub>3</sub> is partially substituted for Hf, was synthesized and STM observations were performed to observe the existence of the streaks and change in the CDW due to Hf substitution. Electrical resistivity measurements showed that the CDW transition temperature increased with Hf substitution. STM observations at 4.2K revealed the existence of the similar streak to those observed in ZrTe<sub>3</sub>. Furthermore, in addition to the CDW inherent to ZrTe<sub>3</sub>, additional harmonic-like structure was observed. In this presentation, we will discuss the details of the change in STM images due to Hf substitution on the Zr site of ZrTe<sub>3</sub>.

[1] D.J. Eaglesham et al., Journal of Physics C: Solid State Physics 17 (1984) L697

[2] S. Kobayashi et al, The Annual Meeting of JPSJ 2019 (Tokyo univ of science)

[3] X. Zhu et al., PHYSICAL REVIEW B 87, 024508 (2013)

[4] Jing Li et al., PHYSICAL REVIEW B 96, 174510 (2017)

[5] S. J. Denholme et al., Scientific Report 7, 45217 (2017)

Keywords: Hf<sub>x</sub>Zr<sub>1-x</sub>Te<sub>3</sub>, ZrTe<sub>3</sub>, CDW, STM

## PCP2-5

### Evaluation of the physical properties and the real space observation in $2H\text{-TaS}_2$ synthesized with flux method

\*Shun Ohta<sup>1</sup>, Sora Kobayashi<sup>1</sup>, Atsushi Nomura<sup>1</sup>, Yuita Fujisawa<sup>2</sup>, Satoshi Demura<sup>3</sup>, Hideaki Sakata<sup>1</sup>

Department of Physics, Tokyo University of Science<sup>1</sup>  
Okinawa Institute of Science and Technology<sup>2</sup>  
College of Science and Technology, Nihon University<sup>3</sup>

The physical properties of the layered compounds can be changed by the intercalation of the metal ion, organic molecules, and so on. In transition metal dichalcogenide (TMDC)  $2H\text{-TaS}_2$ , which shows superconductivity and charge density wave (CDW) state, the intercalation of the metal ion increases the superconducting transition temperature and changes the superstructure. Although intercalation is useful to tune physical properties of TMDC, up to present, the intercalation technique in TMDC is restricted to a few methods, such as electrochemical or vapor transport technique, and intercalants are also restricted. Thus, it is necessary to find the more methods of the intercalation.

In this study, we tried to grow single crystal  $2H\text{-TaS}_2$  with flux method to intercalate elements which are included in the flux. NaCl and KCl were used as flux. It was found that the potassium is included in the single crystals grow by the flux method from the EDX measurements. The measurements of the electrical resistivity showed the transition temperature to the superconducting state became higher than that in the pristine crystal. Scanning tunneling microscopy / spectroscopy (STM/STS) measurements at 4.2 K revealed the superstructure which is different from that of the CDW in the pristine  $2H\text{-TaS}_2$ . Considered these results, it is concluded that the potassium included in the flux is intercalated with  $2H\text{-TaS}_2$  by single crystal growth with flux method. In the presentation, how the potassium is intercalated with  $2H\text{-TaS}_2$  will be discussed.

Keywords: intercalation, CDW,  $2H\text{-TaS}_2$ , STM/STS

## PCP2-6

### Synthesis and physical property measurements of misfit transition-metal dichalcogenide (SbS)(TaS<sub>2</sub>)

Shun Doyama<sup>1</sup>, Shun Ohta<sup>1</sup>, Hideaki Sakata<sup>1</sup>

Tokyo university of science<sup>1</sup>

The misfit layered compound (MS)(TX<sub>2</sub>)<sub>n</sub> (n = 1, 2, 3) has a layered crystal structure in which a MS layer (M = Bi, Pb, Sb, Sn or lanthanide) forming a square lattice is inserted between transition metal dichalcogenide TX<sub>2</sub> (T = Ta, Nb, Ti, V, Cr X = S, Se) which has a triangular lattice. Because the stacking of the triangular and the square lattice breaks spatial inversion symmetry, the spin orbit interaction affects the electronic states in the misfit layered compounds. Furthermore, because of the low dimensionality of the crystal structure, the appearance of charge density wave (CDW) and superconductivity has been reported. However, understanding of the difference of the CDW and the superconducting transition temperatures between the misfit layered compounds has not been fully understood.

In one of misfit compound, (SbS)(TaS<sub>2</sub>)<sub>1</sub>, there are reports on poly crystal synthesis. However, there are no reports on single crystal synthesis and measurements of physical properties such as the CDW and the superconducting transition[1]. Furthermore, there have been no reports of real space observations of this compound so far. In this study, we investigated single crystal (SbS)(TaS<sub>2</sub>)<sub>1</sub>, whose CDW or superconducting transition has not been studied.

We found that single crystal of (SbS)(TaS<sub>2</sub>)<sub>1</sub> can be synthesized by flux method. The structural analysis by X-ray diffraction and electric resistivity measurements down to 1.4K, and scanning tunneling microscopy measurements were performed in the single crystal. We found this material undergoes both CDW and superconducting transition, and transition temperature was 70K and 2.14K, respectively. In STM measurements, only triangular lattice layer was imaged with superlattice due to the effect of underlying square lattice layer and the CDW. In the presentation, CDW and superconducting transition temperature is compared to those of other misfit materials.

[1] Yoshito Gotoh et al. Jpn. J. Appl. Phys. **30** L1039 1991

Keywords: Superconductor, Charge Density Wave, Scanning Tunneling Microscopy, Transition metal dichalcogenide

### Local Density of States in Two-Dimensional Nano-Structured Superconducting Systems with Superconductor–Normal Metal Interfaces

\*Saoto Fukui<sup>1</sup>, Zhen Wang<sup>1</sup>, Masaru Kato<sup>2</sup>

Shanghai Institute of Microsystem and Information Technology, Chinese Academy of Sciences<sup>1</sup>  
Osaka Prefecture University<sup>2</sup>

Superconductor–normal metal (SN) interfaces occur important phenomena such as the Andreev reflection and a proximity effect. Also, superconductor–normal metal–superconductor (SNS) junctions are expected as many applications, for example, a SQUID, a single flux quantum logic, and so on. In recently developments, high-quality junctions with nano-structured superconducting films are made. In nano-structured systems, movements of electrons are restricted strongly and the quantum confinement effect occurs. Also, it is known that superconducting properties such as a critical temperature and a density of state oscillate as a function of a thickness of the superconducting film [1]. The other feature of the quantum confinement effect is a discreteness of energy levels. The quantum confinement effect in the superconductor is investigated actively, while in the case of superconductors with SN interfaces, effects of the quantum confinement effect on various properties are not investigated very much.

We investigate superconducting properties in nano-structured superconductors with SN interfaces, in particular, in the region of the quantum confinement effect. In this research, we focus on the discreteness of energy levels. The discreteness of energy levels affects a local density of state (LDOS), and the LDOS as a function of the energy has some peaks. Then, we investigate behaviors of the LDOS in nano-structured systems with the SN interface and SNS junctions theoretically. Experimentally, the LDOS can be measured through a differential conductance with the STM / STS measurement, so an electronic structure of a surface in the system is important. Then, we consider two-dimensional systems. In order to obtain the electronic structure in this system, we solve the Bogoliubov-de Gennes equations self-consistently with a two-dimensional finite element method [2]. Using solutions, we report dependences of sizes, shapes, potential barriers in SN interfaces, and widths of each metals on the LDOS.

[1] A. A. Shanenko, et al., Phys. Rev. B, **75**, 014519 (2007)

[2] H. Suematsu, et al., Physica C, **412-414**, 548 (2004)

Keywords: superconductor-normal metal interface, Bogoliubov de Gennes equations

## PCP2-8

### Angular dependence of the upper critical field in the high-pressure 1T' phase of MoTe<sub>2</sub>

\*Yajian Hu<sup>1</sup>, Yuk Tai Chan<sup>1</sup>, Kwing To Lai<sup>1</sup>, Kin On Ho<sup>1</sup>, Xiaoyu Guo<sup>1</sup>, Hai-Peng Sun<sup>2,3,4</sup>, King Yau Yip<sup>1</sup>, Dickon H.L. Ng<sup>1</sup>, Hai-Zhou Lu<sup>2,3</sup>, Swee Kuan Goh<sup>1</sup>

The Chinese University of Hong Kong, Hong Kong<sup>1</sup>  
Southern University of Science and Technology, China<sup>2</sup>  
Shenzhen Key Laboratory of Quantum Science and Engineering, China<sup>3</sup>  
Department of Physics, Harbin Institute of Technology, China<sup>4</sup>

Superconductivity in the type-II Weyl semimetal candidate MoTe<sub>2</sub> has attracted much attention due to the possible realization of topological superconductivity. In this work, we constructed a temperature-pressure phase diagram, as shown in Fig.(a). The magnetoresistance (MR) and Hall coefficient of MoTe<sub>2</sub> are found to decrease with increasing pressure. The Kohler's scalings for the MR data above ~11 kbar show a change of exponent whereas the data at lower pressure can be well scaled with a single exponent. These results are suggestive of a Fermi-surface reconstruction when the structure changes from the T<sub>d</sub> to 1T' phase. We have performed a detailed study of the upper critical field H<sub>c2</sub> of MoTe<sub>2</sub> at 15 kbar, which is in the 1T' phase. The H<sub>c2</sub>-temperature phase diagram are constructed with magnetic field B // ab and B ⊥ ab. The data can be satisfactorily described by the Werthamer–Helfand–Hohenberg model with the Maki parameters α ~ 0.77 and 0.45, respectively. The surprisingly enhanced α may stem from a small Fermi surface and a large effective mass of semimetallic MoTe<sub>2</sub>. The angular dependence of H<sub>c2</sub> at 15 kbar can be well fitted by the Tinkham model, as shown in Fig.(b), suggesting the two-dimensional nature of superconductivity in the high-pressure 1T' phase. Furthermore, the calculations and experimental results of the electronic structure of MoTe<sub>2</sub> under pressure will also be discussed.

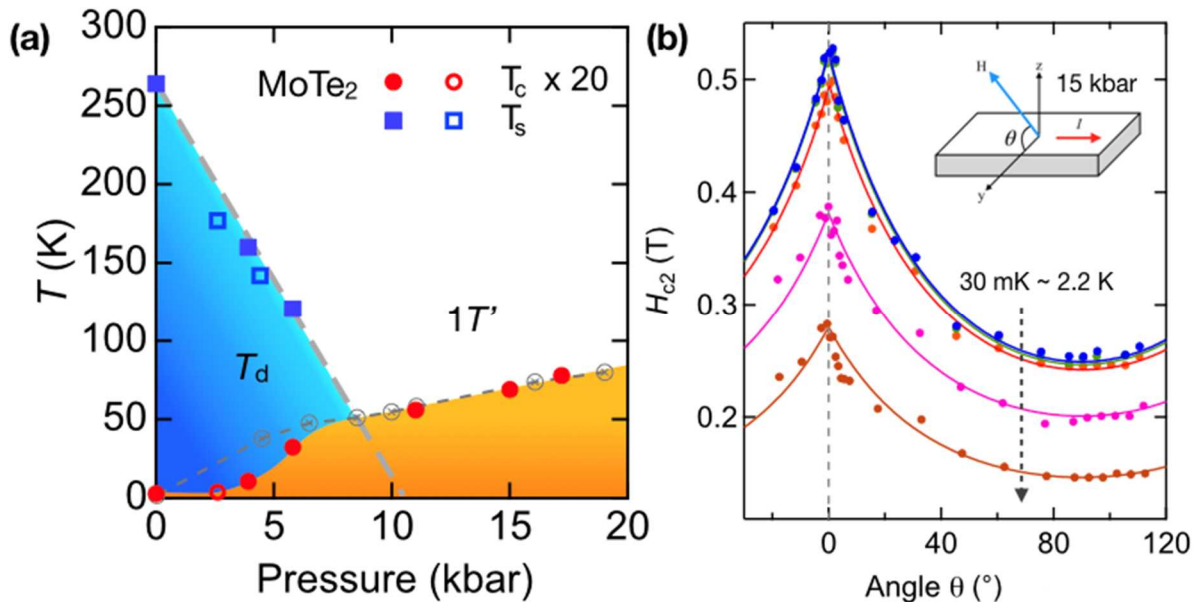


Figure: (a) The temperature-pressure phase diagram of MoTe<sub>2</sub>. (b) Angular dependence of upper critical field of MoTe<sub>2</sub> at 15 kbar. The markers are data and the lines are fitting.

Keywords: Weyl semimetal, Superconductivity, Angular dependence, Electronic structure

## Bogoliubov–de Gennes Approach to Inhomogeneous Superconducting Gap in Nanowires and Nanotubes

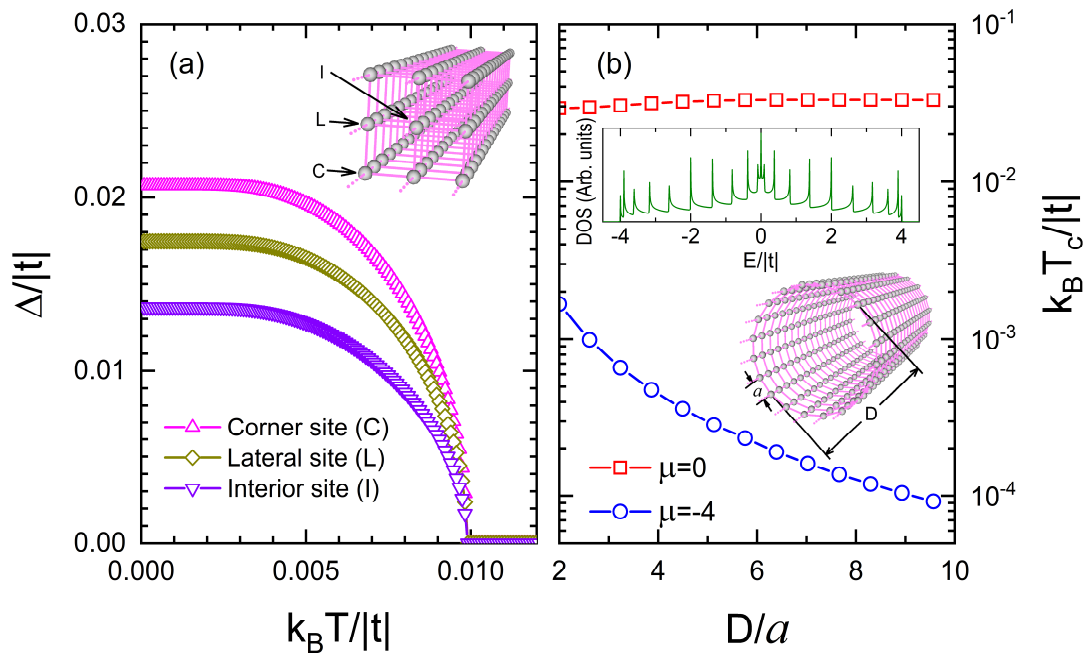
\*German E. Lopez<sup>1</sup>, Chumin Wang<sup>1</sup>

Instituto de Investigaciones en Materiales, Universidad Nacional Autonoma de Mexico, A.P. 70-360, 04510, Mexico City, MEXICO.<sup>1</sup>

Traditional theories of superconductivity have been developed in the reciprocal space based on the translational symmetry. Such symmetry is absent in many inhomogeneous superconductors that contain structural grains or interfaces, whose study requires a real space theory of superconductivity [1]. In this work, we study the inhomogeneity of superconducting gap in nanostructures by using the Bogoliubov–de Gennes equations and an attractive Hubbard model [2]. In Fig. 1(a), the superconducting gap ( $\Delta$ ) versus temperature ( $T$ ) is shown for a nanowire of an infinite-length and a cross section of 9 atoms (illustrated in the inset) with an on-site interaction of  $U = -|t|$  and the chemical potential at  $\mu=0$ , while the critical temperature ( $T_c$ ) as a function of diameter ( $D$ ) is exposed in Fig. 1(b) for an infinite-length nanotube (illustrated in its inset) with  $U = -|t|$ ,  $\mu=0$  (red squares) and  $\mu = -4|t|$  (blue circles), being  $t$  the single electronic hopping integral. Observe the appearance of a unique critical temperature at  $k_B T_c \approx 0.01|t|$  in Fig. 1(a), in spite of different  $\Delta$  at non-equivalent sites. Notice also in Fig. 1(b) both slight increase and decrease behaviors of calculated  $T_c$ , in consistence with those observed in  $WS_2$  [3] and carbon [4,5] nanotubes.

This work was partially supported by *UNAM-IN106317 and CONACyT-252943*. Computations were performed at Miztli of DGTIC, UNAM. G.E.L. thanks the support from UNAM-PAEP 2019.

- [1] P. G. de Gennes, *Superconductivity of Metals and Alloys* (Westview Press, 1999).  
 [2] C. G. Galvan, J. M. Cabrera, L. A. Perez, C. Wang, *Phys. Status Solidi B* **253**, 1638 (2016).  
 [3] F. Qin, *et al.*, *Nano Lett.* **18**, 6789 (2018).  
 [4] Z. K. Tang, *et al.*, *Science* **292**, 2462 (2001).  
 [5] M. Kociak, *et al.*, *Phys. Rev. Lett.* **86**, 2416 (2001).



Keywords: Bogoliubov–de Gennes, Superconducting gap, Critical temperature, Nanostructures

## PCP2-10

### Crystal growth and conduction properties of Pb substituted La(O,F)BiS<sub>2</sub>

\*Yuto Nakayama<sup>1</sup>, Ryunosuke Shirota<sup>1</sup>, Atsushi Nomura<sup>1</sup>, Hideaki Sakata<sup>1</sup>

Tokyo University of Science<sup>1</sup>

La(O,F)BiS<sub>2</sub> is a layered superconductor, which have LaO as a blocking layer and BiS<sub>2</sub> as a conducting layer. Recently, an anomalous hump in temperature dependence of electric resistivity was reported in Pb substituted La(O,F)BiS<sub>2</sub> single crystal with Pb concentration 6~9%. [1] These specimens showed higher superconducting transition temperature (T<sub>c</sub>) than specimens without the hump. The appearance of the hump is thought to be related to a structural change, though the origin has not been elucidated yet. We tried to synthesize La(O,F)BiS<sub>2</sub> single crystals which have Pb concentration much more than that in the samples previously studied to elucidate the effect of Pb substitution in La(O,F)BiS<sub>2</sub>. We synthesized Pb substituted La(O,F)BiS<sub>2</sub> single crystal with Pb concentration up to 75% with flux method. We carried out structure analysis by X-ray diffraction and temperature dependence of the electric resistivity measurements to evaluate the conducting property of the samples. We found that the lattice constant along the c-axis shrank largely when Pb concentration exceeded 10%, indicating possible structural change. In these samples, the superconductivity was suppressed and no T<sub>c</sub> was observed down to 2 K. In the presentation, we also discuss the results of Seebeck coefficient measurements of these samples to investigate the electronic structure.

[1] S. Otsuki, et al. Solid State Communications 270 (2018) 17-21

Keywords: BiS<sub>2</sub>-based superconductor, layered material



## PCP2-11

### Synthesis and superconducting property evaluation of Pb-substituted BiS-based superconductor $\text{LaO}_{1-x}\text{F}_x\text{BiS}_2$

\*Takahito Fukui<sup>1</sup>, Satoshi Demura<sup>1</sup>, Yoshiki Takano<sup>1</sup>

College of Science and Technology, Nihon University Japan<sup>1</sup>

BiS<sub>2</sub>-based superconductor  $\text{LaO}_{1-x}\text{F}_x\text{BiS}_2$  has a layered crystal structure composed of electron-supply layers of La (O,F) layers and conductive layers of two BiS<sub>2</sub> layers. Although superconductivity does not appear in  $\text{LaOBiS}_2$ , it shows superconductivity about 3K by replacing a part of O ions with F ions. In addition, the superconducting transition temperature of  $\text{LaO}_{0.5}\text{F}_{0.5}\text{BiS}_2$  is increased by replacing a part of Bi ions with Pb ions, which is called as Pb substitution effect. [1] While Pb substitution effect was confirmed in  $\text{LaO}_{0.5}\text{F}_{0.5}\text{BiS}_2$ , it has not been known whether the same effect occurs in  $\text{LaO}_{1-x}\text{F}_x\text{BiS}_2$  with different fluorine content so far.

Here, we performed Pb substitution to  $\text{LaO}_{1-x}\text{F}_x\text{BiS}_2$  with various fluorine content to investigate the Pb substitution effect to superconducting properties of these materials. Polycrystalline samples used in this investigation were prepared by solid state reaction in evacuated quartz tube. The superconducting properties for the obtained samples were evaluated from X-ray diffraction, electrical resistivity, and magnetic susceptibility measurements. In this presentation, we will discuss the effect of Pb substitution for the superconducting properties in  $\text{LaO}_{1-x}\text{F}_x\text{BiS}_2$  while comparing results of that of  $\text{LaO}_{0.5}\text{F}_{0.5}\text{BiS}_2$ .

[1] S. Otsuki *et al.*, Solid State Commun., 270 17-21(2018)

## Co-Intercalation of Li and Ethylenediamine into the Bi-based Chalcogenides with the Layered Structure by Solvothermal Technique

\*Shota Ueno<sup>1</sup>, Takashi Noji<sup>1</sup>, Takayuki Kawamata<sup>1</sup>, Masatsune Kato<sup>1</sup>

Department of Applied Physics, Tohoku University, Sendai 980-8579, Japan<sup>1</sup>

We have reported that the co-intercalation of alkali metals or alkaline-earth metals and organic molecules into the transition-metal chalcogenides is effective to induce superconductivity or enhance the superconducting transition temperature  $T_c$  [1,2]. Through the co-intercalation, carriers can be doped and the electronic density of states at Fermi level is expected to increase due to the change of the electronic structure from three-dimensional to two-dimensional by the expansion of spacing between the conductive layers. It is reported that the topological insulator  $\text{Bi}_2\text{Se}_3$  with the layered structure exhibits superconductivity with  $T_c \sim 2\text{-}4\text{ K}$  through the intercalation of several kinds of metals [3-5]. Therefore, the enhancement of  $T_c$  is expected by the expansion of spacing between the conductive Bi-Se layers through the co-intercalation. In this study, we have carried out the co-intercalation of Li and ethylenediamine (EDA) into the Bi-based chalcogenides with the layered structure of  $\text{Bi}_2\text{Se}_3$  and  $\text{SnBi}_2\text{Se}_4$ .

Host materials were prepared by the solid-state reaction method. The co-intercalation was carried out at 180-190°C for 7 days by the solvothermal technique using the Teflon-lined steel autoclave.

As for  $\text{Bi}_2\text{Se}_3$ , new Bragg peaks are observed through the co-intercalation, as shown in Figs. 1(a) and (b). It has been found that the new co-intercalation compound of  $\text{Li}_x(\text{EDA})_y\text{Bi}_2\text{Se}_3$  is successfully synthesized. As for  $\text{SnBi}_2\text{Se}_4$ , it is not clear if the co-intercalated sample is obtained because only one new Bragg peak is observed as shown in Figs. 1(c) and (d). We will report whether superconductivity appears or not.

[1] T. Hatakeda *et al.*: J. Phys. Soc. Jpn. **85**, 103702 (2016). [2] K. Sato *et al.*: J. Phys. Soc. Jpn. **87**, 054704 (2018). [3] Y. S. Hor *et al.*: Phys. Rev. Lett. **104**, 057001 (2010). [4] Z. Liu *et al.*: J. Am. Chem. Soc. **137**, 10512 (2015). [5] Y. Qiu *et al.*: arXiv:1512.03519.

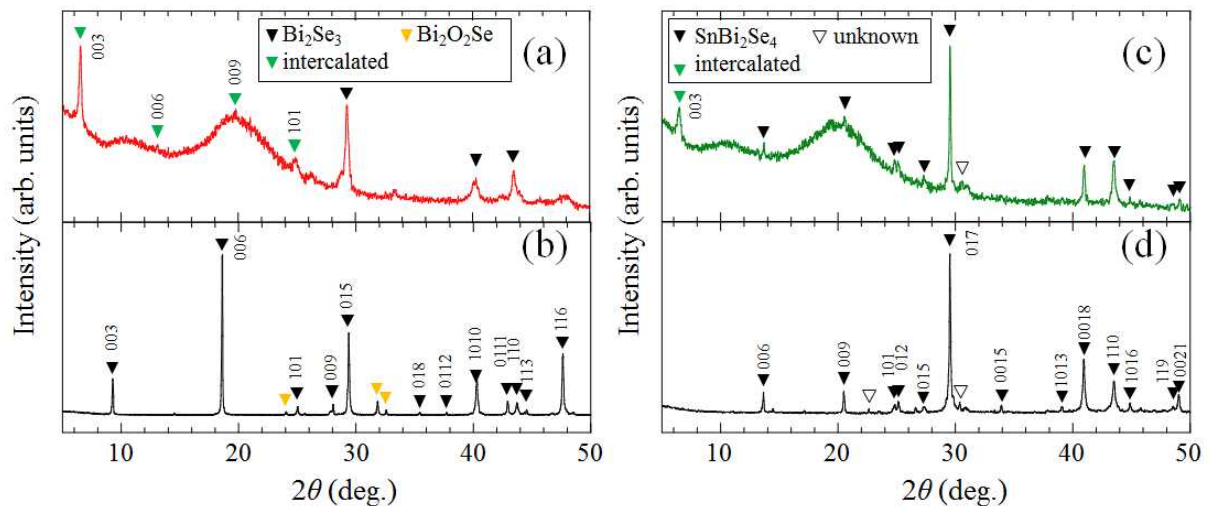


Fig.1. Powder X-ray diffraction patterns of samples obtained through the co-intercalation of Li and EDA for (a)  $\text{Bi}_2\text{Se}_3$  and (c)  $\text{SnBi}_2\text{Se}_4$ . Those of host samples of (b)  $\text{Bi}_2\text{Se}_3$  and (d)  $\text{SnBi}_2\text{Se}_4$  are also shown for reference.

Keywords: Superconductor, Intercalation, Solvothermal Technique

## PCP3-1

### Synthesis and Physical Properties of New Iridium Oxyfluorides Using Topochemical Reaction Method

\*Kenta Kuramochi<sup>1,2</sup>, Tomohito Shimano<sup>1,2</sup>, Taichiro Nishio<sup>1</sup>, Hiroataka Okabe<sup>3</sup>, Kazumasa Horigane<sup>4</sup>, Jun Akimitsu<sup>4</sup>, Tomoki Uchiyama<sup>5</sup>, Yoshiharu Uchimoto<sup>5</sup>, Hiraku Ogino<sup>2</sup>

Department of Physics, Tokyo University of Science, Tokyo, Japan<sup>1</sup>

Superconducting Electronics Group, National Institute of Advanced Industrial Science and Technology, Ibaraki, Japan<sup>2</sup>

Institute of Materials Structure Science/J-PARC Center, High Energy Accelerator Research Organization, Ibaraki, Japan<sup>3</sup>

Research Institute for Interdisciplinary Science, Okayama University, Okayama, Japan<sup>4</sup>

Graduate School of Human and Environmental Studies, Kyoto University, Kyoto, Japan<sup>5</sup>

Ruddlesden-Popper (RP) type Iridate  $\text{Sr}_2\text{IrO}_4$  has been paid much attention due to the interesting physical properties such as  $J_{\text{eff}} = 1/2$  Mott insulating state induced by strong spin-orbit interaction<sup>[1]</sup>. Moreover, the possibilities of unconventional superconductivity in carrier-doped  $\text{Sr}_2\text{IrO}_4$  has been proposed because it has several similarities with the high- $T_c$  cuprate superconductors such as  $\text{La}_2\text{CuO}_4$ <sup>[2]</sup>. Carrier doping such as La substitution for Sr site was already attempted<sup>[3]</sup>, but bulk superconductivity has not yet been reported. So far, we have reported synthesis of new iridium oxyfluoride  $\text{Sr}_2\text{Ir}(\text{O},\text{F})_{6-\delta}$  using topochemical reaction method. This compound has more anisotropic structure due to insertion of fluorine layer into rock salt layer, and suppression of the magnetic ordering in  $\text{Sr}_2\text{IrO}_4$  have been observed with topochemical fluorination. Thus, we utilized topochemical reaction method for other iridates in order to synthesize a novel iridium oxyfluorides.

$\text{Ba}_2\text{IrO}_4$  as precursor was synthesized by a conventional solid-state reaction method under high-pressure. Thereafter, it was mixed with various fluorinating agents such as  $\text{ZnF}_2$ ,  $\text{CuF}_2$  and PTFE (precursor : fluorinating agents = 1 : 1), and the mixture was heated at 250-550 °C for 12 hours in air. Phase identification was performed by powder X-ray diffraction method. Magnetic susceptibility and resistivity were measured using a SQUID magnetometer and a four-probe method. The valence state of Ir ion was evaluated using XAFS study. The figure shows powder XRD pattern of the compounds and the possible crystal structure. New layered iridium oxyfluoride  $\text{Ba}_2\text{Ir}(\text{O},\text{F})_{6-\delta}$  was successfully synthesized by topochemical fluorination with  $\text{ZnF}_2$ ,  $\text{CuF}_2$  and PTFE. This oxyfluoride has the same structure as  $\text{Sr}_2\text{Ir}(\text{O},\text{F})_{6-\delta}$  with largely enhanced  $c$ -axis length because fluorine layer was inserted in the rock salt layer. The magnetization measurements showed

paramagnetic behavior after fluorination. Meanwhile, the electronic transport properties of  $\text{Ba}_2\text{Ir}(\text{O},\text{F})_{6-\delta}$  exhibited semiconducting behavior like  $\text{Sr}_2\text{Ir}(\text{O},\text{F})_{6-\delta}$ . Further detail of the compounds such as valence state of Ir will be given in the presentation.

[1] B. J. Kim *et al.*, *Science* **323**, (2009), 1329. [2] H. Watanabe *et al.*, *PRL* **110**, (2013), 027002. [3] K. Horigane, *et al.*, *PRB* **97**, (2018), 064425.

Keywords: Layered perovskite, Oxyfluorides, Iridates, Topochemical reaction

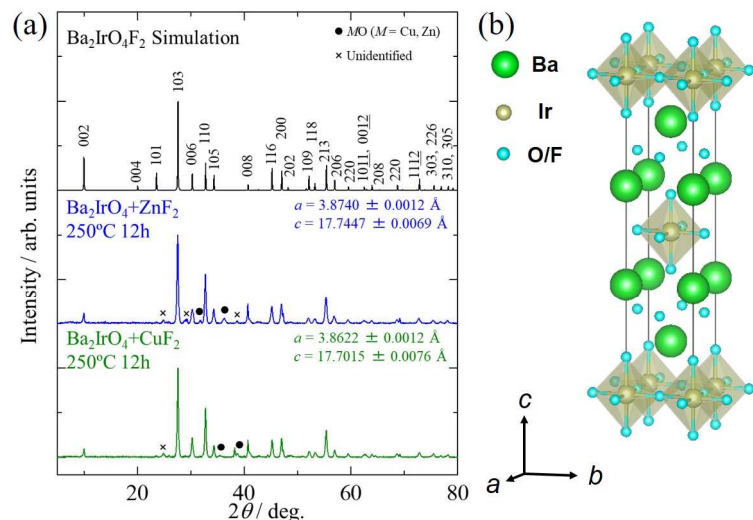


Fig. (a) Powder XRD patterns of  $\text{Ba}_2\text{Ir}(\text{O},\text{F})_{6-d}$  and (b) Crystal structure model of  $\text{Ba}_2\text{Ir}(\text{O},\text{F})_{6-d}$ .

## PCP3-2

### Exploration of New Superconducting Phases in a Scandium Borocarbide System

\*Hiroki Ninomiya<sup>1</sup>, Kunihiko Oka<sup>1</sup>, Izumi Hase<sup>1</sup>, Kenji Kawashima<sup>1,2</sup>, Hiroshi Fujihisa<sup>1</sup>, Yoshito Gotoh<sup>1</sup>, Shigeyuki Ishida<sup>1</sup>, Hiraku Ogino<sup>1</sup>, Akira Iyo<sup>1</sup>, Yoshiyuki Yoshida<sup>1</sup>, Hiroshi Eisaki<sup>1</sup>

National Institute of Advanced Industrial Science and Technology (AIST), Tsukuba, Ibaraki 305-8568, Japan<sup>1</sup>

IMRA Material R&D Co., Ltd., Kariya, Aichi 448-0032, Japan<sup>2</sup>

Superconducting materials containing light elements are advantageous to emerge the relatively high critical temperature ( $T_c$ ), because high-frequency vibration of phonons due to the light mass enhances its  $T_c$  within the BCS theory. Indeed, there are various superconductors in alkali, alkali-earth, and  $d$  transition-metal borides and carbides [1-3].

In this study, we searched for a new superconductor in the ternary Sc-B-C system using an arc-melting method. Although a moderately high- $T_c$  superconductor is expected in combination with the comparatively small ionic radius of Sc and potentially high Debye frequencies originating from B and C, this system remains unexplored.

We attempted to synthesize the Sc-B-C compounds under various conditions of the starting composition, and found that a superconducting transition was observed at around 7.7 K only when the B-poor sample (e.g. nominal composition of Sc:B:C=37:2:61) was prepared [4]. Note that neither B-free nor B-excess samples exhibited the superconductivity down to 2 K. The structural refinements through the Rietveld analysis demonstrated that the compound belongs to the tetragonal space group of  $P4/ncc$ . By using the density functional theory calculations, the precise atomic positions of a small amount of B were examined. As a result, a chemical formula of the present superconducting phase was found to be expressed as  $\text{Sc}_{20}\text{C}_{8-x}\text{B}_x\text{C}_{20}$  ( $x=1$  or  $2$ ).

The sample exhibited the typical type-II superconductivity below  $T_c=7.7$  K. Our specific-heat measurements revealed that  $\text{Sc}_{20}\text{C}_{8-x}\text{B}_x\text{C}_{20}$  was classified as an intermediately coupled superconductor. The electronic structure studies by first principles calculations proposed that the contribution of Sc- $3d$  orbitals was mainly responsible for the superconductivity.

[1] J. Nagamatsu, N. Nakagawa, T. Muranaka, Y. Zenitani, and J. Akimitsu, *Nature* **410**, 63 (2001).

[2] G. Amano, S. Akutagawa, T. Muranaka, Y. Zenitani, and J. Akimitsu, *J. Phys. Soc. Jpn.*, **73**, 530 (2004).

[3] N. Emery, C. Hérold, M. d'Astuto, V. Garcia, Ch. Bellin, J. F. Maréché, P. Lagrange, and G. Louprias, *Phys. Rev. Lett.* **95**, 087003 (2005).

[4] H. Ninomiya, K. Oka, I. Hase, K. Kawashima, H. Fujihisa, Y. Gotoh, S. Ishida, H. Ogino, A. Iyo<sup>1</sup>, Y. Yoshida, and H. Eisaki, to be submitted.

Keywords: New material, Superconductor, Borocarbide, Electronic structure

## PCP3-3

### Crystal Growth and Superconducting Properties of a Chiral Compound TaSi<sub>2</sub>

\*Yuta Hoshidoh<sup>1</sup>, Kaito Koyanagi<sup>1</sup>, Takao Sasagawa<sup>1</sup>

MSL, Tokyo Institute of Technology<sup>1</sup>

Superconductivity was reported, long time ago, in  $MX_2$  ( $M = \text{Nb, Ta}$ ;  $X = \text{Si, Ge}$ ) [1,2]. Though the reported superconducting transition temperature,  $T_c$ , was as high as 16 K for NbGe<sub>2</sub>, there have been only a few follow-up experiments. It is noted that the measurements of superconducting properties under magnetic fields are lacking, and  $T_c$  for each compound remains controversial. The difficulty of establishing the superconductivity in these compounds may be attributed to the fact that it is difficult to synthesize single-phase pure samples. This is because high purity Nb and Ta are not readily available and the melting-points ( $T_m$ ) and reaction-temperatures of the raw materials are very high (e.g.  $T_m \sim 3000^\circ\text{C}$  for Ta).

We are interested in these compounds from the viewpoint of electronic structures. As shown in Fig. 1 (a),  $MX_2$  has a hexagonal crystal structure with the space group P6<sub>2</sub>22, which belongs to the chiral symmetry. It is expected that the spin band splitting occurs in the electronic states when strong spin-orbit interaction (SOI) is present in the chiral symmetry. In fact, by the first principles calculations, we confirmed such spin band splitting in these compounds. Therefore, it became increasingly important to examine and establish the superconductivity in these chiral compounds.

Using Ta (6N) and Si (5N) grains, single-phase polycrystalline samples of TaSi<sub>2</sub> were successfully synthesized by the arc-melting method in a tetra-arc furnace (Fig. 1 (b)). Residual resistivity at 2 K and residual resistivity ratio of the obtained TaSi<sub>2</sub> pellet were 0.22  $\mu\Omega\text{cm}$  and 143, respectively, indicating the high quality of the sample. The temperature dependence of resistivity was measured using a dilution refrigerator down to 55 mK. Below 0.7 K, the resistivity suddenly dropped, indicating a superconducting transition. Although the onset  $T_c \sim 0.7$  K is lower than the previously reported value (4.4 K [1], which is very close to  $T_c$  for Ta), we believe this is the intrinsic superconductivity in TaSi<sub>2</sub>.

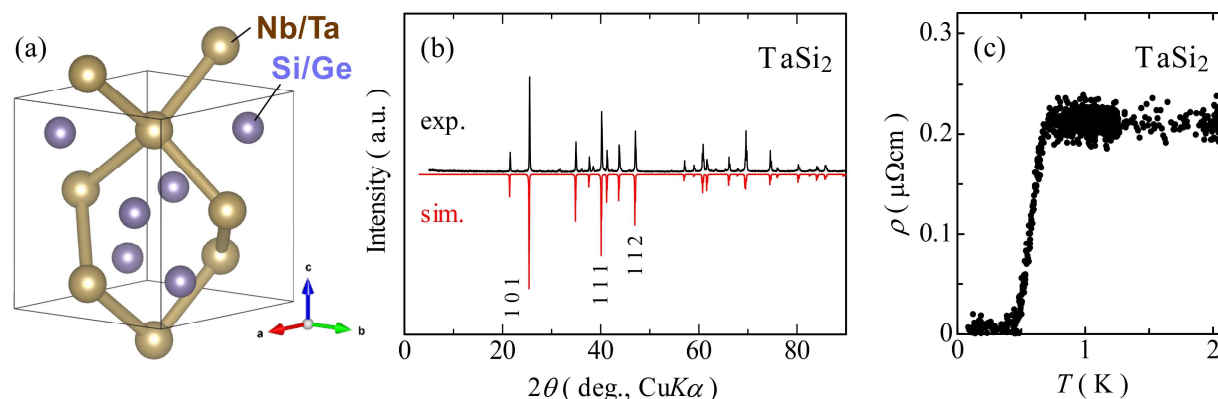


Fig. 1 (a) Crystal structure of  $MX_2$  ( $M = \text{Nb, Ta}$ ;  $X = \text{Si, Ge}$ ). (b) XRD patterns of TaSi<sub>2</sub> (experiment vs. Simulation). (c) Temperature dependence of resistivity in the TaSi<sub>2</sub> pellet.

[1] C. M. Knoedler and D. H. Douglass, J. Low Temp. Phys. **37**, 189 (1979).

[2] J. C. Lasjaunias *et al.*, J. Low Temp. Phys. **92**, 335 (1993).

Keywords: Chiral Compound, Crystal Growth, Spin-orbit Interaction

## PCP3-4

### Superconductivity in a Topological Dirac Nodal-Line Semimetal

\*Masayuki Murase<sup>1</sup>, Takao Sasagawa<sup>1</sup>

Laboratory for Materials and Structures<sup>1</sup>

Topological electronic materials, especially Dirac nodal-line semimetals (DNLSs), have been attracting attention in condensed matter physics. DNLSs have gapless nodal-line Dirac dispersions along the specific momentum-directions in the electronic band structures, which are protected by the nonsymmorphic symmetry of the crystal structures even under the strong spin-orbit-interaction (SOI). ZrSiS and InBi are the DNLSs, belonging to the nonsymmorphic space group P4/nmm. They are known to exhibit large magnetoresistance (MR) due to the existence of the Dirac line node.

LaAgBi<sub>2</sub> (shown in Fig. 1(a)) was reported to exhibit large MR [1]. Recently, we found that LaAgBi<sub>2</sub> was also the DNLS [2] from the fact that it belongs to the same P4/nmm space group and has strong SOI from Bi. As shown in Fig. 1 (b), it should be noted that the Dirac dispersion exactly crosses at the Fermi energy in LaAgBi<sub>2</sub>.

In this study, we explored the possibility of superconductivity in LaAgBi<sub>2</sub> as a DNLS. High-quality single crystals of LaAgBi<sub>2</sub> were obtained by the self-flux method. As shown in Fig. 1 (c), our sample of LaAgBi<sub>2</sub> exhibited the higher residual resistivity ratio of 131 and the larger magnetoresistance of 2400% at 2 K and 9 T than those of previous studies (10 and ~1200%, respectively [1]). Furthermore, we found that the resistivity dropped rapidly below 2 K (inset of Fig. 1 (c)). As increasing the applied magnetic fields, the resistivity-drop was suppressed, indicating the resistivity behavior below 2 K is due to superconductivity. We will report the details of superconducting properties, including anisotropy, at lower temperatures.

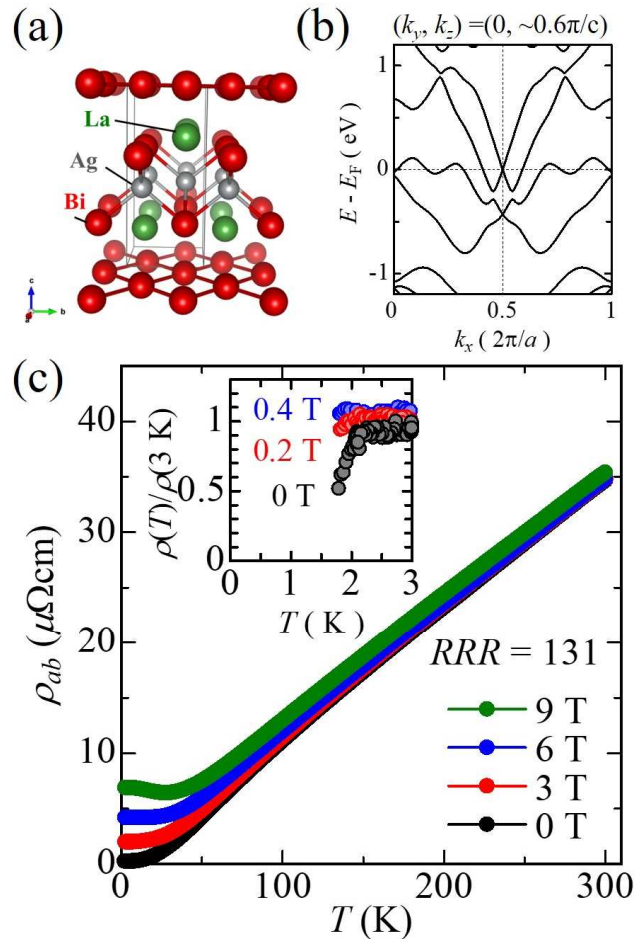


Fig. 1 (a) The crystal structure of LaAgBi<sub>2</sub>. (b) The electronic dispersions plotted along the  $k_x$  direction at the fixed  $(k_y, k_z) = (0, \sim 0.6\pi/c)$ . (c) Temperature dependence of resistivities under various magnetic fields. Inset: The plot of  $\rho(T)/\rho(3\text{ K})$  versus temperature below 3 K.

## PCP3-5

### Effect of non-magnetic rare earth substitution for A site on mixed anion APX superconductors

\*Hijiri Kito<sup>1</sup>, Kenji Kawashima<sup>1,2</sup>, Shigeyuki Ishida<sup>1</sup>, Kunihiro Oka<sup>1</sup>, Hiroshi Fujihisa<sup>1</sup>, Yoshito Goth<sup>1</sup>, Akira Iyo<sup>1</sup>, Hiraku Ogino<sup>1</sup>, Hiroshi Eisaki<sup>1</sup>, Yoshiyuki Yoshida<sup>1</sup>

National Institute of Advanced Industrial Science and Technology (AIST)<sup>1</sup>  
IMRA Material R&D Co., Ltd<sup>2</sup>

Non-magnetic rare earth atom substitution effect for A site in APX-based Zr(P, S)<sub>2</sub> system, Hf(P, Se)<sub>2</sub> and Hf(P, S)<sub>2</sub> superconductors (see Fig. (a)) for improvement of superconducting transition temperature ( $T_c$ ) have been examined.

In Zr (P, Se)<sub>2</sub>[1], the  $T_c$  improvement with partial substitution of a non-magnetic rare earth Lu atom for Zr site and the doping behavior by partial substitution were discussed [2, 3]. By partially substituting a non-magnetic rare earth Lu atom for Zr site in ZrPS, the lattice constants  $a$  and  $c$  decrease monotonically with increasing nominal substitution  $y$  in contrast to the case of non-magnetic rare earth substitution of Zr sites in Zr (P, Se)<sub>2</sub>[1]. It is shown that the maximum  $T_c$  for ZrPS was increased from 3.70 K [1] to 6.36 K (see Fig. (b)). In HfP<sub>1.55</sub>Se<sub>0.45</sub>, lattice constants  $a$  decrease and  $c$  increase monotonically with increasing nominal substitution  $y$  when Lu atoms are partially substituted for Hf atoms.  $T_c$  was also increased from 4.88 K [1] to 5.89 K. In HfP<sub>1.45</sub>S<sub>0.55</sub>, lattice constants  $a$  decrease slightly and  $c$  increase monotonically with increasing nominal substitution  $y$  when Lu atoms are partially substituted for Hf atoms.  $T_c$  was also increased from 3.16 K [1] to 5.86 K. In this presentation, the doping behavior by partial substitution and the increase of  $T_c$  is discussed.

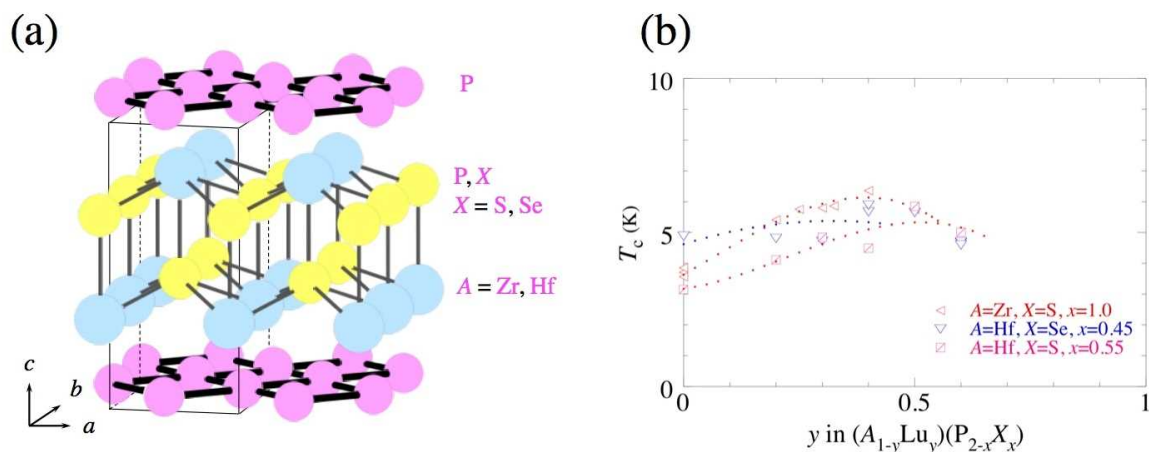


Fig. (a) The crystal structure for PbFCl-type AP<sub>2-x</sub>X<sub>x</sub> (A=Zr, Hf; X=S, Se), (b)  $T_c$  dependence on substitution nominal amount  $y$  for (A<sub>1-y</sub>Lu<sub>y</sub>)(P<sub>2-x</sub>X<sub>x</sub>) (A=Zr, Hf; X=S, Se).

[1] H. Kitô *et al.* J. Phys. Soc. Jpn. 83 (2014) 074713.

[2] H. Kitô *et al.* J. Phys. Conf. Ser. 1054 (2018) 012003.

[3] K. Iwakiri *et al.*, J. Phys. Conf. Ser. 1054 (2018) 012002.

Keywords: substitution effect, Mixed anion superconductor, AP<sub>2-x</sub>X<sub>x</sub> (A=Zr, Hf; X=S, Se)

## PCP3-6

### Electronic Structure of novel Superconductor doped-ZrPSe

\*Izumi Hase<sup>1</sup>, Takashi Yanagisawa<sup>1</sup>, Hijiri Kito<sup>1</sup>, Kousuke Iwakiri<sup>2</sup>, Taichiro Nishio<sup>2</sup>, Hiroshi Fujihisa<sup>1</sup>, Yoshihisa Gotoh<sup>1</sup>, Hiroshi Eisaki<sup>1</sup>, Kenji Kawashima<sup>3</sup>

AIST<sup>1</sup>

Tokyo Sci. Univ.<sup>2</sup>

IMRA Material R&D Co. Ltd.<sup>3</sup>

Recently found superconductor  $ZrP_{2-x}Se_x$  has the same structure with iron-based superconductor LiFeAs.  $ZrP_{1.25}Se_{0.75}$  already has  $T_c \sim 5.8K$ , and the substitution of non-magnetic rare-earth elements for Zr even increases  $T_c$  [1-3]. Moreover, these doped-ZrPSe are also isostructural to ZrSiS, which has Dirac cone protected by non-symmorphic symmetry and three-dimensional Dirac line nodes [4-6].

Therefore, doped-ZrPSe can give a promising platform for investigating the interplay between the Dirac line nodes and the superconductivity. In order to study these points, it is necessary to clarify the electronic structure of doped-ZrPSe.

In this paper we report the results of the first-principles calculations for cation and anion co-doped system  $(Zr_{1-y}Y_y)P(As_{0.25}Se_{0.75})$  using virtual crystal approximation. We found that the density of states at the Fermi level ( $=D(E_F)$ ) shows a dome-shape with respect to the doping concentration  $y$ , as shown in the Figure. This result qualitatively explains the observed  $y$  dependence of  $T_c$ , especially for  $(Zr_{1-y}Y_y)P_{1.25}Se_{0.75}$ . We also found the similarity of the band structure between ZrSiS and doped-ZrPSe. Characteristic band crossing near  $E_F$  along M-G axis, which is found to be the Dirac line node in ZrSiS, is also found in doped-ZrPSe. This result strongly suggests that the superconductivity and the Dirac line node are co-existed in doped-ZrPSe.

[1] H. Kito *et al.* J. Phys. Soc. Jpn. **83** (2014) 074713.

[2] S. Ishida *et al.* Supercond. Sci. Technol. **29** (2016) 055004.

[3] K. Iwakiri *et al.* J. Phys. Soc. Jpn. **1054** (2018) 012002.

[4] L. M. Schoop *et al.* Nat. Commun. **7** (2016) 11696.

[5] Q. Xu *et al.* Phys. Rev. B **92** (2015) 205310.

[6] M. Neupane *et al.* Phys. Rev. B **93** (2016) 201104.

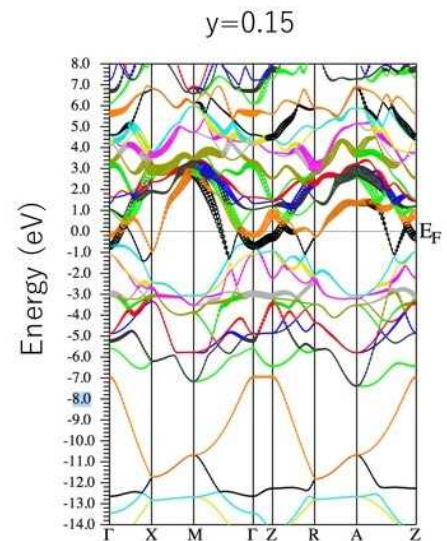
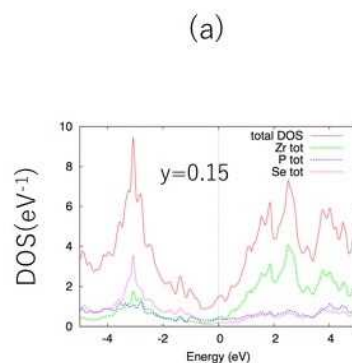
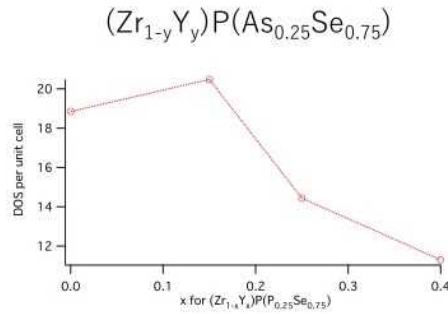


Fig. (a) Density of states at the Fermi level of  $(Zr_{1-y}Y_y)P(As_{0.25}Se_{0.75})$  as a function of  $y$ . (b) Density of states curve of  $(Zr_{0.85}Y_{0.15})P(As_{0.25}Se_{0.75})$ . (c) Energy dispersion of  $(Zr_{0.85}Y_{0.15})P(As_{0.25}Se_{0.75})$ . The width of the band represents the contribution of Zr d- $e_g$  orbitals.

Keywords: doped-ZrPSe, band structure calculation, doping dependence, Dirac line nodes



## PCP3-7

### Index theorem, skyrmions and the Witten effect in topological quantum systems

\*Takashi Yanagisawa<sup>1</sup>

National Institute of Advanced Industrial Science and Technology<sup>1</sup>

Topological materials have attracted much attention from both physicists and mathematicians recently. Topological properties are closely related to the index theorem. The index theorem known as the Atiyah-Singer index theorem is formulated on a manifold without boundary. An interesting phenomenon will appear when considering the index theorem for manifolds with boundaries. We discuss such interesting phenomena in topological systems including a topological superconductor that emerge from the boundary effect. The boundary effect will result in fractional quantization of charges (that is, the existence of magnetic and electric charges). The Witten effect will also be very attractive when the Dirac electron exists, for example, on the surface of topological materials.

Keywords: topological materials, index theorem, monopoles, Witten effect

## PCP3-8

### Many-variable variational Monte-Carlo studies of superconductivity with incipient bands in two-band Hubbard models

\*Daichi Kato<sup>1</sup>, Kazuhiko Kuroki<sup>1</sup>

Osaka university<sup>1</sup>

The "incipient" band, which is not within, but close to the Fermi level, can contribute significantly to spin-fluctuation-mediated pairing [1,3,4]. The incipient band pairing can achieve both strong pairing interactions and light electron mass, possibly resulting in extremely high  $T_c$ . The previous studies argued that superconductivity with incipient bands can be induced by engineering of band structures and carrier concentrations in the weak coupling regime [2]. On the other hand, in the case of the strong coupling regime, the pairing mechanism continues to be a matter of debate. Using a many-variable variational Monte-Carlo method [5] for two-band Hubbard models, we find a possible evidence for a correlation-driven Lifshitz transition at the emergence of superconductivity with incipient bands. We also find that in the presence of large Fermi surfaces in the weak coupling limit, incipient bands tend to stick to the Fermi level when the electron correlation is increased.

[1] K. Kuroki, T. Higashida, and R. Arita, *Phys. Rev. B* **72**, 212509 (2005).

[2] K. Matsumoto, D. Ogura, and K. Kuroki, *Phys. Rev. B* **97**, 014516 (2018).

[3] P.J. Hirschfeld, M.M. Korshukov, and I.I. Mazin, *Rep. Prog. Phys.* **74**, 124508 (2011).

[4] H. Miao et al., *Nat. Comm.* **6**, 6056 (2015).

[5] <https://github.com/issp-center-dev/mVMC>

Keywords: Strongly correlated electron systems, Unconventional superconductivity, Incipient bands, Correlation driven Lifshitz transition

## PCP3-9

### Characterization of rice hull magnetic activated carbon and a rotary drum type magnetic separator with ferromagnetic mesh filters

\*Tatsuya Shiina<sup>1</sup>, Yu Komatsu<sup>1</sup>, Osuke Miura<sup>1</sup>

Electrical Engineering and Computer Science, Graduate School of Systems Design, Tokyo Metropolitan University, Japan<sup>1</sup>

We have developed rice hull magnetic activated carbon (RH-MAC) and studied its adsorption properties for heavy and valuable metal ions in water and magnetic separation properties using a rotary drum type magnetic separator with ferromagnetic mesh filters. RH-MAC was synthesized by impregnating rice hull with an iron nitrate solution and heat-treatments in nitrogen and carbon dioxide atmosphere. In those processes, a lot of meso-pores and nano-size magnetite were generated inside the activated carbon. The magnetization of RH-MAC increased with increasing concentration of iron nitrate solution. The maximum magnetization of RH-MAC3 made from 1.6 mol/L iron nitrate solution reached 22.2 Am<sup>2</sup>/kg at 1 T. RH-MAC had excellent properties for metal ions especially for Cd and Rb ions. To evaluate the magnetic separation properties for RH-MAC, a rotary drum type magnetic separator with the multiple magnetic mesh filters wrapped around a permanent magnet drum was used. It was conformed that capacity rate of RH-MAC increased by multiplying magnetic mesh filters, and the capture rate of RH-MAC3 reached 94% at the flow rate about 900 ml/min with 0.5T and the capture rate reached 98.2% by using triple magnetic mesh filter at the flow rates of 250 ml/min. We also simulated the magnetic particle trajectory by the finite element method for magnetic separation. The simulation results qualitatively matched up to the experimental results. To realize a high speed water processing, we proposed a high magnetic field rotary drum type magnetic separator using a superconducting magnet.

Keywords: Rice hull magnetic activated carbon, High gradient magnetic separation

## PCP4-1

### $^{31}\text{P}$ NMR studies of an optimally doped superconductor $\text{Ba}_{0.5}\text{Sr}_{0.5}\text{Fe}_2(\text{As}_{1-x}\text{P}_x)_2$ ( $x \sim 0.4$ )

\*Yutaka Itoh<sup>1</sup>, Seiji Adachi<sup>2</sup>

Kyoto Sangyo University, Japan<sup>1</sup>

Superconducting Sensing Technology Research Association, Japan<sup>2</sup>

We report  $^{31}\text{P}$  NMR studies of an oriented polycrystalline superconductor of  $\text{Ba}_{0.5}\text{Sr}_{0.5}\text{Fe}_2(\text{As}_{0.6}\text{P}_{0.4})_2$  ( $T_c = 29$  K). The P-substituted  $\text{Ba}_{0.5}\text{Sr}_{0.5}\text{Fe}_2\text{As}_2$  is one of the high- $T_c$  superconductors as well as  $\text{BaFe}_2\text{As}_2$  and  $\text{SrFe}_2\text{As}_2$  [1]. The  $^{31}\text{P}$  nuclear spin-lattice relaxation rate  $1/T_1$  shows an asymptotic behavior of  $a+bT$  ( $a$  and  $b$  are constants) at higher temperatures than about 100 K and the minimum at 40 K with an upturn toward  $T_c$ . The  $a$  term in  $1/T_1$  indicates the presence of two dimensional antiferromagnetic spin fluctuations. The negative Weiss temperature  $\Theta = -15$  K of the Curie-Weiss-type antiferromagnetic spin susceptibility  $\chi(Q) \propto 1/(T + \Theta)$  in the analysis of  $1/T_1 T$  suggests a weakly antiferromagnetic ground state in the suppression of superconductivity. No spin pseudogap characterizes the weakly antiferromagnetic spin fluctuations above  $T_c$ .

[1] S. Adachi, Y. Murai, and K. Tanabe: *Physica C* **483**, 67 (2012).

Keywords: BaSr123, NMR

## PCP4-2

### Composition dependence of penetration depth in $\text{FeSe}_{1-x}\text{Te}_x$ films measured by superconducting resonators

\*Sota Nakamura<sup>1</sup>, Hodaka Kurokawa<sup>1</sup>, Naoki Shikama<sup>1</sup>, Yuki Sakishita<sup>1</sup>, Fuyuki Nabeshima<sup>1</sup>, Atsutaka Maeda<sup>1</sup>

Department of Basic Science, the University of Tokyo<sup>1</sup>

The relation between the structural (nematic) transition and superconductivity have attracted much interest in FeSe. Te-substituted  $\text{FeSe}_{1-x}\text{Te}_x$  exhibits the rapid increase of the superconducting transition temperature,  $T_c$ , upon disappearance of the structural transition caused by the increase of  $x$ [1,2]. The rapid change of  $T_c$  may suggest a possible change in the superconducting properties. However, only thin-film growth techniques make it possible to obtain single crystalline samples of  $\text{FeSe}_{1-x}\text{Te}_x$  in the composition region [1,2]. In this study, we measured temperature dependence and its magnitude of the penetration depth in  $\text{FeSe}_{1-x}\text{Te}_x$  films to investigate the relation between superconducting gap structure and the structural transition, by the microwave transmission line resonator technique. [3]. We fabricated coplanar resonators of  $\text{FeSe}_{1-x}\text{Te}_x$  films by using a sandblasting method and obtained the penetration depth from the resonant frequency. The merit of this technique is that the absolute magnitude of the penetration depth is obtained without the aid of any other measurement.

The measured penetration depth as a function of temperature was well represented by the power-law,  $\lambda(T) = \lambda(0) + AT^n$  for  $0.1 < T/T_c < 0.2$  which agrees with the so far established behavior[4]. Figure.1 shows the low-temperature-limiting  $\lambda(0)$  and the power,  $n$ , as a function of Te content,  $x$ , together with  $T_c$ . It is remarkable that  $\lambda(0)$  does not change largely when we crossed the orthorhombic-tetragonal boundary, which is in contrast to the  $T_c$  behavior. As for the power,  $n$ , the end material FeSe, exhibiting the structural transition, shows  $n = 1.55$ , whereas, other samples without structural transition shows  $n > 2$ . We will discuss the implications of these results, in terms of the change in the structure of the superconducting gap function as a function of Te substitution.

[1] Y. Imai, *et al.*, *Sci. Rep.* **7**, 46653 (2017).

[2] Y. Imai, *et al.*, *PNAS*, **112**, 1937(2015).

[3] K. Watanabe, *et al.*, *Jpn. J. Appl. Phys.* **33**, 5708 (1994).

[4] V. Mishra *et al.*, *Phys. Rev. B* **84**, 014524(2011).

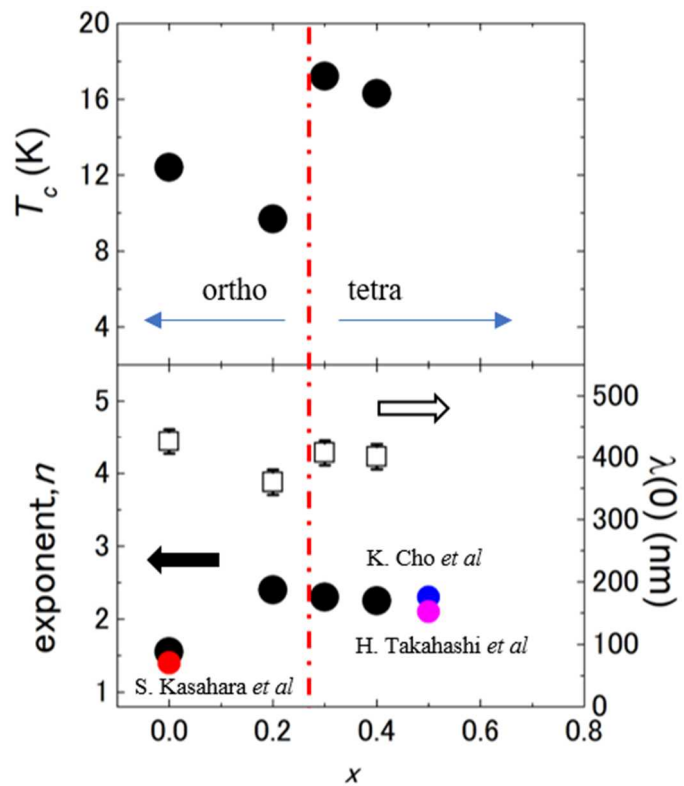


Fig1.  $x$  dependence of  $T_c$ ,  $\lambda(0)$  and exponent,  $n$

Keywords: iron-based superconductor, microwave, superconducting gap

## PCP4-3

### Transport properties of electron-doped $\text{FeSe}_{1-x}\text{S}_x$ and $\text{FeSe}_{1-y}\text{Te}_y$ films with electric double layer transistor

\*Naoki Shikama<sup>1</sup>, Yuuki Sakishita<sup>1</sup>, Fuyuki Nabeshima<sup>1</sup>, Atustaka Maeda<sup>1</sup>

Department of Basic Science, the University of Tokyo, Japan<sup>1</sup>

FeSe shows the structural phase transition without an antiferromagnetic transition unlike other iron-based superconductors, and provides a unique playground to study the role of the structural phase (nematic) transition. We found that  $T_c$  of  $\text{FeSe}_{1-x}\text{S}_x$  films monotonically decreases when the structural phase transition disappears [1], while that of  $\text{FeSe}_{1-y}\text{Te}_y$  films jumps just after the structural phase transition disappears [2]. The contrastive behavior between  $\text{FeSe}_{1-x}\text{S}_x$  and  $\text{FeSe}_{1-y}\text{Te}_y$  may suggest that the structural phase transition does not play a universal role for  $T_c$ .

It is well-known that electron doping to FeSe increases its  $T_c$  up to 40-45 K [3]. It is of great interest to investigate the  $T_c$  behavior in such a high  $T_c$  electron-doped FeSe upon S/Te substitution, especially at the orthorhombic-tetragonal boundary. In this study, we fabricated the electric double layer transistor (EDLT) configuration of  $\text{FeSe}_{1-x}\text{S}_x$  and  $\text{FeSe}_{1-y}\text{Te}_y$  films on  $\text{LaAlO}_3$  substrate, and measured transport properties under gate voltage to investigate the behavior of  $T_c$  of the tetragonal phase and orthorhombic phase for the electron-doped FeSe films.

Figure 1 shows the temperature dependence of the electron-doped  $\text{FeSe}_{0.89}\text{S}_{0.11}$ ,  $\text{FeSe}_{0.8}\text{Te}_{0.2}$  [4] and FeSe films. Electron-doped  $\text{FeSe}_{0.89}\text{S}_{0.11}$  and  $\text{FeSe}_{0.8}\text{Te}_{0.2}$  also show high  $T_c$ . Figure 2 shows the phase diagram of the electron-doped  $\text{FeSe}_{1-x}\text{S}_x$  and  $\text{FeSe}_{1-y}\text{Te}_y$  films.  $T_c$ 's of electron doped  $\text{FeSe}_{1-x}\text{S}_x$  and  $\text{FeSe}_{1-y}\text{Te}_y$  films are lower than that of FeSe. Unlike the "bulk"  $\text{FeSe}_{1-x}\text{S}_x$  and  $\text{FeSe}_{1-y}\text{Te}_y$  films,  $T_c$  gradually decreases as  $x$  or  $y$  increases. We will discuss the origin of the difference in the behavior of  $T_c$  at the orthorhombic-tetragonal boundary between the "bulk" and electron-doped films.

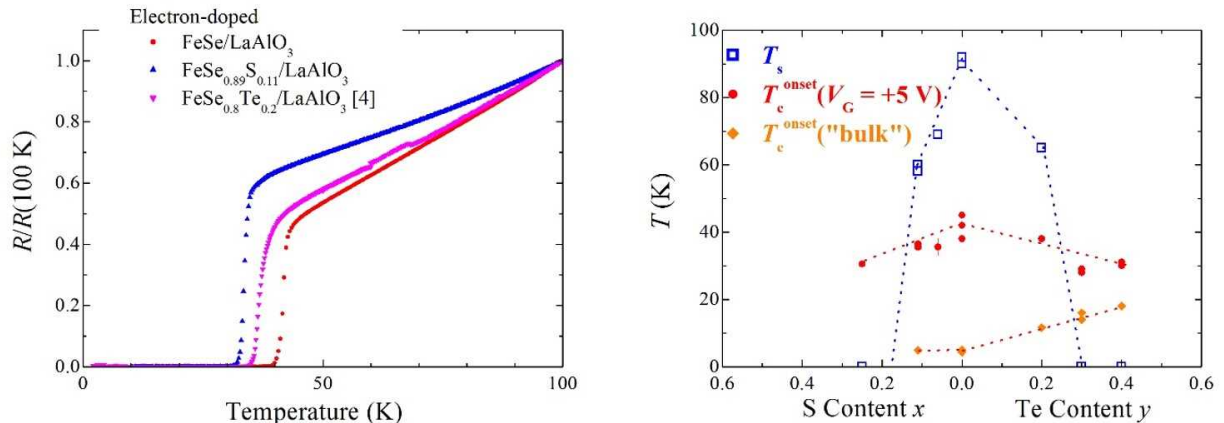


Fig. 1 Temperature dependence of resistivity of the electron-doped  $\text{FeSe}_{0.89}\text{S}_{0.11}$ ,  $\text{FeSe}_{0.8}\text{Te}_{0.2}$  [4] and FeSe under gate voltage  $V_G = +5$  V.

Fig. 2 Phase diagram of the electron-doped  $\text{FeSe}_{1-x}\text{S}_x$  and  $\text{FeSe}_{1-y}\text{Te}_y$  films.

[1] F. Nabeshima *et al.*, J. Phys. Soc. Jpn. **87**, 073704 (2018). [2] Y. Imai *et al.*, Sci. Rep. **7**, 46653 (2017).

[3] J. Shiogai *et al.*, Nat. Phys. **12**, 42(2016). [4] S. Kouno *et al.*, Sci. Rep. **8**, 14731 (2018).

Keywords: iron chalcogenide, thin films, electric double layer transistor

## PCP4-4

### Effect of in-plane strain on transport properties of FeSe single crystals

\*Yuki Ohata<sup>1</sup>, Masamichi Nakajima<sup>1</sup>, Setsuko Tajima<sup>1</sup>

Department of Physics, Osaka University, Japan<sup>1</sup>

The band structure of iron-based superconductors is sensitive to the local crystal structure. A good example is a thin film of FeSe with epitaxial strain. From angle-resolved photoemission spectroscopy measurements, a systematic change of the band structure was observed according to the degree of in-plane strain [1]. Reflecting the band structure, superconducting transition temperature  $T_c$  also shows a systematic change with in-plane strain [2]. Although a study using thin films turned out to be effective, the quality of the film varies depending on substrate materials, and compounds to which such an approach is applicable would be limited. Here we report the electronic transport properties for FeSe single crystals with applying biaxial strain. FeSe single crystals were attached on two kinds of substrates (soda-lime glass and polycarbonate sheets) using cyanoacrylate adhesives. Since each substrate material has a different thermal-expansion coefficient, different compressive strain is imposed on FeSe at low temperatures, the magnitude of which is 0.38% for glass and 0.85% for polycarbonate. The compressive strain enhances  $T_c$  from 8.5 K for the strain-free sample to 13.1 K for the sample on polycarbonate, consistent with the study of the thin films [2]. We analyzed the magnetoresistance and the Hall effect at 30 K using a three-carrier model, in which one hole and two electron carriers are considered. The result for the strain-free sample is in agreement with the previous study [3]. For the samples on glass and polycarbonate, hole and electron carrier densities systematically increase with compressive strain, which means that we definitely succeeded in controlling the band structure of single-crystalline FeSe.

[1] G. N. Phan *et al.*, Phys. Rev. B **95**, 224507 (2017).

[2] F. Nabeshima *et al.*, Jpn. J. Appl. Phys. **57**, 120314 (2018).

[3] M. D. Watson *et al.*, Phys. Rev. Lett. **115**, 027006 (2015).

Keywords: iron-based superconductor, FeSe, in-plane strain, transport property

## PCP4-5

### Low-oxygen Annealing Process of FeSe Superconducting Materials

\*Botao Shao<sup>1</sup>, Shengnan Zhang<sup>1</sup>, Jixing Liu<sup>1</sup>, Jianqing Feng<sup>1</sup>, Chenshan Li<sup>1</sup>

Northwest Institute for Non-Ferrous Metal Research, Xi'an 710016, China<sup>1</sup>

Among various Fe-based superconducting materials, FeSe-based superconducting materials are considered to be ideal candidates for the exploring of superconducting mechanism due to their simplest crystal structure and tunable superconducting critical temperature. Besides, FeSe-based superconductors also can be adopted for practical applications based on their advantages, such as high upper critical field, high current capacity under high field, and low anisotropy. Therefore, it is necessary to optimize the fabrication process and superconducting performance of FeSe superconducting materials. Based on our previous study, with the introduction of high energy ball milling process and the change of initial Fe:Se ratio in the FeSe based superconductor, the content of tetragonal phase can be effectively improved. However, the existence of interstitial irons in the superconducting tetragonal phase  $\beta$ -FeSe can not be eliminated, which have obvious negative influence on the performance of the FeSe-based superconducting material. In this experiment, FeSe bulks with different Fe:Se ratios of 1.00, 1.05, 1.10, 1.15 and 1.20 were prepared with solid state sintering process. By comparing the superconducting properties of these sample both before and after annealing, the best Fe:Se ratio was determined to be 1.15. On this basis, many important parameters, including the annealing temperature, annealing time and oxygen partial pressure of the annealing atmosphere were systematically optimized. The phase composition and microstructure of the system were characterized after annealing, combined with the analysis of superconducting properties measurements. The results showed that during the low-oxygen annealing process, the interstitial irons inside the system was induced and diffused to the surface, which finally reduced the interstitial iron content of the tetragonal phase  $\beta$ -FeSe, thus increased the superconducting phase content and the critical transition temperature of the system. The optimum annealing process of 400 °C-5 %O<sub>2</sub>-10 h for Fe<sub>1.15</sub>Se samples was obtained.

Keywords: Fe-based superconducting materials, FeSe, interstitial irons, annealing



## PCP4-6

### Critical current densities and superconducting properties for Fe (Te<sub>1-x</sub>Se<sub>x</sub>)<sub>1-y</sub>S<sub>y</sub>

\*Kota Miyaki<sup>1</sup>, Osuke Miura<sup>1</sup>, Yoshikazu Mizuguchi<sup>2</sup>

Department of Electrical Engineering and Computer Science, Tokyo Metropolitan University, Japan.<sup>1</sup>

Department of physics, Tokyo Metropolitan University, Japan<sup>2</sup>

We have fabricated Fe(Te<sub>1-x</sub>Se<sub>x</sub>)<sub>1-y</sub>S<sub>y</sub> high-quality bulk single crystals by the melting method with low heat treatment. First, three single crystals of  $x = 0.4, 0.45,$  and  $0.46$  were fabricated with the composition ratio of Fe (Te<sub>1-x</sub>Se<sub>x</sub>)<sub>1-y</sub>S<sub>y</sub> as  $y = 0$ , and their superconducting properties were evaluated. Temperature dependence of magnetization showed that low- $T_c$  region exists inside the crystals for  $x=0.4$  and  $0.45$ . The highest  $T_c$  of 14.4 K was obtained for  $x=0.45$  crystal, and it decreased for  $x=0.4$  and  $0.46$ . The highest  $J_c$  under the magnetic field parallel to the  $c$ -axis at 4.2 K was obtained for  $x=0.4$  crystal, and achieved 0.15 and 0.05 MA / cm<sup>2</sup> at 0 T and 7 T respectively. At high temperature of 9 K,  $x=0.4$  crystal had the highest  $J_c$  up to 3 T. To further improvement of superconducting properties we studied to fabricate single crystals in which the composition ratio of Fe (Te<sub>0.6</sub>Se<sub>0.4</sub>)<sub>1-y</sub>S<sub>y</sub> changes to  $y = 0.05, 0.1, 0.15$  and  $0.2$ .

Keywords: Single crystal, Fe (Te<sub>1-x</sub>Se<sub>x</sub>)<sub>1-y</sub>S<sub>y</sub>

## PCP4-7

### Effects of Point Defects Introduced by Co-doping and Proton Irradiation in $\text{CaKFe}_4\text{As}_4$

\*Yuto Kobayashi<sup>1</sup>, Sunseng Pyon<sup>1</sup>, Ayumu Takahashi<sup>1</sup>, Tsuyoshi Tamegai<sup>1</sup>

Department of Applied Physics, The University of Tokyo<sup>1</sup>

Introduction of defects to superconductors enhances their critical current density ( $J_c$ ). Recently, a new iron-based superconductor,  $\text{CaKFe}_4\text{As}_4$ , with a new type of structure is found [1], and its  $J_c$  is evaluated to be  $\sim 2 \text{ MA/cm}^2$  at 2 K and self-field [2].

To enhance  $J_c$  in  $\text{CaKFe}_4\text{As}_4$ , we introduced point defects by chemical and physical methods. In the chemical method, we have grown high-quality single crystals in which a part of Fe is replaced by Co up to 9 %. Co-doping is believed to make the inherently overdoped  $\text{CaKFe}_4\text{As}_4$  closer to optimally doped one. Figure 1 shows  $J_c$  -  $H$  properties of  $\text{CaK}(\text{Fe}_{1-x}\text{Co}_x)_4\text{As}_4$  up to  $x = 0.09$  at  $T = 5 \text{ K}$ . A relatively strong magnetic field dependence of  $J_c$  in the pristine  $\text{CaKFe}_4\text{As}_4$  is weakened by modest Co-doping ( $0.03 < x < 0.07$ ), leading to large  $J_c$  at high fields. It clearly demonstrates that the introduced Co work as point defects.

In the physical method, 3 MeV protons are irradiated into  $\text{CaKFe}_4\text{As}_4$ , which are known to produce point defects. In order to compare effects of two different kinds of point defects on  $J_c$  and get some insight into the effect of coexisting point defects, the pristine, 3% Co-doped, and 7% Co-doped crystals are irradiated. Figure 2 shows the irradiation dose dependence of  $J_c$  of these three crystals at  $T = 5 \text{ K}$  and  $H = 4 \text{ T}$ .  $J_c$  of all these three crystals is enhanced by the introduction of point defects by protons up to  $0.1 \times 10^{16} \text{ ions/cm}^2$ . It means that proton-induced point defects cooperatively pin vortices with chemically induced point defects. Quantitative comparison shows that 7 % Co-doping has nearly the same effect as that induced by  $0.1 \times 10^{16} \text{ ions/cm}^2$  proton irradiation.

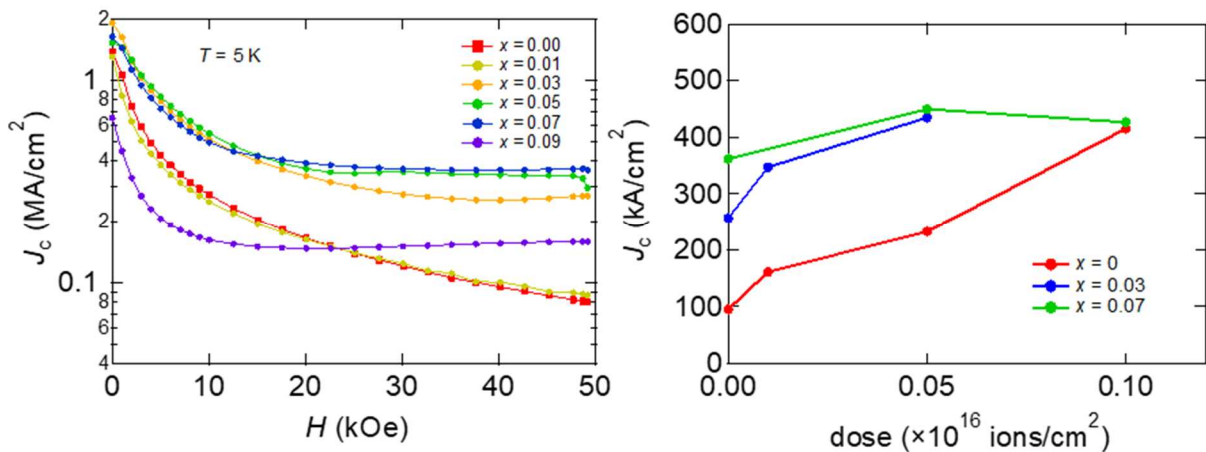


Figure 1: Magnetic field dependence of  $J_c$  in  $\text{CaK}(\text{Fe}_{1-x}\text{Co}_x)_4\text{As}_4$  at  $T = 5 \text{ K}$ .

Figure 2: Proton irradiation dose dependence of  $J_c$  in  $\text{CaK}(\text{Fe}_{1-x}\text{Co}_x)_4\text{As}_4$  at  $T = 5 \text{ K}$  and  $H = 4 \text{ T}$ .

[1] A. Iyo *et al.*, J. Am. Chem. Soc. **138**, 3410 (2016).

[2] S. Pyon *et al.*, Phys. Rev. B **99**, 104506 (2019).

Keywords: Iron-based superconductor, critical current density, particle irradiation, point defects

## PCP4-8

### Effects of Splayed Columnar Defects on Critical Current Density in $\text{CaKFe}_4\text{As}_4$

\*Yuto Kobayashi<sup>1</sup>, Sunseng Pyon<sup>1</sup>, Ayumu Takahashi<sup>1</sup>, Tsuyoshi Tamegai<sup>1</sup>

\*Ayumu Takahashi<sup>1</sup>, Sunseng Pyon<sup>1</sup>, Yuto Kobayashi<sup>1</sup>, Tadashi Kambara<sup>2</sup>, Atsushi Yoshida<sup>2</sup>, Satoru Okayasu<sup>3</sup>, Ataru Ichinose<sup>4</sup>, Tsuyoshi Tamegai<sup>1</sup>

Department of Applied Physics, The University of Tokyo, 7-3-1 Hongo, Bunkyo-ku, Tokyo 113-8656, Japan<sup>1</sup>

Nishina Center, RIKEN, 2-1 Hirosawa, Wako, Saitama 351-0198, Japan<sup>2</sup>

Advanced Science Research Center, Japan Atomic Energy Agency, Tokai, Ibaraki 319-1195, Japan<sup>3</sup>

Central Research Institute of Electric Power Industry, Nagasaka, Yokosuka, Kanagawa 240-0196, Japan<sup>4</sup>

Introduction of columnar defects to superconductors through particle irradiation enhances their critical current density ( $J_c$ ) [1,2]. Further enhancement of  $J_c$  by dispersing the direction of columnar defects has been confirmed in cuprates  $\text{YBa}_2\text{Cu}_3\text{O}_{7-\delta}$  [3] and iron-based superconductors (IBSs)  $\text{Ba}_{1-x}\text{K}_x\text{Fe}_2\text{As}_2$  [4] single crystals. Moreover, in such systems with splayed columnar defects, an anomalous peak effect in  $J_c$  at a certain magnetic field determined by the irradiation dose as well as an in-plane anisotropy of  $J_c$  between those parallel and perpendicular to the splay direction were observed [4, 5].

Here, we introduce splayed columnar defects to  $\text{CaKFe}_4\text{As}_4$  single crystals, which was recently found as a new type of IBSs (1144-type IBS) [6], by irradiating 2.6 GeV U and 320 MeV Au ions and measure their  $J_c$  properties.  $J_c$  in  $\text{CaKFe}_4\text{As}_4$  is also enhanced by splayed columnar defects at 5 K under zero field from 1.5 MA/cm<sup>2</sup> in the pristine crystal to 17 MA/cm<sup>2</sup> as shown in Fig. 1(a) for the case of  $\theta_{\text{CD}} = \pm 20^\circ$  and  $B_\Phi = 4 \text{ T} + 4 \text{ T}$ . It should be noted that the anomalous peak effect at  $\sim 1/3 B_\Phi$  as observed in  $\text{Ba}_{0.6}\text{K}_{0.4}\text{Fe}_2\text{As}_2$  (Fig. 1(b)) in the same irradiation condition disappears in  $\text{CaKFe}_4\text{As}_4$ . We interpret that the suppression of the anomalous peak effect in  $\text{CaKFe}_4\text{As}_4$  is due to the presence of planar defects parallel to the  $ab$ -plane, which is unique to this material. We also compare the in-plane anisotropy of  $J_c$  in  $\text{Ba}_{0.6}\text{K}_{0.4}\text{Fe}_2\text{As}_2$  and  $\text{CaKFe}_4\text{As}_4$  with splayed columnar defects.

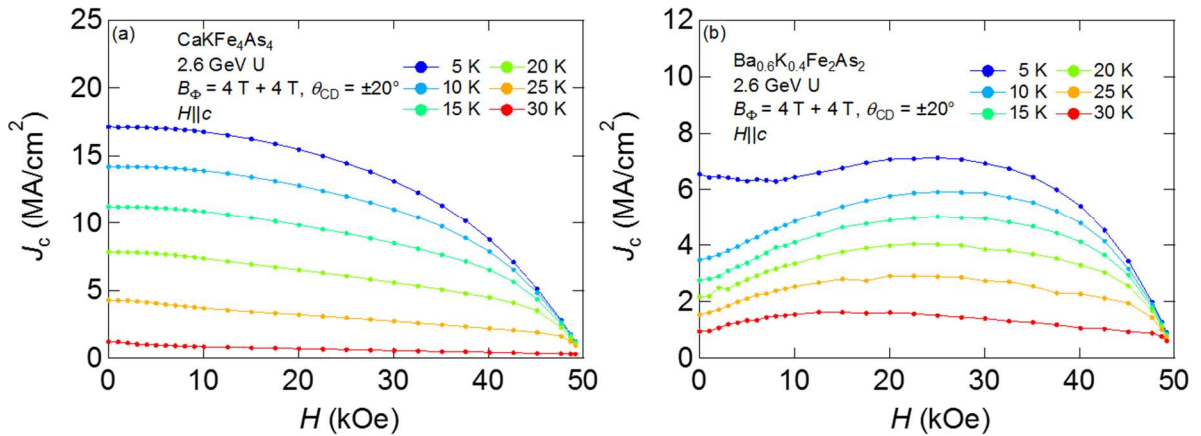


Fig. 1: Magnetic field dependences of  $J_c$  at various temperatures in (a)  $\text{CaKFe}_4\text{As}_4$  and (b)  $\text{Ba}_{0.6}\text{K}_{0.4}\text{Fe}_2\text{As}_2$  that are irradiated by 2.6 GeV U ions with  $B_\Phi = 4 \text{ T} + 4 \text{ T}$  and  $\theta_{\text{CD}} = \pm 20^\circ$ .

[1] L. Civale *et al.*, Phys. Rev. Lett. **67**, 648 (1991). [2] T. Tamegai *et al.*, Supercond. Sci. Technol. **25**, 084008 (2012). [3] L. Krusin-Elbaum *et al.*, Phys. Rev. Lett. **76**, 2563 (1996).

[4] A. Park *et al.*, Physica C **530**, 58 (2016). [5] A. Park *et al.*, Phys. Rev. B **97**, 064516 (2018).

[6] A. Iyo *et al.*, J. Am. Chem. Soc. **138**, 3410 (2016).

Keywords: Iron-based superconductors, Particle irradiation, Critical current density, Columnar defect

## PCP5-1

### Superconductivity in Uncollapsed Tetragonal $\text{LaFe}_2\text{As}_2$

\*Akira Iyo<sup>1</sup>, Shigeyuki Ishida<sup>1</sup>, Hiroshi Fujihisa<sup>1</sup>, Yoshito Gotoh<sup>1</sup>, Izumi Hase<sup>1</sup>, Yoshiyuki Yoshida<sup>1</sup>, Hiroshi Eisaki<sup>1</sup>, Kenji Kawashima<sup>1,2</sup>

National Institute of Advanced Industrial Science and Technology (AIST)<sup>1</sup>  
IMRA Material R&D Co., Ltd.<sup>2</sup>

We report synthesis, crystal structure and superconductivity in  $\text{ThCr}_2\text{Si}_2$ -type  $\text{LaFe}_2\text{As}_2$  (La122). La122 was synthesized at 960°C for 1.5 h under a pressure of 3.4 GPa. An as-synthesized La122, which was *not* a superconductor, had a collapsed tetragonal structure with a short  $c$ -axis length of 11.0144(4) Å as observed in  $\text{CaFe}_2\text{As}_2$  under pressure. The collapsed tetragonal transformed into an uncollapsed tetragonal by annealing the as-synthesized La122 at 500°C. The  $c$ -axis length remarkably extended to 11.7317(4) Å and superconductivity emerged at 12.1 K in the uncollapsed tetragonal La122. Ab-initio electronic structure calculations showed that a cylindrical hole-like Fermi-surface around the  $\Gamma$  point that plays an important role for an  $s_{\pm}$  wave pairing in iron-based superconductors was missing in the uncollapsed tetragonal La122 due to heavily electron-doping. Superconductivity in La122 may be closely related to that induced in  $\text{CaFe}_2\text{As}_2$  under pressure.

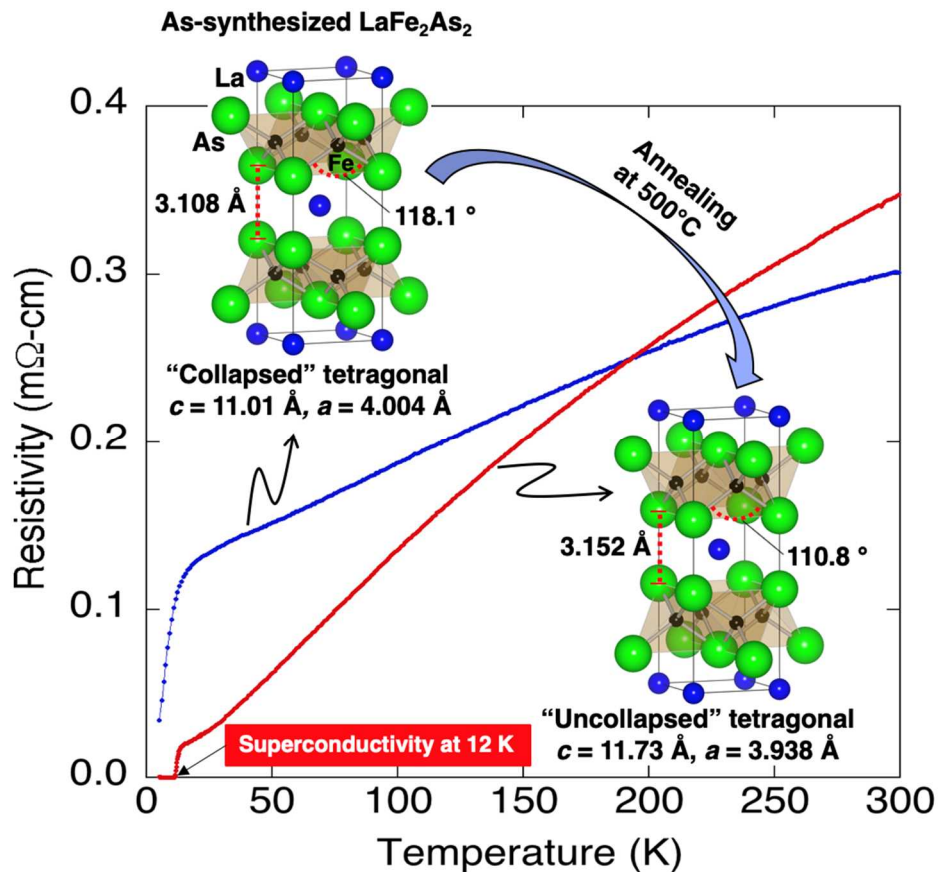


Figure 1 Temperature dependence of resistivity and crystal structures for as-synthesized and annealed  $\text{LaFe}_2\text{As}_2$ .

Keywords: New superconductor, 122-type Iron-based superconductor, Collapsed tetragonal structure, Band structure calculation

## PCP5-2

### Electronic phase diagram of $\text{Sr}_2\text{V}_{1-x}\text{Sc}_x\text{FeAsO}_3$

\*Masamichi Nakajima<sup>1</sup>, Taihei Wakimura<sup>1</sup>, Shigeki Miyasaka<sup>1</sup>, Setsuko Tajima<sup>1</sup>

Osaka University, Japan<sup>1</sup>

In iron-based superconductors, various electronic orders emerge in an iron layer due to intertwined electronic degrees of freedom. Iron-based superconductors with a perovskite-type thick blocking layer, e.g.  $\text{Sr}_2\text{VFeAsO}_3$ , offer various possibilities of chemical substitution into the blocking layer, which keeps the iron layer clean, and are suitable for a study to investigate the electronic state in the iron layer.  $\text{Sr}_2\text{VFeAsO}_3$  shows superconductivity, while non-superconducting isostructural counterpart  $\text{Sr}_2\text{ScFeAsO}_3$  exhibits antiferromagnetic ordering [1]. In this work, we synthesized polycrystalline  $\text{Sr}_2\text{V}_{1-x}\text{Sc}_x\text{FeAsO}_3$  and studied how the electronic state evolves on going from  $\text{Sr}_2\text{VFeAsO}_3$  to  $\text{Sr}_2\text{ScFeAsO}_3$ . With increasing Sc content  $x$ , a superconducting transition temperature systematically decreases. We revealed that the antiferromagnetic phase shows up for  $x > 0.45$  adjacent to the superconducting phase.  $\text{Sr}_2\text{VFeAsO}_3$  shows not only superconductivity but also an enigmatic electronic order at  $T_0 \sim 150$  K. The phase transition at  $T_0$  is present up to  $x = 0.17$  and disappears with further Sc substitution. The suppression of the transition is slower than the case for Cr substitution [2]. In light of a proposed scenario that the transition at  $T_0$  arises from frustration between stripe-type and Neel-type antiferromagnetic fluctuations of Fe and V spins, respectively [3], the frustration is lifted by non-magnetic Sc substitution at V sites, giving rise to the suppression of the transition.

[1] J. Munevar *et al.*, Phys. Rev. B **84**, 024527 (2011).

[2] T. Wakimura *et al.*, Supercond. Sci. Technol. **32**, 064003 (2019).

[3] J. M. Ok *et al.*, Nat. Commun. **8**, 2167 (2017).

Keywords: Iron-based superconductors,  $\text{Sr}_2\text{VFeAsO}_3$ , Chemical substitution

## PCP5-3

### Study of $\mu$ SR in Iron-Based Superconductor $\text{LaFeAs}_{1-x}\text{P}_x\text{O}_{0.9}\text{F}_{0.1}$

\*Shinzaburo Sano<sup>1</sup>, Dai Tomono<sup>2</sup>, Wataru Higemoto<sup>3,4</sup>, Tsuyoshi Kawashima<sup>1</sup>, Masamichi Nakazima<sup>1</sup>, Shigeki Miyasaka<sup>1</sup>, Akira Sato<sup>1</sup>, Koichiro Shimomura<sup>5</sup>, Setsuko Tajima<sup>1</sup>

Department of Physics, Osaka University, 1-1 Machikaneyama-cho, Toyonaka, Osaka 560-0043, Japan<sup>1</sup>

Research Center for Nuclear Physics (RCNP), Osaka University, 10-1 Mihogaoka, Ibaraki, Osaka 567-0047, Japan<sup>2</sup>

Advanced Science Research Center, Japan Atomic Energy Agency, 2-4, Ooaza Shirakata, Tokai, Naka, Ibaraki 319-1195, Japan<sup>3</sup>

Department of Physics, Tokyo Institute of Technology 2-12-1, Ohokayama, Meguro, Tokyo 152-8550, Japan<sup>4</sup>

Institute of Materials Structure Science, KEK, 1-1 Oho, Tsukuba, Ibaraki 305-0801, Japan<sup>5</sup>

In the iron-based superconductors  $\text{LaFeAs}_{1-x}\text{P}_x\text{O}_{1-y}\text{F}_y$ , the electron doping level and the local crystal structure can be controlled by the F substitution for O and P substitution for As. With these chemical substitutions, Fermi surface (FS) topology changes giving three different superconducting (SC) phases [1]. For example, at  $y=0.1$ , the As-rich compounds are in the first superconducting phase (SC1), while the P-rich compounds are in the second superconducting phase (SC2) [2]. The theoretical study by Kuroki and coworkers has indicated that the different nesting in LaFeAsO-type and LaFePO-type FSs induces the different SC gap symmetries, i.e., full and nodal gaps [3].

In the present work, we have investigated the difference between SC gap symmetry in SC1 and SC2 using  $\mu$ SR measurement in  $\text{LaFeAs}_{1-x}\text{P}_x\text{O}_{0.9}\text{F}_{0.1}$  ( $x=0.0\sim 0.8$ ). The  $\mu$ SR measurement were performed at TRIUMF in Canada and Research Center for Nuclear Physics (RCNP), Osaka University in Japan using a He gas-flow cryostat in a magnetic field of 250G. At  $x=0$ , the temperature ( $T$ ) dependence of the muon spin relaxation rate  $\sigma$  shows a rapid increase with decreasing  $T$  below  $T_c$  and a saturation at low temperatures, indicating the s-wave behavior. In contrast,  $\text{LaFeAs}_{1-y}\text{P}_y\text{O}_{0.9}\text{F}_{0.1}$  ( $y=0.2\sim 0.8$ ) show the slightly different  $T$  dependence of the relaxation rate  $\sigma$ . In these P doping compounds, the  $T$  dependence of the relaxation rate  $\sigma$  does not show a clear saturation at low temperatures and cannot be fitted by the simple s-wave model. These results suggest that the P-doped compounds have several SC gaps with different gap sizes or a nodal SC gap, and the SC gap symmetries in the SC1 and SC2 phases may be different.

[1] S. Miyasaka *et al.*, Phys. Rev. B **95**, 214515 (2017).

[2] K. T. Lai *et al.*, Phys. Rev. B **90**, 064504 (2014).

[3] K. Kuroki *et al.*, Phys. Rev. B **79**, 224511 (2009).

Keywords: Iron-based superconductors,  $\mu$ SR, superconducting gap

## PCP5-4

### Synthesis of the Mother Phase of the Iron-Based Superconductor, SmFeAsO via Low-Temperature Heat Treatment

\*Ryosuke Sakagami<sup>1,2</sup>, Simon R. Hall<sup>2</sup>, Jason Potticary<sup>2</sup>, Masanori Matoba<sup>1</sup>, Yoichi Kamihara<sup>1,2,3</sup>

Department of Applied Physics and Physico-Informatics, Faculty of Science and Technology, Keio University, Japan<sup>1</sup>

Complex Functional Materials Group, School of Chemistry, Univ. of Bristol, United Kingdom<sup>2</sup>

Center for Spintronics Research Network (CSRN), Keio University, Japan<sup>3</sup>

Low-temperature heat treatment of the iron-based superconductor<sup>1,2</sup> is effective for fabrication of the iron-based superconducting wires and tapes with high transport critical current density. To determine the lowest temperature for the formation of a crystallographic phase of SmFeAsO, we demonstrate the evolution of the SmFeAsO during a solid-state reaction in a mixture of SmAs, Fe<sub>2</sub>As, FeAs, and Sm<sub>2</sub>O<sub>3</sub> heated to heat-treatment temperatures from 580°C to 950°C. X-ray diffraction (XRD) measurements indicated that a significant increasing of the SmFeAsO phase appears at heat-treatment temperatures not lower than 620°C. Scanning electron microscopy (SEM) with energy-dispersive X-ray spectroscopy (EDX) analysis showed a compound uniformly composed of samarium, iron, arsenic, and oxygen (Sm-Fe-As-O) having surface areas on the order of 10 μm<sup>2</sup> surrounded by grains of SmAs, Fe<sub>2</sub>As, FeAs, and Sm<sub>2</sub>O<sub>3</sub> in a sample heated to 580°C. This work therefore shows the SmFeAsO phase grows at 620°C and suggested that the SmFeAsO phase emerge at 580°C.

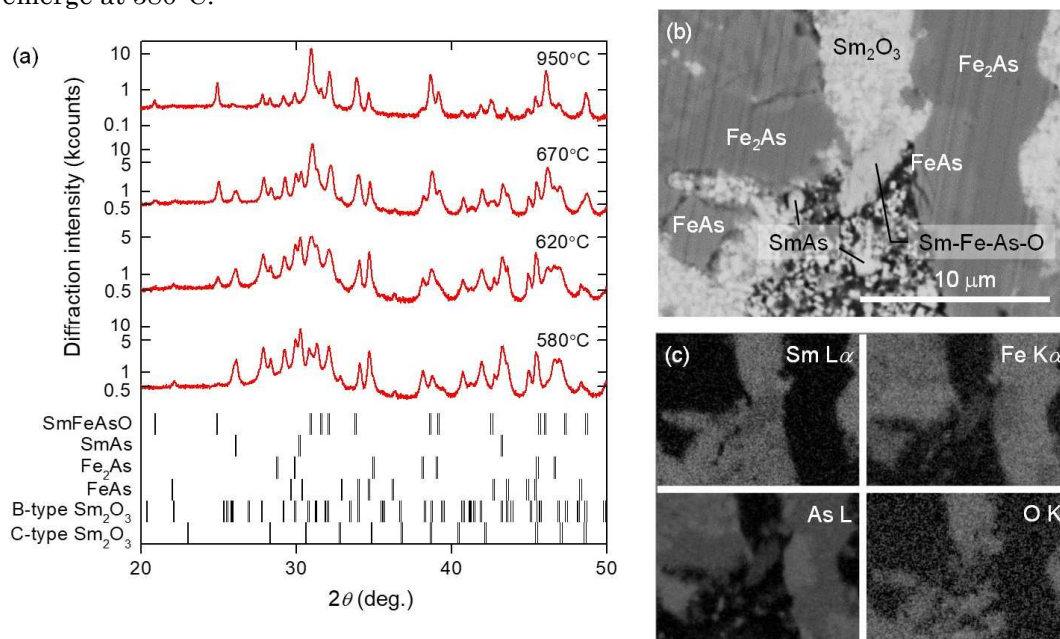


Fig. (a) Heat-treatment temperature dependence of X-ray diffraction (XRD) patterns at room temperature of the pulverized samples heated from SmAs, Fe<sub>2</sub>As, FeAs, and Sm<sub>2</sub>O<sub>3</sub> as starting materials. The vertical bars at the bottom represent diffractions due to SmFeAsO, SmAs, Fe<sub>2</sub>As, FeAs, B-type Sm<sub>2</sub>O<sub>3</sub>, and C-type Sm<sub>2</sub>O<sub>3</sub> from above. Heat-treatment temperatures are denoted near the patterns. (b) Back-scattered electron (BSE) scanning electron microscope (SEM) image and (c) energy-dispersive X-ray spectroscopy (EDX) elemental mapping of a polished sample heated to 580°C from SmAs, Fe<sub>2</sub>As, FeAs, and Sm<sub>2</sub>O<sub>3</sub> as starting materials.

[1] Y. Kamihara *et al.*, *J. Am. Chem. Soc.* **130**, 3296 (2008).

[2] Z.-A. Ren *et al.*, *Chin. Phys. Lett.* **25**, 2215 (2008).

Keywords: Iron-Based Superconductor, Solid-State Reaction, Low-Temperature Heat Treatment, Crystallographic phase

## Fabrication of superconducting NdFeAs(O,H) epitaxial thin films

\*Keisuke Kondo<sup>1</sup>, Seiya Motoki<sup>1</sup>, Takafumi Hatano<sup>1</sup>, Takahiro Urata<sup>1</sup>, Kazumasa Iida<sup>1,2</sup>, Hiroshi Ikuta<sup>1</sup>

Department of Material Physics, Nagoya University, Japan<sup>1</sup>  
JST CREST, Japan<sup>2</sup>

$LnFeAs(O,F)$  ( $Ln$ : lanthanide) exhibits the highest superconducting transition temperature ( $T_c$ ) up to 58 K among the Fe-based superconductors. However, the amount of F that can be substituted for O is limited to about 20% and it is difficult to investigate the physical properties in the overdoped region. On the other hand, Hanna *et al.* reported that the substitution limit can be increased to about 80% by changing the substituting elements from F to H[1]. Furthermore, SmFeAs(O,H) epitaxial thin films on MgO (001) substrates were grown recently using a topotactic reaction  $SmFeAsO + (x/2)CaH_2 \rightarrow SmFeAs(O_{1-x}H_x) + (x/2)CaO$ [2]. It is interesting whether  $LnFeAs(O,H)$  thin films for other  $Ln$  can be realized. Here, we report on the fabrication of NdFeAs(O,H) thin films using the same H doping method[2], and their structural and electro-magnetic properties.

Parent NdFeAsO thin films having a thickness of 20 - 30 nm were grown on MgO (001) substrates by molecular beam epitaxy[3]. The NdFeAsO film and CaH<sub>2</sub> powder were sealed in an evacuated quartz tube. The whole arrangement was then annealed under various conditions. Figure 1 (a) and (b) show the results of X-ray diffraction (XRD) measurement and the temperature dependence of resistance for one of the NdFeAs(O,H) films. For comparison, the data of an as-grown film are also shown. From the XRD measurements, no impurities were observed both for as-grown and annealed films. The 00 $l$  peaks shifted to higher angles. The  $c$ -axis length changed from 8.587 Å to 8.466 Å. These results suggest that a phase-pure NdFeAs(O,H) film was obtained. The resistance measurement showed an onset  $T_c$  of 48 K and zero resistance at 45 K, respectively. The magnetization measurements exhibited a self-field critical current density of over 8 MA/cm<sup>2</sup> at 4 K, which is roughly comparable to our NdFeAs(O,F) films.

[1] T. Hanna *et al.*, *Phys. Rev. B* **84**, 024521 (2011). [2] J. Matsumoto *et al.*, arXiv:1903.11819 (2019). [3] T. Kawaguchi *et al.*, *Appl. Phys. Express* **4**, 083102 (2011).

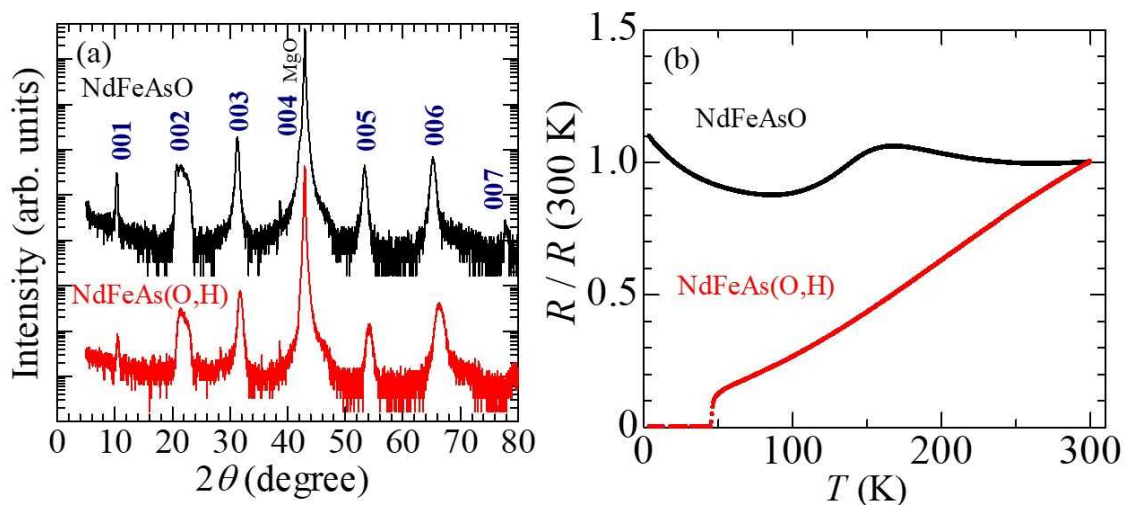


Fig.1. (a) XRD patterns and (b) the temperature dependence of resistance of non-doped and doped NdFeAs(O,H) thin films.

Keywords: oxypnictides, hydrogen doping, epitaxial thin films, topotactic reaction



## PCP5-6

### New strategies in PLD growth of iron-oxypnictides

\*Silvia Haindl<sup>1</sup>, Michiko Sato<sup>2</sup>, Masato Sasase<sup>2</sup>, Hidenori Hiramatsu<sup>2,3</sup>, Hideo Hosono<sup>2,3</sup>, Erik Kampert<sup>4</sup>, Ian MacLaren<sup>5</sup>

Tokyo Tech World Research Hub Initiative (WRHI), Institute of Innovative Research, Tokyo Institute of Technology<sup>1</sup>

Materials Research Center for Element Strategy, Tokyo Institute of Technology<sup>2</sup>

Laboratory for Materials and Structures, Institute of Innovative Research, Tokyo Institute of Technology<sup>3</sup>

Dresden High Magnetic Field Laboratory (HLD-EMFL), Helmholtz-Zentrum Dresden-Rossendorf<sup>4</sup>

School of Physics and Astronomy, University of Glasgow<sup>5</sup>

Pulsed laser deposition (PLD) in thin film growth of iron oxypnictides (ZrCuSiAs-type structure) faces several difficulties. Recently, further advances were made in the *in-situ* deposition of fluorine-doped oxypnictide films using fluorine diffusion from the substrate [1,2] or in hydrogen-doping based on an *ex-situ* diffusion process and a topotactic reaction [3]. Here we present a new strategy in the deposition of iron oxypnictides based on an iron pnictide template (BaFe<sub>2</sub>As<sub>2</sub>). This approach does not only allow a reduction of lattice mismatch between film and substrate but also offers a compatible chemical bonding environment at the interface resulting in a common FeAs-layer. For the purpose of investigating how superconductivity is affected by this specific template approach we turned to Co-doped iron oxypnictides (SmOFe<sub>1-x</sub>Co<sub>x</sub>As and LaOFe<sub>1-x</sub>Co<sub>x</sub>As). Our analysis combines structural and analytic investigations using XRD, TEM, electrical transport measurements and AES depth profiling. We will finally discuss the role of diffusion processes in iron oxypnictides in comparison with previous results on F-doped thin films with a diffusion-gradient hybrid structure [4]. The results demonstrate how diffusion affects the superconducting state of individual iron-pnictide layers.

#### References

- [1] S. Haindl, K. Hanzawa, H. Sato, H. Hiramatsu, H. Hosono, *Sci. Rep.* **6**, 35797 (2016)
- [2] S. Haindl, S. Molatta, H. Hiramatsu, H. Hosono, *J. Phys. D: Appl. Phys.* **49**, 345301 (2016)
- [3] J. Matsumoto, K. Hanzawa, M. Sasase, S. Haindl, T. Katase, H. Hiramatsu, H. Hosono, *arXiv:1903.11819* (submitted)
- [4] S. Haindl, E. Kampert, M. Sasase, H. Hiramatsu, H. Hosono, *Supercond. Sci. Technol.* **32**, 044003 (2019)

Keywords: iron pnictides, thin films, pulsed laser deposition

## PCP5-7

### AC, DC and magnetic relaxation studies of cuprate and pnictide superconducting single crystals exhibiting a second magnetization peak

\*Adrian Crisan<sup>1</sup>, Lucica Miu<sup>1</sup>

National Institute of Materials Physics Bucharest, 405A Atomistilor Street, 077125 Magurele, Romania<sup>1</sup>

We investigated the AC magnetic response of several  $\text{La}_{2-x}\text{Sr}_x\text{CuO}_4$  and 122-type pnictide superconducting single crystals exhibiting a pronounced DC Second Magnetization Peak (SMP). It was found that in the case of small demagnetization effects (LSCO samples) the AC magnetic signal across the SMP remains in the linear regime, with no detectable distortions in the SMP range, which indicates reduced values of the Campbell penetration depth.

The nonlinear AC Bean regime far below the Irreversibility Line has been observed in plate-like 122-type pnictide specimens in perpendicular magnetic fields with strong demagnetization effects. The origin of SMP in superconducting single crystals with fourfold symmetric inter-vortex interactions (such as  $\text{La}_{2-x}\text{Sr}_x\text{CuO}_4$  and the 122-type iron pnictides) has been directly related to the structural rhomb-to-square vortex-phase transition (ST). At the same time, for various superconducting systems, the SMP was attributed to a pinning-induced disordering of the quasi-ordered vortex solid, the proliferation of dislocations in the vortex system leading to a better accommodation of vortices to the pinning centres.

We discuss the relevance of these two models for the SMP in fourfold symmetric superconductors, by investigating the isothermal DC magnetic hysteresis curves  $m(H)$ , the DC magnetization relaxation, and the AC magnetic response of overdoped  $\text{BaFe}_2(\text{As}_{1-x}\text{P}_x)_2$  single crystal, where both the SMP and the ST are expected to be present. It was found that the ST leads to a “shoulder” on the  $m(H)$  curves, affecting the onset of the SMP. The enhancement of the  $m(H)$  shoulder with decreasing temperature leads to the intersection of magnetic hysteresis curves, and, consequently, to a peak in the temperature variation of the critical current density. However, in AC magnetic measurements, when the vortex system is dynamically ordered in the ST range, there is no sign for such a peak at the structural transition temperature. This indicates that the  $m(H)$  shoulder is generated by a precipitous pinning-induced proliferation of dislocations in the vortex system at the ST, where the “squash” vortex-lattice elastic modulus softens.

Keywords: single crystals, pnictides, cuprates, Second Magnetization Peak

## PCP6-1

### Variational Monte Carlo Study of Excited States in Strongly Correlated Hubbard model

\*Hisatoshi Yokoyama<sup>1</sup>, Kenji Kobayashi<sup>2</sup>, Tsutomu Watanabe<sup>2</sup>, Masao Ogata<sup>3</sup>

Department of Physics, Tohoku University, Japan<sup>1</sup>

Department of Natural Science, Chiba Institute of Technology, Japan<sup>2</sup>

Department of Physics, University of Tokyo, Japan<sup>3</sup>

In recent experimental research, excited states were artificially produced by irradiating various (doped) Mott insulators with pulsed light or by modulating the periodic potential of optical lattices in cold atom systems, and relaxation processes from them were actively studied. For example, it was discussed that when one excites parent compounds (antiferromagnetic Mott insulators) of cuprate superconductors, the features of metallization are different between the compounds for hole-doped and electron-doped systems [1]. So far, most theoretical studies have addressed dynamical relaxation processes, but it is also important to elucidate static properties of many-body excited states because they are not necessarily what are expected from the band theories. For example, how much doublon density, namely, light intensity is needed to make a Mott insulator metallic.

In this work, we study static properties in the initial quasi-steady states after an excitation beyond the Hubbard gap, by applying a variational Monte Carlo (VMC) method to a two-dimensional Hubbard model with diagonal transfer ( $t$ ). We can make a trial wave function for an initial excited state by regulating the lowest number of doublons  $D_L$  to  $D_L > 0$ , legitimately at least in the Mott insulating regime; for the ground state,  $D_L = 0$ . We primarily consider fundamental features of excited states at half filling for intermediate and strong correlations, for instance, the threshold of doublon density to metallize a Mott insulator as a function of  $U/t$  and  $t'/t$  [2] or how superconducting (SC) correlation is enhanced immediately below the Mott transition point  $U_c/t$ , as compared to the ground state. Secondly, how this SC correlation evolves as doping rate increases. In the presentation, we explain the details of formalism and discuss basic results.

[1] H. Okamoto *et al.*, Phys. Rev. B **82**, 060513(R) (2010), *ibid.* **83**, 125102 (2011).

[2] H. Yokoyama, T. Miyagawa, M. Ogata, J. Phys. Soc. Jpn. **80**, 084607 (2011).

Keywords: excited state, cuprate superconductor, Mott transition, variational Monte Carlo method

## PCP6-2

### Model Construction and Fluctuation Exchange Study of a New Cuprate Superconductor $\text{Ba}_2\text{CuO}_{3+\delta}$

\*Kimihiro Yamazaki<sup>1</sup>, Masayuki Ochi<sup>1</sup>, Kazuhiko Kuroki<sup>1</sup>, Hiroshi Eisaki<sup>2</sup>, Shinichi Uchida<sup>2,3</sup>, Hideo Aoki<sup>2,4</sup>

Department of Physics, Osaka University, Osaka 560-0043, Japan<sup>1</sup>

National Institute of Advanced Industrial Science and Technology, Tsukuba 305-8568, Japan<sup>2</sup>

Institute of Physics, Chinese Academy of Science, Beijing 100190, China<sup>3</sup>

Department of Physics, University of Tokyo, Hongo, Tokyo 113-0033, Japan<sup>4</sup>

Despite a long history exceeding three decades, the high- $T_c$  cuprate superconductors have basically the same essential ingredient, the  $\text{CuO}_2$  plane. Typically, high- $T_c$  cuprates have a layered perovskite structure, where the Cu-O octahedron is elongated along the  $c$  axis, so that the  $3dx^2-y^2$  orbital is located at the top among the  $3d$  bands. In a previous study[1], it was shown that the separation of the  $3dx^2-y^2$  orbital from other (especially  $3d3z^2-r^2$ ) orbitals plays an important role in realizing high  $T_c$   $d$ -wave superconductivity. Therefore, a large apical O height should in general favor high  $T_c$  as far as the  $\text{CuO}_2$  plane is concerned with about 15% hole doping being “optimal” for the highest  $T_c$ .

Recently, Li *et al.* [2] reported high- $T_c$  superconductivity in a new cuprate  $\text{Ba}_2\text{CuO}_{3+\delta}$  with a  $\text{K}_2\text{NiF}_4$ -like layered structure. There, they find several unique features which strongly suggest that the material is a different type of cuprate superconductor that opens up a new paradigm. Namely, a large amount of O vacancies are present within the  $\text{CuO}_2$  planes, and a great amount of holes are doped which should cause a large deviation of the Cu valence from 2+. Also, the distance between Cu and the apical O is shorter than the in-plane Cu-O distance, so that the octahedron is compressed along the  $c$  axis. This should result in a crystal field where the  $3d3z^2-r^2$  orbital is lifted in energy above the  $3dx^2-y^2$  orbital. These findings suggest that the mechanism of superconductivity in the  $\text{Ba}_2\text{CuO}_{3+\delta}$  may be considerably different from that for the conventional cuprates.

For the 2-1-3 composition in particular, the chain structure is known to be stable in an actual material  $\text{Sr}_2\text{CuO}_3$ . As another possibility within the 2-1-3 composition, here we consider a Lieb lattice type structure. First principles total-energy calculation performed with the VASP code shows that the chain and the Lieb lattice structures are close in the total energy, so that the latter may also be considered as a candidate. Focusing on these two structures, we construct multi-orbital Hubbard models, and discuss the possibility of superconductivity within the fluctuation exchange approximation.

[1] H. Sakakibara *et al.*, Phys. Rev. B **89**, 224505 (2014).

[2] W. M. Li *et al.*, Proc. Natl. Acad. Sci. U.S.A. **116**, 12156 (2019).

Keywords: Cuprates, Theory,  $\text{Ba}_2\text{CuO}_{3+\delta}$ , Lieb lattice

## PCP6-3

### Anisotropy in strongly correlated electrons and its relationship with superconductivity

\*Kenji Kobayashi<sup>1</sup>, Hisatoshi Yokoyama<sup>2</sup>

Department of Natural Science, Chiba Institute of Technology, Japan<sup>1</sup>

Department of Physics, Tohoku University, Japan<sup>2</sup>

Recently, symmetry-breaking phenomena have been successively found in various superconductors; electronic nematic order breaking the rotational symmetry [1] and charge density wave breaking the translational symmetry [2] were experimentally discovered along with superconductivity (SC). Thus, it is urgent to clarify the relationship between these novel symmetry breaking phenomena and SC because they may provide important insights into the relationship between SC and the enigmatic pseudogap state. Pomeranchuk instability, a spontaneous breaking of four-fold rotational symmetry of the Fermi surface without lattice distortion, is a noteworthy candidate for the nematicity observed in cuprate superconductors [3].

In this presentation, we check whether an anisotropy spontaneously appears or not in strongly correlated electrons that have a complex phase diagram of SC and antiferromagnetism (AF). To this end, we use a variational Monte Carlo method (VMC) for the square-lattice Hubbard model with diagonal transfer  $t'$  and large  $U$ , and consider the relationship between the anisotropy and SC when the model parameters varied.

We introduce the following features in trial wave functions: (1) Band renormalization effect owing to electron correlation is introduced by adjusting the parameters of hopping integrals, some of which have degree of freedom of anisotropy in  $x$  and  $y$  directions. (2) As multi-body correlation factors, a doublon-holon binding factor and an on-site Gutzwiller factor are used to capture the essence of strong correlation.

First, we calculate the properties of pure SC, pure AF, and normal states individually by VMC method and consider what is the most important factor in Pomeranchuk instability by comparing the magnitude of  $x$ - $y$  anisotropy. Next, we adopt a mixed state of AF and SC orders as a trial wave function, by which we can treat the orders continuously from their coexistence to the mutual exclusivity. With this wave function, we will clarify the relationship between anisotropy and SC or AF order in the strongly correlated regime.

[1] Y. Sato, *et al.*, Nat. Phys. **13**, 1074 (2017).

[2] S. Kawasaki, *et al.*, Nat. Commun. **8**, 1267 (2017).

[3] H. Yamase, *et al.*, Phys. Rev. B **72**, 035114 (2005); H. Yamase and W. Metzner, Phys. Rev. B **73**, 214517 (2006); B. Edegger, *et al.*, Phys. Rev. B **74**, 165109 (2006).

Keywords: Cuprate superconductor, Hubbard model, Nematicity, Pomeranchuk instability

## PCP6-4

### Study of Optical Properties in Triple-Layer Cuprate Bi2223

\*Yuta Ito<sup>1</sup>, Katsuya Mizutamari<sup>1</sup>, Masamichi Nakajima<sup>1</sup>, Nae Sasaki<sup>2</sup>, Shunpei Yamaguchi<sup>2</sup>, Takao Watanabe<sup>2</sup>, Shigeki Miyasaka<sup>1</sup>, Setsuko Tajima<sup>1</sup>

Department of Physics, Osaka University, Osaka 560-0043, Japan<sup>1</sup>

Graduate School of Science and Technology, Hirosaki University, Hirosaki 036-8561, Japan<sup>2</sup>

$\text{Bi}_2\text{Sr}_2\text{Ca}_2\text{Cu}_3\text{O}_{10}$ , "Bi2223", which is one of the multilayer cuprate superconductors, has three  $\text{CuO}_2$  layers per unit cell. The optimally doped Bi2223 shows the superconductivity below  $T_c = 110\text{K}$ . Recently the superconducting gap in each layer has been determined by angle-resolved photoemission[1] and Raman scattering spectroscopy[2]. The observed gap sizes and the gap/ $T_c$  ratio were much larger than those of single- and double-layer cuprates.

Because of this relatively higher  $T_c$  and larger superconducting gap, it is expected that the change of the optical feature by superconducting transition appears at higher energy region and at higher temperatures above  $T_c$ . However, there has been so far no report of optical spectra of Bi2223 probably because of a lack of large crystals. In this work, we performed in-plane ( $E \perp c$ ) optical reflectivity measurements by Fourier transform infrared (FTIR) spectroscopy in optimally doped Bi2223. We succeeded in observing a rise of reflectivity below  $T_c$  around  $1000\text{ cm}^{-1}$ , suggesting the suppression of the optical conductivity with forming Cooper pairs.

[1] S. Ideta, *et al.*, Phys. Rev. Lett. **104**, 227001 (2017)

[2] G. Vincini, *et al.*, Phys. Rev. B **98**, 144503 (2019)

Keywords: High- $T_c$  cuprate, Optical properties, Superconducting gap

## PCP6-5

### Simulation of THz emission from various shaped intrinsic Josephson junction arrays

Yusuke Fujiki<sup>1</sup>, Masaru Kato<sup>1</sup>

Department of Physics and Electronics, Osaka Prefecture University, Japan<sup>1</sup>

High- $T_c$  cuprate superconductors have several special properties: higher superconducting transition temperature and unconventional Cooper pairing. Additionally, in these materials, superconducting layers and insulating layers are piled up alternately, thus the Josephson junctions between layers are formed spontaneously. These junctions are called the intrinsic Josephson junctions.

If a voltage is applied to the Josephson junctions, an ac current flows by the Josephson effect. Because of this ac current, this electromagnetic (EM) wave is emitted from junctions, and frequency of this wave reaches to the THz regime.

The frequency of the THz wave depends on the applied voltage, also the shape of the material. In some shapes, the EM wave have a circular polarization.

In this study, we simulate the EM field in the junction and the EM wave emitted to outside of the junction numerically using the finite element method and the boundary element method. In a junction array, we use the finite element method and solve Josephson relation considered coupling between the junctions [1], spatial variations of phase differences in magnetic wave, and the Maxwell equation.

And outside of the junctions, we obtain emitted EM wave by using the boundary element method. Then we investigate the dependence of the EM wave on the shape of the junction array.

[1] T. Koyama, H. Matsumoto, M. Machida, K. Kadowaki, Phys. Rev. B **79**, 104522 (2009)

Keywords: High- $T_c$  cuprate superconductors, Intrinsic Josephson junctions, THz emission, Finite element method

## PCP6-6

### Exotic Properties of High Temperature Cuprates Superconductor

\*Kazuhisa Nishi<sup>1</sup>

University of Hyogo, Japan<sup>1</sup>

In spite of much interest in various exotic properties of superconducting cuprates such as the pseudogap, strange metal in normal state, anomalies in the optical sum rules, and several exotic phases of the electron-nematic order *etc* [1], its microscopic mechanism still remains unsolved issues. Here these properties are considered using our recently proposed theory emphasizing that the electronic state of superconductors can be described by the composed fermions [2,3,4]. It is found that the anisotropic pseudogap can be derived from pseudogap state with the representation in momentum space, and that  $T$ -linearity of the electrical resistivity in optimal doping can be derived from considering the interplay between the composite fermion bands. It is also found that the anomaly of optical sum rules can be explained in a similar mechanism.

- [1] B. Keimer *et al.* Nature **518** (2015) 179.
- [2] K. Nishi, J. Phys. Conf. Ser. **871** (2017) 012033.
- [3] K. Nishi, J. Phys. Conf. Ser. **1054** (2018) 012013.
- [4] K. Nishi, Phys. Lett. A **382** (2018) 3293.

Keywords: high temperature superconductor, cuprates, exotic properties



## PCP6-7

### Superconductivity in the heavily Pb-doped Bi-2212 phase of $(\text{Bi,Pb})_2\text{Sr}_2\text{CaCu}_2\text{O}_{8-\delta}$

\*Koki Takano<sup>1</sup>, Ryohei Ito<sup>1</sup>, Takayuki Kawamata<sup>1</sup>, Takashi Noji<sup>1</sup>, Masatsune Kato<sup>1</sup>

Department of Applied Physics, Tohoku University, Japan<sup>1</sup>

The superconducting transition temperature  $T_c$  of the Bi-2212 phase of  $\text{Bi}_2\text{Sr}_2\text{CaCu}_2\text{O}_{8+\delta}$  is  $\sim 80$  K. The reason of the relatively low  $T_c$  is that the hole-concentration is situated in the overdoped region because extra oxygen atoms easily introduced in the BiO plane supply the  $\text{CuO}_2$  plane with holes excessively. The structural disorder caused by extra oxygen atoms also suppresses superconductivity. Recently, we have succeeded in increasing  $T_c$  up to 102 K in  $\text{Bi}_{1.64}\text{Pb}_{0.36}\text{Sr}_2\text{CaCu}_2\text{O}_8$  by the optimization of the content of  $\text{Pb}^{2+}$ -substitution for  $\text{Bi}^{3+}$  and the complete removal of extra oxygen atoms through the reduction annealing [1]. With further increasing Pb-content, it is expected that the oxygen deficiency occurs. In this study, we have investigated the effects of the oxygen deficiency on  $T_c$  in the heavily Pb-doped Bi-2212 phase of  $(\text{Bi,Pb})_2\text{Sr}_2\text{CaCu}_2\text{O}_{8-\delta}$ .

Polycrystalline samples of  $\text{Bi}_{2-x}\text{Pb}_x\text{Sr}_2\text{CaCu}_2\text{O}_{8-\delta}$  ( $0 \leq x(\text{Pb}) \leq 1$ ) were prepared by the solid-state reaction method and annealed in flowing gas of Ar in the final step to suppress the formation of impurity phases with  $\text{Pb}^{4+}$ . As shown in Fig. 1, almost single-phase samples can be obtained for  $x(\text{Pb}) \leq 0.6$  through the Ar-annealing at 710-750°C. As for  $x(\text{Pb}) = 0.8$ , almost single-phase sample is obtained through the Ar-annealing at 730°C. We will report the effects of the oxygen deficiency on  $T_c$ .

[1] K. Sugawara *et al.*, J. Phys.: Conf. Ser. **1054** (2018) 012008.

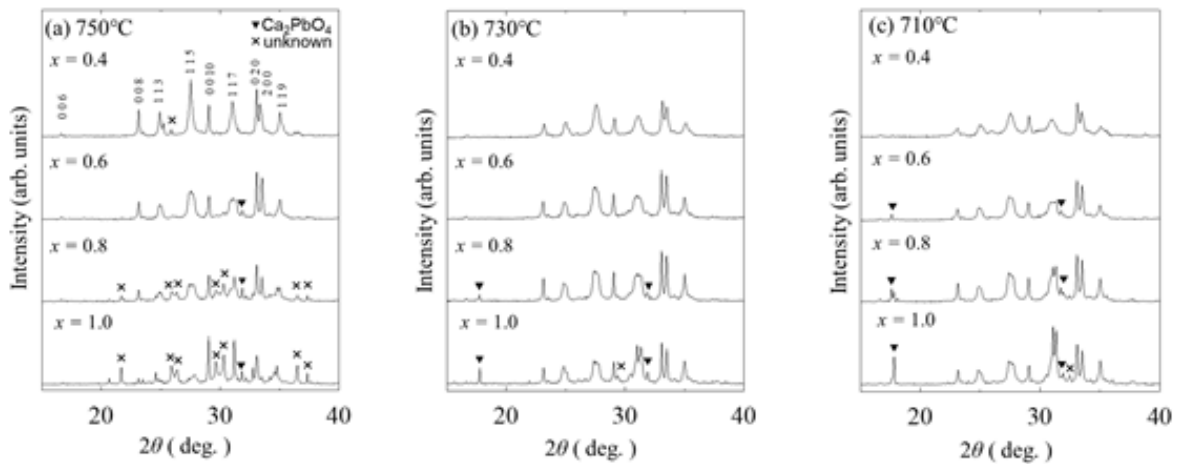


Fig.1. Powder X-ray diffraction patterns of  $\text{Bi}_{2-x}\text{Pb}_x\text{Sr}_2\text{CaCu}_2\text{O}_8$  ( $0.4 \leq x(\text{Pb}) \leq 1$ ) obtained after the Ar-annealing at (a)750°C, (b)730°C and (c)710°C.

Keywords: Bi-2212, Pb-substitution, Oxygen deficiency

## PCP7-1

### Accurate Determination of Composite Crystal Structure of $\text{Sr}_{14-x}\text{Ca}_x\text{Cu}_{24}\text{O}_{41}$ Using the Akaike Information Criterion

\*Yoshito Gotoh<sup>1</sup>

National Institute of Advanced Industrial Science and Technology (AIST) Japan<sup>1</sup>

The composite crystal structures of the spin-ladder compound,  $\text{Sr}_{14-x}\text{Ca}_x\text{Cu}_{24}\text{O}_{41}$  have been accurately determined using the Akaike Information Criterion (AIC) to solve the possible overfitting of atomic parameters. For  $\text{Sr}_{14}\text{Cu}_{24}\text{O}_{41}$  as parent material of  $\text{Sr}_{14-x}\text{Ca}_x\text{Cu}_{24}\text{O}_{41}$ , the minimizing AIC method removes an anomalous behavior of the Cu-O bonds along the 1-D Cu-O chain in the two-legged  $\text{Cu}_2\text{O}_3$  ladder. Our study reveals the importance of the Cu-O-Cu rung with a strong Cu-O bond in  $\text{Sr}_{14-x}\text{Ca}_x\text{Cu}_{24}\text{O}_{41}$ .

In the modulated structure of  $\text{Sr}_{14}\text{Cu}_{24}\text{O}_{41}$ , non-symmetric hole transfers from the O atom in the  $\text{CuO}_2$  chain to the Cu-O-Cu rung in the ladder have been elucidated. The Bond-valence sum analysis of the modulated  $\text{CuO}_2$  substructure of  $\text{Sr}_{14}\text{Cu}_{24}\text{O}_{41}$  shows the role of large displacive modulation of O atom in the  $\text{CuO}_2$  chain and the valence fluctuation of Cu atom with a periodicity almost 200 times that of the average  $\text{CuO}_2$  lattice. There exist the  $\langle\text{Cu}^{2+}\rangle$ - $\langle\text{Cu}^{3+}\rangle$ - $\langle\text{Cu}^{2+}\rangle$  arrangements without the discommensuration in the  $\text{CuO}_2$  chain. The mutual incommensurability between the average substructures is precisely characterized and the chemical formula of  $\text{Sr}_{14}\text{Cu}_{24}\text{O}_{41}$  should be exactly expressed as  $(\text{Sr}_2\text{Cu}_2\text{O}_3)_{0.6995}\text{CuO}_2$ .

The minimizing AIC method has enabled us to successfully select the correct superspace group of  $\text{Sr}_{14-x}\text{Ca}_x\text{Cu}_{24}\text{O}_{41}$ .

[1] Y. Gotoh *et al.*, Phys. Rev. B **68**, 224108 (2003).

[2] Y. Gotoh, J. Phys. Soc. Jpn., **87**, 124601 (2018).

Keywords: Cuprate spin-ladder compound, Composite crystal, Model selection, AIC

## PCP7-2

### Synthesis and Superconductivity in Pb-doped NbSr<sub>2</sub>RECu<sub>2</sub>O<sub>z</sub> ( $z \approx 8$ ; RE: rare-earth element)

\*Yoshihiro Yamada<sup>1</sup>, Tamon Wada<sup>1</sup>, Toshihiko Maeda<sup>1</sup>

Kochi University of Technology<sup>1</sup>

Substitution effects of Pb for Nb in NbSr<sub>2</sub>RECu<sub>2</sub>O<sub>z</sub> (Nb-"1-2-1-2"; RE: rare-earth element) are investigated. The first Nb-"1-2-1-2", NbBa<sub>2</sub>LaCu<sub>2</sub>O<sub>z</sub> and NbBa<sub>2</sub>PrCu<sub>2</sub>O<sub>z</sub>, were synthesized for the first time in 1991 by Ichinose *et al.* [1] and they did not exhibit superconductivity. Kim *et al.* [2] reported in 2013 that Sn doping into their related compounds, NbSr<sub>2</sub>RECu<sub>2</sub>O<sub>z</sub> (RE=Sm, Eu), made them superconducting with superconducting transition temperature ( $T_c$ ) of ~30K by generating carriers due to Sn<sup>4+</sup> partial substitution for Nb<sup>5+</sup>. In this study, doping effects of Pb<sup>4+</sup> instead of Sn<sup>4+</sup> in the Sr-containing Nb-"1-2-1-2" are reported mainly focusing on the occurrence of superconductivity.

Samples were prepared by a solid-state reaction method using Nb<sub>2</sub>O<sub>5</sub>, PbO, SrCO<sub>3</sub>, RE<sub>2</sub>O<sub>3</sub> (RE=Nd, Sm, Eu, Gd) and CuO. Nominal compositions of (Nb<sub>1-x</sub>Pb<sub>x</sub>)Sr<sub>2</sub>RECu<sub>2</sub>O<sub>z</sub> ( $0 \leq x \leq 0.4$ ) were used. Sintering was carried out in air at temperatures of 1000~1080°C and post-annealing was performed in a flowing O<sub>2</sub> gas at 800°C. Characterization of the samples was carried out by means of powder X-ray diffraction (XRD) and the electrical resistivity was measured by a four-probe method.

For the Pb-doped Nb-"1-2-1-2", superconductivity is observed only for the post-annealed samples of RE=Sm, RE=Eu and RE=Gd. This shows that oxygen nonstoichiometry plays an crucial role for the occurrence of superconductivity in these compounds. The maximum value of  $T_c$  observed in this study is 43 K (onset) for (Nb<sub>0.8</sub>Pb<sub>0.2</sub>)Sr<sub>2</sub>EuCu<sub>2</sub>O<sub>z</sub>. Some characteristics of the superconductivity in the Nb-"1-2-1-2" will be discussed.

[1] A. Ichinose *et al.*, J. Ceram Soc. Jpn. **97**, 1065-1070 (1989). (in Japanese)

[2] K. Kim *et al.*, Physica C **492**, 165-167 (2013).

Keywords: Cuprate Superconductor, Nb-"1-2-1-2", Pb-doping, Oxygen nonstoichiometry

## PCP7-3

### Synthesis and Superconductivity of Pb-based "1-2-0-1" Cuprates

\*Toshihiko Maeda<sup>1</sup>, Ryutaro Koresawa<sup>1</sup>, Aoi Sato<sup>1</sup>, Tamon Wada<sup>1</sup>

Kochi University of Technology<sup>1</sup>

Three kinds of homologous series are known at present in Pb-based cuprate superconductors. Among them,  $(\text{Pb,Cu})\text{Sr}_2(\text{Y,Ca})_{n-1}\text{Cu}_n\text{O}_{2n+3}$  characteristically contains  $(\text{Pb,Cu})\text{O}$  monolayer in its crystal structure and is known to form in an oxidizing atmosphere. In this series, two compounds of  $n=1$  and  $n=2$  have been synthesized. Chemical formula of the former is represented as  $(\text{Pb,Cu})(\text{Sr}_{0.5}\text{La}_{0.5})_2\text{CuO}_5$  ( $n=1$ ;  $(\text{Pb,Cu})$ -"1-2-0-1") in which 50 % of  $\text{Sr}^{2+}$  site is replaced by  $\text{La}^{3+}$ . Synthesis and superconductivity with superconducting transition temperature ( $T_c$ ) of 25 K of this  $(\text{Pb,Cu})$ -"1-2-0-1" are reported for the first time by Adachi *et al.* [1,2]. For this compound, however, it has not been made clear how the charge carriers responsible for superconductivity forms. In this study, effects of oxygen non-stoichiometry on superconductivity of the  $(\text{Pb,Cu})$ -"1-2-0-1" are investigated. Additionally, we have attempted to substitution effects of Nd and Sm for La on phase formation of  $(\text{Pb,Cu})$ -"1-2-0-1".

Samples are prepared by a solid-state reaction method of  $\text{PbO}$ ,  $\text{CuO}$ ,  $\text{SrCO}_3$  and  $\text{RE}_2\text{O}_3$  (RE: La, Nd and Sm) using nominal compositions of  $(\text{Pb}_{0.5}\text{Cu}_{0.5})(\text{Sr}_{1-x}\text{RE}_x)_2\text{CuO}_z$  ( $x=0.0$  to  $1.0$ ). For the former, calcination and sintering are carried out respectively at  $850^\circ\text{C}$  for 10 h in air and at  $950$ - $1050^\circ\text{C}$  for 2 h in air or flowing  $\text{O}_2$  gas. Some samples are subjected to quenching procedure, *i.e.*, after post-annealing at  $800^\circ\text{C}$  for 1.5 h in air, samples are rapidly cooled on a copper plate in air. For the latter, calcination and sintering are carried out respectively at  $800^\circ\text{C}$  for 12 h in air and at  $850$ - $920^\circ\text{C}$  for 10 h in air or flowing  $\text{O}_2$  gas. Samples are characterized by means of powder X-ray diffractometry ( $\text{CuK}\alpha$ ;  $\theta$ - $2\theta$ ) and temperature dependence of electrical resistivity ( $\rho$ ) is measured by a four-probe method.

For the case of  $\text{RE}=\text{La}$ , superconductivity is observed for samples of  $x=0.4$ ,  $0.5$  and  $0.6$ , and  $T_c$  tends to be raised by the quenching. Only these three samples contain  $(\text{Pb,Cu})$ -"1-2-0-1" as a dominant phase. Effects of oxygen nonstoichiometry on superconductivity are now being investigated. For the cases of  $\text{RE}=\text{Nd}$  and  $\text{Sm}$ , formation of the "1-2-0-1" phase are not observed.

Keywords:  $\text{Pb}$ -"1-2-0-1", Cuprate superconductor

## PCP7-4

### High-field measurements on bulk $\text{YBa}_2\text{Cu}_3\text{O}_y$ samples prepared by the Infiltration-Growth (IG) technique

\*Quentin Nouailhetas<sup>1,2</sup>, Michael Koblichka<sup>2,3</sup>, Kévin Berger<sup>1</sup>, Bruno Douine<sup>1</sup>, Anjela Koblichka-Veneva<sup>3</sup>, Masato Murakami<sup>3</sup>, Namburi Devendra Kumar<sup>5</sup>, S Pavan Kumar Naik<sup>4</sup>

GREEN - EA 4366, Université de Lorraine, Faculté des Sciences et Technologies, BP 70239, 54506 Vandœuvre-lès-Nancy Cedex, France<sup>1</sup>

Experimental Physics, Saarland University, P.O. Box 151150, 66041 Saarbrücken, Germany<sup>2</sup>

Department of Materials Science and Engineering, Shibaura Institute of Technology, 3-7-5

Toyosu, Koto-ku, Tokyo 135-8548, Japan<sup>3</sup>

Superconducting Electronics Group, Electronics and Photonics Research Institute, National Institute of Advanced Industrial Science and Technology (AIST) 1-1-1 Central 2, Tsukuba, 3055-8568, Japan<sup>4</sup>

Department of Engineering, University of Cambridge, Trumpington Street, Cambridge CB2 1PZ, United Kingdom<sup>5</sup>

With the objective to concurrence the well-known melt texturing YBCO samples in term of irreversible field and critical current, infiltration growth YBCO bulks (IG-processed) show a recent increase of interest due to their advantage of better controlling the shape of the final product and better mechanical stability. Two types of IG-processed YBCO samples were developed: standard bulk samples and superconducting foams which show the advantage of a huge cooling capacity and a low weight due to his low density, particularly appreciated for space applications.

Intended for use as permanent superconducting magnets (trapped field (TF) magnets), precedents works were done to evaluate the pinning properties of such materials by pinning force scaling (Dew-Hughes and Kramer) but only under relatively low magnetic field (up to 9 T). Considering a very high irreversible field ( $H_{irr}$ ), even at 77 K, a lot of assumptions and extrapolations were needed.

Small pieces of both designs (standard bulk and foam) were cut and mechanically polished ( $1 \times 1 \times 0.1 \text{ mm}^3$ ) according to the crystallographic orientation ( $H // c$ ). To experimentally determine the pinning properties for magnetic field above 9 T, we were able to make measurements at high magnetic field (above 30 T) for different temperatures between 85 K and 40 K with the help of EMFL facilities using Cantilever Torque Magnetometry at the High Magnetic Field Laboratory of Nijmegen.

Keywords: IG-processed YBCO, Material characterization, superconducting Bulks, High field measurements

## PCP7-5

### Advances in Novel $\text{YBa}_2\text{Cu}_3\text{O}_{x-\delta}$ Superconducting Materials

\*William Dee Rieken<sup>1</sup>, Atit Bhargava<sup>2</sup>, Rie Horie<sup>3</sup>, Jun Akimitsu<sup>3</sup>, Hiroshi Daimon<sup>1</sup>

Graduate School Of Materials Science, Nara Institute Of Science and Technology<sup>1</sup>

Scotch College<sup>2</sup>

Research Institute For Interdisciplinary Science, Okayama University<sup>3</sup>

We report the fabrication of high-temperature superconductor  $\text{YBa}_2\text{Cu}_3\text{O}_{x-\delta}$  (YBCO) in the various new forms of wafers, bi-wafers, and spiral morphologies made by solution chemistry [1]. Reagent grade oxides of Yttrium Oxide ( $\text{Y}_2\text{O}_3$ ), Barium Oxide (BaO) and Copper Oxide (CuO) in stoichiometric proportions prepared in solution, and upon precipitation, an intimate mixture of fine-grained materials was obtained [2]. The precipitate calcined at 773 K for two h, then subsequently converted to YBCO morphologies by heating to 1223 K in oxygen for 12 h. X-ray diffraction in one case showed that the powder consisted of nanorods and nanotubes predominantly of the  $\text{YBa}_2\text{Cu}_3\text{O}_{x-\delta}$  phase. A critical superconducting transition temperature  $T_c$  of 92 K achieved in a critical magnetic field of 10 Oe, along with observing the Meissner effect using MMPS.

Herein, this presentation presents additional material of this novel discovery not presented in our previous work [3] of these. Transmission electron microscope (TEM) and scanning electron microscope (SEM) images (Fig. 1—2) reveal the tubular morphology of the structures. A significant finding is that these morphologies are superconducting without the need for further sintering or oxygenation, providing an avenue for the application of  $\text{YBa}_2\text{Cu}_3\text{O}_{x-\delta}$  to substrates at room temperatures or direct use in the form of a superconducting powder.

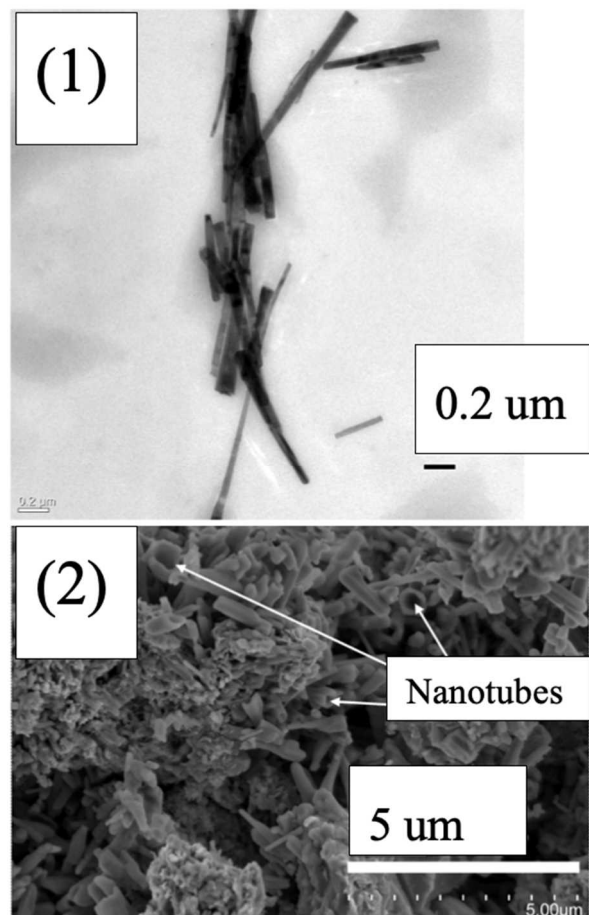
Figure (1): TEM image of superconducting nanorods and nanotubes showing thickness as little as 50 nm and lengths of several micrometers. Figure (2): SEM image of slice of material clearly showing nanotubes.

[1] S.P. Naik and P.M.S. Raju, *AIMS Materials Science*, **3(3)**, 916 (2016).

[2] A. Bhargava, I. Mackinnon, T. Yamashita, and D. Page, *Physica C*, **241**, 53 (1995).

[3] W. Rieken, A. Bhargava, R. Horie, J. Akimitsu, H. Daimon, et al., *Jpn. J. Appl. Phys.*, (2017)

Keywords: Superconductor, Morphology, YBCO, Solution Chemistry



## PCP7-6

### Properties of electron-doped high temperature superconductor $\text{Nd}_{2-x}\text{Ce}_x\text{CuO}_4$ Films deposited by TFA-MOD

\*Keita Sakuma<sup>1</sup>, Yoshinori Kamada<sup>1</sup>, Syuji Anno<sup>1</sup>, Masashi Miura<sup>1</sup>

Seikei University<sup>1</sup>

Superconducting materials with a high in-field critical current density ( $J_c$ ) and a low-cost process are required for superconducting applications such as nuclear magnetic resonance equipment, generators, and energy storage devices. The in-field  $J_c$  is strongly related to not only the vortex pinning but also crystallinity and critical temperature ( $T_c$ ). The trifluoroacetates metal organic deposition (TFA-MOD) process is effective process to crystalize the high crystallinity film and introduce the artificial pinning centers. We reported that the TFA-MOD derived hole-doped high temperature superconductor (HTS) ( $\text{Y}_{0.77}\text{Gd}_{0.23}\text{Ba}_2\text{Cu}_3\text{O}_y$ ) ((Y,Gd)BCO) film shows high in-field  $J_c$  due to high crystallinity and  $T_c$  even with the introduction of high density of adding artificial pinning centers [1]. Although electron-doped  $\text{RE}_{2-x}\text{Ce}_x\text{CuO}_4$  (RECCO, RE = Nd, Pr, Eu...) is also high temperature superconductor,  $J_c$  in RECCO film has not yet been clarified.

In this work, we report that the structural and electrical properties of TFA-MOD derived  $\text{Nd}_{2-x}\text{Ce}_x\text{CuO}_4$  (NCCO,  $x = 0, 0.15$ ) films grown on the substrates with various lattice mismatch. The X-ray diffraction result shows that  $c$ -axis oriented NCCO films were grown on  $\text{LaAlO}_3$  and  $\text{DyScO}_3$  substrate. The  $c$ -axis oriented NCCO films show high crystallinity ( $\Delta\omega \approx 0.14^\circ$ ). The  $\rho$ -T curve of the NCCO ( $x = 0.15$ ) film on  $\text{LaAlO}_3$  shows superconducting transition ( $T_c \approx 9$  K). This  $T_c$  value is lower than that of the bulk value ( $\sim 24$  K). The low  $T_c$  could be attributed to the lattice mismatch between the NCCO and the  $\text{LaAlO}_3$  substrate ( $-4.0\%$ , compressive strain). The structural and electrical properties of NCCO films grown on substrates with various lattice mismatch will be reported.

[1] M. Miura et al., NPG Asia Materials 9, (2017) e447

Acknowledgements: MM is supported by JSPS KAKENHI (17H03239 and 17K18888).

Keywords: Electron-doped HTS, TFA-MOD

## PCP7-7

### Enhanced critical current density in TFA-MOD $(Y_{0.77}Gd_{0.23})Ba_2Cu_3O_y+BaHfO_3$ films on $CeO_2$ buffered $R-Al_2O_3$ substrates

\*Taiki Furuya<sup>1</sup>, Yoshinori Kamada<sup>1</sup>, Keita Sakuma<sup>1</sup>, Masashi Miura<sup>1</sup>

Seikei University Japan<sup>1</sup>

$REBa_2Cu_3O_y$  (REBCO) coated conductors produced by the trifluoroacetate metal organic deposition (TFA-MOD) process are promising candidates for applications, because of the low cost and high superconducting performance. The  $R-Al_2O_3$  substrate is a good candidate for a high sensitivity REBCO resonator filter because of the low dielectric constant. For the resonator filter application, a  $(Y_{0.77},Gd_{0.23})Ba_2Cu_3O_y$  ((Y,Gd)BCO) film with high critical current density ( $J_c$ ) is required because the surface resistance ( $R_s$ ) is strongly correlated with  $J_c$  ( $R_s \propto \mu(1/J_c)$ ) [1]. Recently, the TFA-MOD (Y,Gd)BCO films on  $CeO_2$  buffered  $R-Al_2O_3$  substrates indicate that the high self-field  $J_c$  ( $J_c^{s.f.}$ ) of (Y,Gd)BCO films increases with increasing density of incoherent  $BaMO_3$  (M=Zr, Hf, Sn) nanoparticles (NPs) [2,3]. For further improvement of the  $J_c$ , introducing a high density of BMO NPs as flux pinning centers without degradation of crystallinity and critical temperature ( $T_c$ ) is key.

In this work, in order to investigate the effect of  $BaHfO_3$  (BHO) NPs on the superconducting properties, we fabricated the (Y,Gd)BCO and (Y,Gd)BCO+BHO films on  $CeO_2$  buffered  $R-Al_2O_3$  substrates using the TFA-MOD process. The (Y,Gd)BCO+BHO film shows higher  $J_c^{s.f.}$  without  $T_c$  degradation compared with that of standard (Y,Gd)BCO film. We will discuss the mechanism of improvement of the  $J_c^{s.f.}$  by the introduction of BHO NPs based on crystallinity,  $T_c$  and microstructure.

Acknowledgements: This work is supported by JSPS KAKENHI (17H032398) and Heiwa Nakajima Foundation. A part of this work was supported by JSPS KAKENHI (18KK0414), Kato Foundation for Promotion of Science (KJ-2744) and Promotion and Mutual Aid Corporation for private Schools of Japan (Science Research Promotion Fund).

#### Reference

- [1] A. Saito *et al.*, *IEEE Trans. Appl. Supercond.*, **15** (2005) 3696-3699.
- [2] M. Miura *et al.*, *Scientific Reports* **6** (2016) 20436.
- [3] M. Miura *et al.*, *NPG Asia Materials* **9** (2017) e447.

Keywords:  $R-Al_2O_3$ , TFA-MOD,  $REBa_2Cu_3O_y$ , resonator filter